Late Ordovician Conodonts and Brachiopods from near Greenvale in the Broken River Province, North Queensland

Yong Yi Zhen[1], Ian G. Percival[1] and Peter D. Molloy[2]

[1]Geological Survey of New South Wales, 947-953 Londonderry Road, Londonderry, NSW 2753, Australia (yong-yi.zhen@industry.nsw.gov.au);
[2]Deceased; formerly of School of Earth and Planetary Sciences, Macquarie University, NSW 2109, Australia.

Published on 15 December 2015 at http://escholarship.library.usyd.edu.au/journals/index.php/LIN

Zhen, Yong Yi, Percival, Ian G. and Molloy, Peter D. (2015). Late Ordovician conodonts and brachiopods from near Greenvale in the Broken River Province, north Queensland. *Proceedings of the Linnean Society of New South Wales* **137**, 85-133.

Late Ordovician conodonts and brachiopods are described from limestones (previously referred to the Carriers Well Formation) in the Wairuna Formation of the Broken River Province. The conodonts include the new genus and species *Molloydenticulus bicostatus*. *Scabbardella altipes, Besselodus fusus* sp. nov. and *Protopanderodus liripipus* dominate the conodont fauna of 24 species, which is typical of the *Protopanderodus* biofacies, with two large, robust species of *Protopanderodus* making up about one-quarter of recovered elements. Associated lingulate brachiopods include species of *Acrosaccus*, *Atansoria*, *Biernatia*, *Conotreta*, *Elliptoglossa*, *Hisingerella*, *Nushbiella*, *Paterula* and *Scaphelasma*, identical with those known from the Malongulli Formation and correlative units of the Macquarie Volcanic Province in central New South Wales. Many of the same conodont species found in allochthonous limestones in the basal Malongulli Formation also occur in the fauna from north Queensland, supporting its assignment to the *Taoqupognathus tumidus–Protopanderodus insculptus* conodont Biozone of late Eastonian age, equivalent to the middle Katian Stage. Subtle palaeoecological differences between the fauna of the deeper water Malongulli Formation limestones and that from the Broken River Province limestones indicate that the latter were likely originally deposited on or near the shelf edge. Recognition of this unstable depositional environment confirms interpretation of these limestones as allochthonous, having been reworked into younger basinal sediments of the Wairuna Formation.

Manuscript received 13 May 2015, accepted for publication 9 December 2015.

KEYWORDS: Biogeography, biostratigraphy, brachiopods, conodonts, Katian, Late Ordovician, North Queensland, palaeoecology

INTRODUCTION

Whereas Late Ordovician conodont and brachiopod faunas from New South Wales are very well known, as the result of more than four decades of detailed systematic studies, those from rocks of equivalent age in Queensland have not had the benefit of such concerted research and hence are relatively poorly documented. The situation in Queensland is compounded by the scarcity of sedimentary rocks of this age, which are limited to the Fork Lagoons beds of the Anakie Inlier in central Queensland (Withnall et al. 1995), and what has previously been referred to in the literature as the Carriers Well Limestone, or more recently, the Carriers Well Formation (Withnall and Lang 1993). The conodont fauna from limestone in the Fork Lagoons beds was monographed by Palmieri (1978), but apart from abstracts listing conodonts from the Carriers Well Limestone (Simpson 1997, 2000) supplemented by illustrations of a few conodont species (Talent et al. 2002, 2003), and descriptions of associated tabulate corals (Dixon and Jell 2012), there has been no detailed study of the Carriers Well fauna. Our contribution will help to remedy that, at least for the conodonts and accompanying microbrachiopods, and in doing so will reveal palaeontological confirmation of the recognition of a strong tectonic and geochemical affinity between the Broken River Province of north Queensland and the Macquarie Volcanic Province of central NSW (Henderson et al. 2011).

REGIONAL GEOLOGIC AND STRATIGRAPHIC SETTING

The Broken River Province is situated approximately 200 km west of Townsville in north Queensland (Fig. 1). It is part of one of several Palaeozoic basins, including the Burdekin River Basin, Clarke River Basin, and Hodgkinson Province (to the north towards Cairns) that together make up the Mossman Orogen (Henderson et al. 2013). These basins occupy the northern Tasmanides of eastern Australia, east of the Gondwana craton and its intracratonic basins; further south into NSW, the Tasmanides includes the New England Orogen and the Lachlan Orogen (Glen 2005, 2013).

Stratigraphy of the Broken River Province is well understood for its Silurian to Carboniferous sequences, largely as a result of detailed mapping by the Geological Survey of Queensland (summarised in Withnall et al. 1993) combined with a tightly constrained biostratigraphic framework based on conodonts that was developed over a decade by John Talent, Ruth Mawson and their students (Talent et al. 2002). The Ordovician sedimentological history of the region is less certain, as it relies on relatively few limestone outcrops to produce age-diagnostic fossils. There is general agreement that much of the Ordovician succession, including clastic and carbonate sedimentary rocks and volcanics, consists of allochthonous blocks. However, whether such blocks have been reworked into younger sediments as a result of erosion and downslope movement (Talent et al. 2002, 2003), or whether they have been incorporated into melanges by accretionary tectonism (Henderson et al. 2011), remains contentious. Increased support for the former scenario has been generated as a result of the present study, but the tectonic model proposed by Henderson et al. (2011), especially its finding of significant geochemical similarity with the volcanic islands forming part of the Macquarie Volcanic Province in NSW, remains relevant to understanding the Late Ordovician development of the Tasmanides.

AGE AND CORRELATION OF THE CONODONT FAUNA

Conodonts recovered from limestones within the Wairuna Formation at the Kaos Gully locality (samples with prefix KCY and KAOS) include 23 identifiable species, including *Aphelognathus* sp., *Belodina confluens* Sweet, 1979, *B*. sp., *Coelocerodontus trigonius* Ethington, 1959, *Besselodus fusus* sp. nov., *Drepanodus arcuatus* Pander, 1856, *Drepanoistodus suberectus* (Branson and Mehl, 1933), *Molloydenticulus bicostatus* gen. et sp. nov., *Panderodus gracilis* (Branson and Mehl, 1933), *P. nodus* Zhen, Webby and Barnes, 1999, *Panderodus* sp., *Paroistodus*? *nowlani* Zhen, Webby and Barnes, 1999, *Paroistodus* sp., *Periodon grandis* (Ethington, 1959), *Phragmodus undatus* Branson and Mehl, 1933, *Pseudooneotodus mitratus* (Moskalenko, 1973), *Protopanderodus insculptus* (Branson and Mehl, 1933), *P. liripipus* Kennedy, Barnes and Uyeno, 1979, *Scabbardella altipes* (Henningsmoen, 1948), *Strachanognathus parvus* Rhodes, 1955, *Spinodus spinatus* (Hadding, 1913), *Taoqupognathus tumidus* Trotter and Webby, 1995 and *Yaoxianognathus* sp. (Fig. 2). Although the main limestone body is exposed more or less continuously along Kaos Gully for about 144 m, only 43 samples from the lower part of the section have yielded conodonts (Table 1). The basal part (about 16 m thick) of the limestone succession contains *B. confluens, P. gracilis, Ph. undatus, P. liripipus, S. altipes* and *Yaoxianognathus* sp., and is correlated with the *T. blandus* Biozone (Fig. 2). The remainder of the fauna is interpreted as representing a single zonal assemblage that is referred to herein as the *Taoqupognathus tumidus-Protopanderodus insculptus* Biozone. As *T. tumidus* was only recovered from two samples in the Kaos Gully section (Table 1), this biozone is defined there by the range of *P. insculptus*, which is present from 16.1 m to 59.3 m above the base of the limestone outcrop. In eastern Australia, *P. insculptus* has only been reported as occurring in the *T. tumidus* Biozone in association with *Protopanderodus liripipus* and *T. tumidus*, and is not recorded from the underlying *T. blandus* Biozone.

The fauna from Kaos Gully is identical with that previously documented from allochthonous limestone clasts in the lower part of the Malongulli Formation overlying the Cliefden Caves Limestone Subgroup (Trotter and Webby 1995), which shares 18 species (three-quarters of those occurring in the Wairuna Formation limestones) with the north Queensland fauna. A graptolite assemblage of Ea3 age (the *kirki* Biozone) including *Dicranograptus* cf. *hians kirki*, *Leptograptus eastonensis*, *Dicellograptus elegans*, and *Normalograptus tubuliferus*, was reported from the base of the Malongulli Formation, directly underlying the main breccia containing the conodont fauna (Moors 1970; Trotter and Webby 1995, p. 475). Graptolites from the upper part of the Malongulli Formation suggest an early Bolindian age (*uncinatus* Biozone: Percival 1976; Jenkins 1978; Percival et al. 2015). Therefore, age of the conodont fauna from the allochthonous clasts in the lower part of the Malongulli Formation can be constrained by the

graptolites occurring immediately below and above as middle Katian (Ea3 and possibly into Ea4, not older than the *kirki* Biozone and not younger than the *gravis* Biozone).

Two spot samples from the two small limestone bodies exposed in Gray Creek near the creek crossing (Gray Creek locality CWZ-1 and Gray Creek bank locality CWZ-2) yielded 29 coniform specimens.

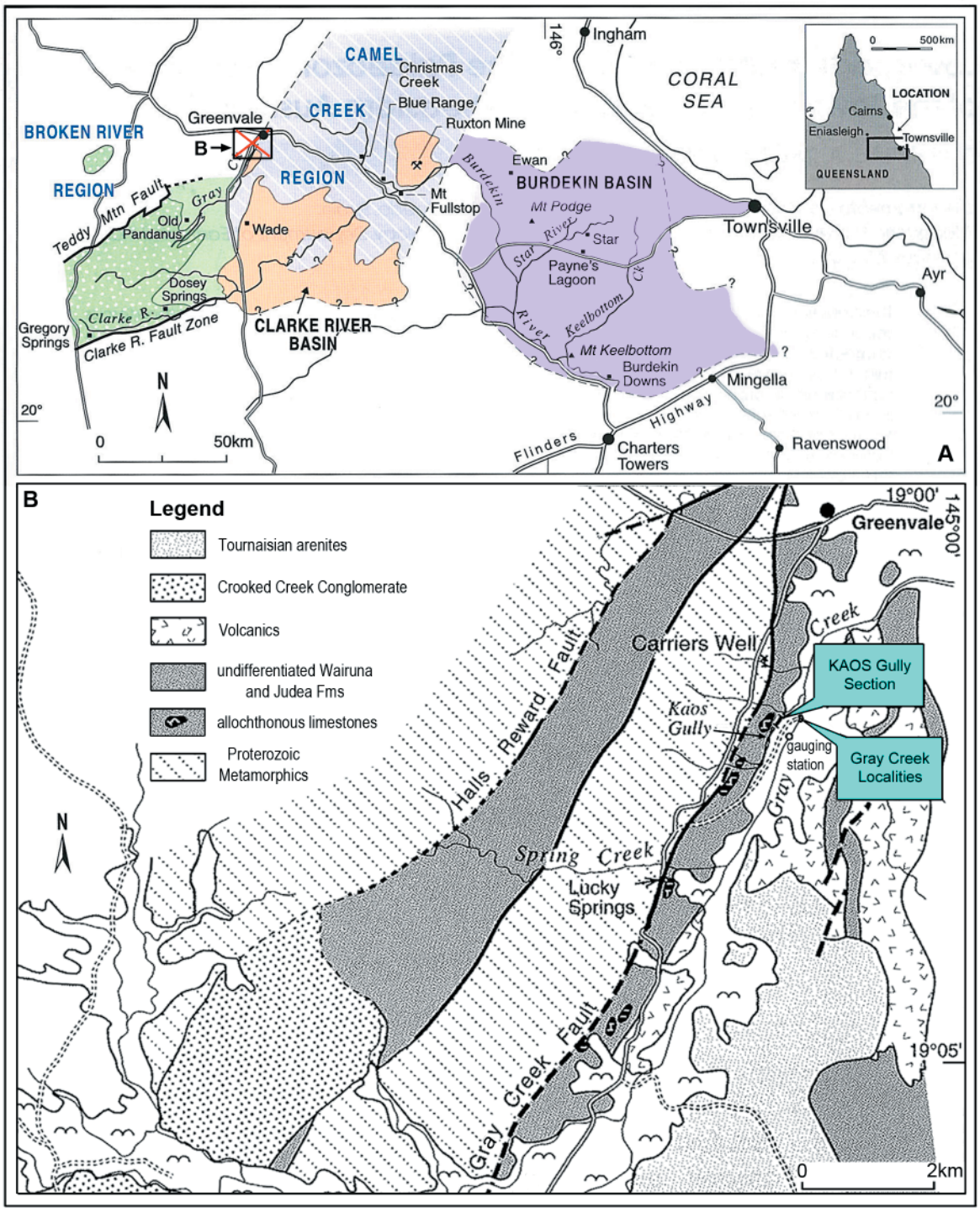

Figure 1. Maps showing the studied area in north Queensland and sample locations. A, Map of Townsville hinterland, north Queensland showing the locations and structural settings of the Gray Creek area, south of Greenvale (modified from Brime et al., 2003); B, Map showing the sample locations of the Kaos Gully section and the two spot samples in Gray Creek near Carriers Well, about 2 km south of Greenvale (modified from Talent et al., 2003).

Table 1. Distribution of conodont species in the samples studied from allochthonous limestones within the Wairuna Formation of north Queensland.

species / samples	KAOS-60	KAOS-59.3	KAOS-56.8	KAOS-50.5	KAOS-50.4	KAOS-50.3	KAOS-50	KAOS-49.8	KAOS-49.6	KAOS-48.2	KAOS-47.8	KAOS-47.5	KAOS-47.4	KAOS-47.1	KAOS-46.8	KAOS-46.2	KAOS-45.9	KAOS-45.6	KAOS-44.8	KAOS-43.9	KAOS-43.7	KAOS-43.3	KAOS-43	KAOS-42.8	KAOS-42.6	KAOS-42.2	KAOS-41.7	KAOS-41.6	KAOS-41.4	KAOS-41.3	KAOS-39.3	KAOS-19.2	KAOS-19	KAOS-18.2	KAOS-17.5	KAOS-17.2	KAOS-17	KAOS-16.1	KAOS-14.6	KCY-6	KCY-5	KCY-4b	KCY-1	CWZ-2	CWZ-1	**Total**
Aphelognathus sp.	1																																														**1**
Belodina confluens Sweet, 1979				1						5									1	9						1	1	1											3	13			5			**40**
Belodina sp.																			1																											**1**
Coelocerodontus trigonius Ethington, 1959										1									1	5				2	2	1													1	5			1			**19**
Besselodus fusus sp. nov.																				442						5	4	2		2	1		1						125			2			**581**
Drepanodus arcuatus Pander, 1856				3															3																											**14**
Drepanistodus suberectus (Branson and Mehl, 1933)			2	2	3									1					29	8				3	4		5	5		2	3						1	12		1				**75**
Molloydenticulus bicostatus gen. et sp. nov.			1																6	195							5	1										41						**249**
Nordiodus italicus Serpagli, 1967																																											2	17	**19**
Paroistodus? *nowlani* Zhen, Webby and Barnes, 1999																																												**3**
Paroistodus sp.																									1					1										3						**5**
Panderodus gracilis (Branson & Mehl, 1933)																		1	3					1	4	5													8			1			**23**
Panderodus nodus Zhen, Webby and Barns, 1999																																								1					**1**
Panderodus sp.																				1	1												1	1											**4**
Periodon grandis (Ethington, 1959)										1				1																			1										12		**4**
Phragmodus undatus Branson and Mehl, 1933																																													**2**
Pseudooneotodus mitratus (Moskalenko, 1973)					2	1					1																																		**5**
Protopanderodus insculptus (Branson & Mehl, 1933)			1		8	16	1	1			2	15		3										1	1													4	6						**91**
Protopanderodus liripipus Kennedy, Barnes & Uyeno, 1979			1	3	18	25				5	1	25		10	4	25	4		48	53							43	2			45	15		15	1	1	1		1	32	130	30				**572**
Scabbardella altipes (Henningsmoen, 1948)	1	1			11	82	3			20	4	41	3	5	5	14	9	7	1	45	130		1		8	17	22	7	69	7	1	34	29	5	4	1	3	2	2	62	181	5		7		**843**
Strachanognathus parvus Rhodes, 1955																				18								1											1						**20**
Spinodus spinatus (Hadding, 1913)				6														1																											**7**
Taoqupognathus tumidus Trotter and Webby, 1995																				3																				1						**4**
Yaoxianognathus sp.																					1																								1		**1**
Total specimens	**2**	**3**	**6**	**47**	**131**	**4**	**1**	**25**	**7**	**89**	**3**	**18**	**9**	**52**	**16**	**7**	**1**	**9**	**139**	**866**	**1**	**1**	**1**	**23**	**39**	**35**	**16**	**127**	**13**	**1**	**88**	**52**	**9**	**25**	**3**	**2**	**5**	**3**	**103**	**536**	**35**	**9**	**9**	**20**	**2594**

The Gray Creek samples are dominated by a single species assigned herein to *Nordiodus italicus* Serpagli, 1967, which has not been recorded in any of the samples from the Kaos Gully locality. Based on four other species (*Coelocerodontus trigonius*, *Besselodus fusus* sp. nov., *Periodon grandis*?, and *Scabbardella altipes*) that also occur in the Kaos Gully samples, these two small limestone bodies are regarded as contemporaneous with that at Kaos Gully. Talent et al. (2003) also reported the occurrence of *Amorphognathus ordovicicus* at the Gray Creek locality, which indicates a similar or slightly younger age.

Zhen et al. (1999, fig. 4) and Zhen (2001) established three successive conodont biozones in the Eastonian of central NSW, defined on the

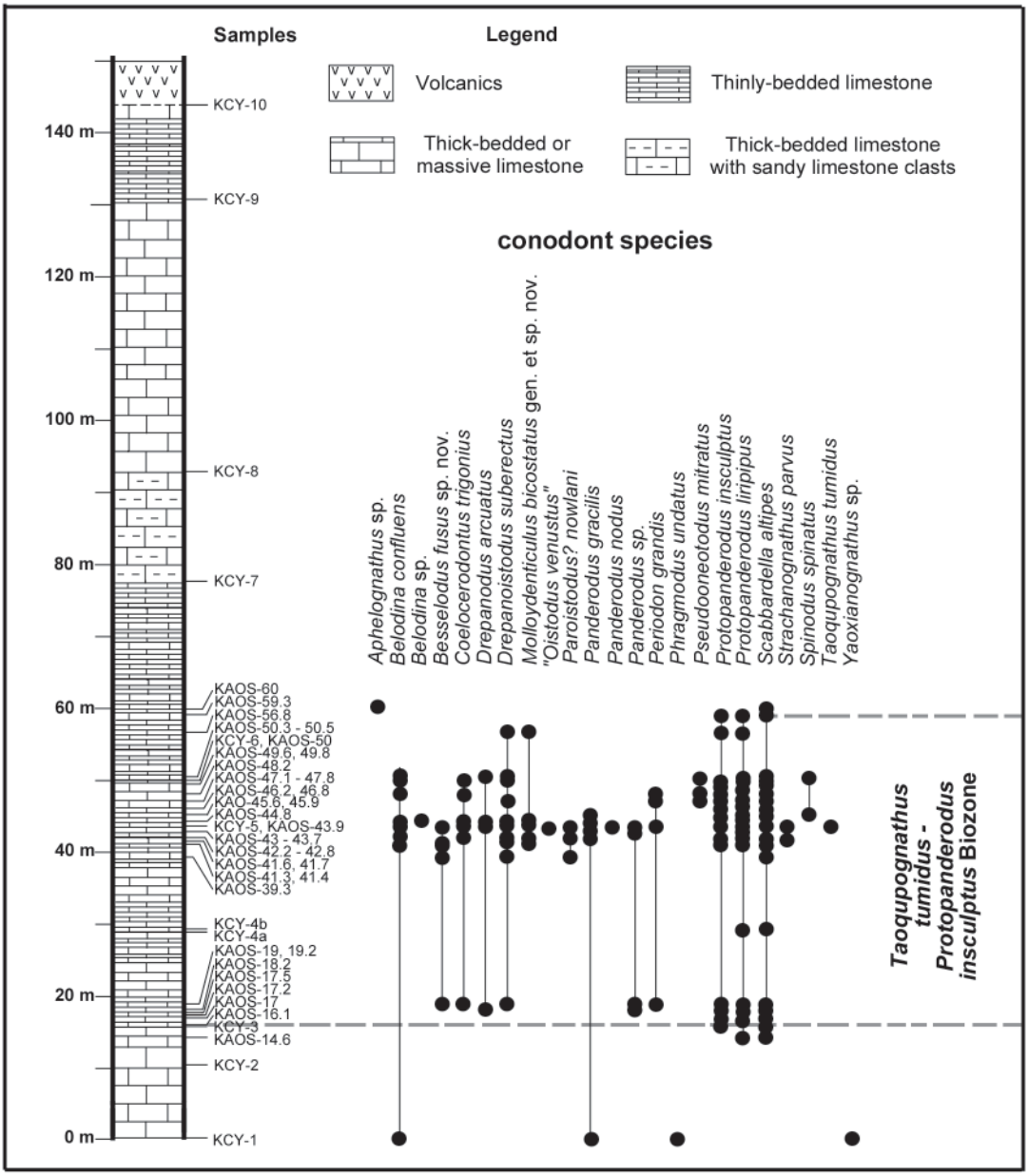

Figure 2. Stratigraphic section showing the sample horizons and ranges of the conodont species in the limestone body exposed along Kaos Gully, south of Greenvale, north Queensland. Samples with prefix KCY were collected by Y.Y. Zhen in 2010 (samples KCY-7 to KCY-10 from the upper part of the section were unproductive), and the remaining 39 productive samples with prefix KAOS were collected previously by John Talent and Ruth Mawson (Macquarie University) from the lower part of the same limestone body. Note that thicknesses shown are apparent, rather than true.

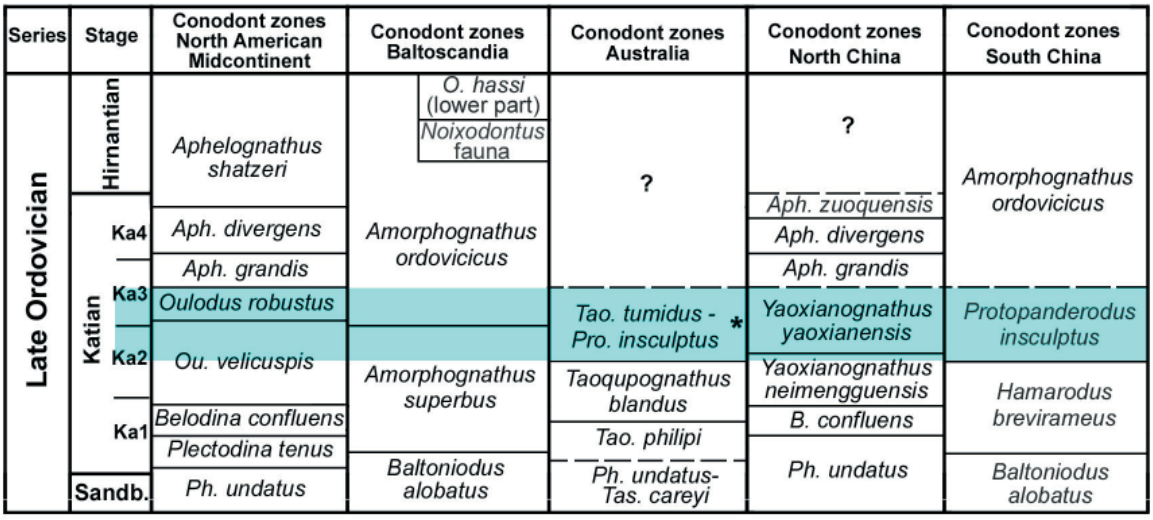

Figure 3. Conodont-based correlation of the allochthonous limestones (indicated by *) within the Wairuna Formation with other Late Ordovician conodont successions established in Australia (*Ph. - Phragmodus, Pro. – Protopanderodus, Tao. – Taoqupognathus, Tas. – Tasmanognathus*), North China (An and Zheng, 1990; Mei, 1995; Zhen et al., 2015; *B. - Belodina, Aph. – Aphelognathus*), South China (An, 1987; Wang et al., 2011; *Hamar. – Hamarodus*), Baltoscandia (Webby et al., 2004; Männik and Viira, 2012; Ferretti et al., 2014; *O. – Ozarkodina*) and North American Midcontinent (Webby et al., 2004; Goldman et al., 2007; Saltzman et al., 2014; *Ou. – Oulodus*). Coloured band in blue represents the middle Katian (late Ka2 to early Ka3) defined by the conodont biozones across different parts of the world.

stratigraphical distribution of *Taoqupognathus* species, from oldest (*T. philipi* Biozone) succeeded by the *T. blandus* Biozone followed by the youngest (*T. tumidus* Biozone). Although *T. tumidus* is relatively rare in the material from north Queensland, being represented by only four specimens, it and the associated species definitely support correlation with the *T. tumidus* Biozone, widely recognized in NSW and other parts of eastern Gondwana and peri-Gondwana.

In North China, the *T. blandus* Biozone can be correlated with the upper *Belodina confluens* Biozone (upper part of the Yaoxian Formation, where *Taoqupognathus blandus* makes its first appearance) and the *Y. neimengguensis* Biozone (spanning the lower part of the Taoqupo Formation) of the Ordos Basin in North China. The *T. tumidus* Biozone correlates with the *Y. yaoxianensis* Biozone of North China (Zhen 2001, text-fig. 3), where *T. tumidus* was reported from the top of the Taoqupo Formation (Zhen et al. 2003), and possibly from the Beiguoshan Formation (correlated to the upper part of the Taoqupo Formation) in the Ordos Basin, and with the *Protopanderodus insculptus* Biozone in South China (Fig. 3).

Kaljo et al. (2012) reported *Molloydenticulus bicostatus* gen. et sp. nov. (referred by them to *Nordiodus*? sp.), *Protopanderodus liripipus* and *P. insculptus* from the lower part of the Tirekhtyakh Formation (sample 115-6/3 from Member 59) in the Mirny Creek section of NE Russia. Co-occurrence of these three species in the faunas documented herein from North Queensland and other parts of eastern Australia (Trotter and Webby 1995) implies a slightly older age (Ka2 to Ka3) for the lower part of the Tirekhtyakh Formation, rather than late Katian (Ka4) as Zhang and Barnes (2007a) and Kaljo et al. (2012) suggested.

CONODONT PALAEOECOLOGY

The conodont fauna from allochthonous limestone in the Kaos Gully section is quantitatively dominated by three species – *Scabbardella altipes* (32.5%), *Besselodus fusus* sp. nov. (22.4%), and *Protopanderodus liripipus* (22.1%) – which constitute over three-quarters of the total number of the specimens recovered (Table 1). *Protopanderodus* and *Spinodus* are widely interpreted to have inhabited relatively deep waters in shelf margin to slope settings (Pohler 1994; Zhang 1998; Löfgren 2003, 2004; Zhen and Percival 2004; Mellgren and Eriksson 2006). Although *Spinodus* is very rare in the material from north Queensland, the two species of *Protopanderodus* that are present make up nearly one-quarter of the total number of specimens, and so this fauna represents a typical *Protopanderodus* biofacies.

The strong taxonomic similarity of this fauna to that in allochthonous limestone clasts from the lower part of the Malongulli Formation in central NSW (Trotter and Webby 1995) has been noted above. However, abundant occurrence of siliceous sponge spicules and radiolarians and the association with argillaceous carbonates suggest that the majority of these Malongulli Formation carbonate clasts represent periplatformal deposits that formed downslope from the island shelf-edge (Webby 1992). Moreover the much higher diversity of the Malongulli limestone clasts fauna with their mixture of typical shallow-water forms, such as *Pseudobelodina* and *Chirognathus*, with characteristic deeper water forms, e.g. *Protopanderodus insculptus* and *P. liripipus* suggested that these clasts might be derived from a variety of sources ranging from the inner platform to slope. In contrast, the fauna from Kaos Gully lacks typical shallow water forms suggesting that the single allochthonous block was likely deposited in a shelf-edge setting. This interpretation is consistent with the common occurrence of corals, stromatoporoids, codiacean algae and bryozoans in these limestone bodies (Dixon and Jell 2012), as well as sedimentological data of these often massive or thick-bedded limestone bodies scattered in the Wairuna Formation.

BRACHIOPOD FAUNA AND PALAEOECOLOGY

Linguliform microbrachiopods recognized in Late Ordovician limestones from the Broken River Province include *Elliptoglossa adela* Percival, 1978, *Paterula malongulliensis* Percival, 1978 and *Hisingerella hetera* (Percival, 1978), in addition to new species of *Acrosaccus*, *Atansoria*, *Biernatia*, *Conotreta*, *Nushbiella* and *Scaphelasma*. Previous discussion of the interpreted palaeoecology of some of these species (Percival 1978) pointed towards a deeper water environment, including both benthic habitats (supported above the sea floor on sponges) and planktic habits, drifting attached to algae. All the new species listed above have been found in limestones (almost exclusively allochthonous) in the Malongulli Formation and correlative units of the Macquarie Volcanic Province in central NSW, and are being described elsewhere on the basis of that more abundant material. There is no doubt, given the identical faunal components, that the depositional environment and palaeoecological setting of the north Queensland limestones was very similar to that of central NSW. But it was not identical, and on the basis of the presence of an abundant and diverse sponge fauna in the Malongulli Formation (and its apparent absence from the Carriers Well limestones) combined with evidence of a shallow-water sedimentological and faunal component in the latter (e.g. Dixon and Jell 2012), we interpret the Carriers Well carbonates as having been deposited at the shelf edge. This would have presumably been unstable and subject to erosion, providing the source of allochthonous blocks to be redeposited into younger sediments. The Malongulli Formation in comparison includes autochthonous graptolitic siltstones and spiculites as matrix to a mixture of spicule-rich limestones interpreted as periplatformal or upper slope in origin (Webby 1992), combined at some horizons with shallower shelfal limestones that have been reworked downslope.

MATERIAL AND SAMPLING LOCALITIES

The conodont fauna documented herein is represented by 2565 discrete identifiable conodont specimens recovered from a total of 43 productive samples (Table 1) from the lower part of an allochthonous limestone block exposed along Kaos Gully, a tributary of Gray Creek (Fig. 1). The Kaos Gully section extends from the base of the limestone at Lat. 19°02.037' S Long. 144°58.372' E (sample KCY-1) to its top at 19°01.970' S 144°58.405' E (sample KCY-10). Conodonts from these samples are opaque black with a CAI of 5-6, indicating a high level of maturation (Epstein *et al*. 1977). Preservation of the conodont specimens varies from reasonably well-preserved to rather strongly deformed or poorly preserved. The upper part of the section was also intensively sampled for conodonts, but none of the samples collected has yielded conodonts. The main limestone block in the Kaos Gully locality is more or less continuously exposed for about 144 m along the gully, and consists of thick-medium bedded greyish limestone in the lower part, thinly bedded, often laminated sandy limestone in the middle, and thick-bedded to massive limestone at the top, which is overlain by brownish volcanics. Ten samples (only four of which were productive, see Table 1) with prefix KCY were collected by Zhen in 2010, and the remaining 39 productive samples with prefix KAOS were collected previously by John Talent and Ruth Mawson (Macquarie University) from the same limestone body. Two additional samples, yielding 29 conodont specimens (Table 1), were also collected by Zhen from the two minor limestone bodies exposed in Gray Creek, one from a large massive limestone block exposed in the middle of the Gray Creek (CWZ-1: 19°02.080' S, 144°58.564' E), and the other (CWZ2,

Gray Creek bank locality: 19°02.162' S, 144°58.535' E) from massive grey limestone exposed on its east bank, next to the track crossing the creek.

SYSTEMATIC PALAEONTOLOGY

All photographic illustrations shown in Figures 4 to 21 are SEM photomicrographs of conodonts and brachiopods captured digitally (numbers with the prefix IY and PI CWL are the file names of the digital images). Figured specimens bearing the prefix MMMC (4756 to 4954 inclusive; 199 specimens in total) are deposited in the microfossil collection of the Geological Survey of New South Wales, housed at the WB Clarke Geoscience Centre at Londonderry in outer western Sydney. Those conodont taxa that are described herein (by Zhen) are alphabetically listed according to their generic assignment, with family level and higher classification omitted. Authorship of the new taxa of conodonts is attributable solely to Zhen. Conodont species that are either rare in the collection, or those that have been adequately described elsewhere in the literature, are documented only by illustration.

CONODONTS (Zhen)

Genus BELODINA Ethington, 1959

Type species

Belodus compressus Branson and Mehl, 1933 (amended by Bergström and Sweet 1966, and by Leslie 1997).

Belodina confluens Sweet, 1979
Fig. 4b-g

Synonymy

Belodina compressa (Branson and Mehl); Bergström and Sweet, 1966, p. 312-319, pl. 31, figs 12-19 (*cum. syn.*); Barnes, 1967, text-figs 1-2; Palmieri, 1978, *partim* only pl. 3, figs 12–15, 20-21, 23–25, pl. 4, figs 1–17, text-fig. 5.6-5.10, 5.16-5.19 (not fig. 11 = S1 of *Belodina baiyanhuaensis* Qiu in Lin, Qiu and Xu, 1984); Nowlan, 1979, pl. 35.1, text-figs 35.1-35.2.

Belodina grandis (Stauffer); Philip, 1966, fig. 2 (= S2 element).

Belodina wykoffensis (Stauffer); Philip, 1966, fig. 3 (= S1 element).

Eobelodina fornicala (Stauffer); Philip, 1966, figs 4, 8 (= M element).

Belodina dispansa (Glenister); Philip, 1966, fig. 1 (= S3 element).

Belodina monitorensis Ethington and Schumacher; Pickett, 1978, cover photo, figs 7-8.

Belodina sp. A s.f. Palmieri, 1978, pl. 3, figs 1-2, text-fig. 5.1 (= S1 element).

Belodina sp. B s.f. Palmieri, 1978, pl. 3, figs 3-6 (3-4 = S2 element, 5-6 = S1 element), text-fig. 5.2-5.3 (5.2 = S2 element, 5.3 = S1 element).

Belodina sp. D s.f. Palmieri, 1978, *partim* only pl. 3, fig. 18, text-fig. 5.13-5.15 (= S3 element) (not pl. 3, figs 16-17, 19, 22, text-fig. 5.11-5.12 = S1 of *Belodina baiyanhuaensis* Qiu in Lin, Qiu and Xu, 1984).

Belodina confluens Sweet, 1979, p. 59-60, fig. 5.10, 5.17, fig. 6.9; Sweet in Ziegler, 1981, p. 73-77, pl. 2, figs 8-14 (*cum syn.*); Nowlan, 1983, p. 662, pl. 3, figs 3-4; Pei and Cai, 1987, p. 70, pl. 9, figs 9, 14, pl. 14, figs 14-16, text-fig. 3.22-3.23; Nowlan and McCracken, in Nowlan et al., 1988, p. 12, pl. 1, figs 16-21 (*cum syn.*); McCracken and Nowlan, 1989, p. 1888, pl. 1, figs 19-21; pl. 2, figs 1-2; Uyeno, 1990, p. 71, pl. 1, figs 8-9; Pickett and Ingpen, 1990, p. 6, cover photo, K; Savage, 1990, p. 829, fig. 9.1-9.6; Bergström, 1990, pl. 3, figs 8–12; Trotter and Webby, 1995, p. 481, pl. 2, figs 18–20, 24-25, 27–30; Zhen and Webby, 1995, pl. 1, figs 16–21; Bergström and Bergström, 1996, fig. 9P; Nowlan et al., 1997, fig. 1.1-1.2; Wang and Zhou, 1998, pl. 3, fig. 9; Zhen et al., 1999, pl. 1, figs 7–9; Furey-Greig, 1999, p. 309, pl. 1, figs 1-11; Percival, 1999, fig. 3.28-29; Furey-Greig, 2000a, p. 91, fig. 4A-F; Furey-Greig, 2000b, p. 137, fig. 5.1-5.4; Zhao et al., 2000, p. 191, pl. 49, figs 4-13; McCracken, 2000, p. 189, pl. 1, figs 10-11, pl. 2, figs 8-10 (*cum syn.*); Wang and Qi, 2001, pl. 1, figs 15, 26; Nowlan, 2002, pl. 1, figs 7-10; Talent et al., 2002, pl. 1, figs A-B; Zhen et al., 2003, fig. 4E-G; Zhang and Barnes, 2007b, fig. 10.11-10.13; Zhang, 2011, fig. 18.14-18.17; Zhang et al., 2011, fig. 13.29-13.31; Chen et al., 2013, fig. 4d'-f'; Zhang, 2013, fig. 10.19-10.21; Zhang and Pell, 2013 fig. 3C; Dumoulin et al., 2014, pl. 5, fig. f.

Belodina sp. A Trotter and Webby, 1995, p. 481, pl. 2, figs 12-13 (= S2 element).

Belodina sp. B Trotter and Webby, 1995, p. 481, pl. 2, fig. 14 (= S2 element).

Belodina sp. A Furey-Greig, 1999, p. 309, pl. 1, fig. 12 (= S1 element).

Belodina sp. C Furey-Greig, 1999, p. 309, pl. 1, figs 14-15 (14= S1 element, 15= M element).

Eobelodina occidentalis Ethington and Schumacher; Pickett, 1978, cover photo, figs 1-2.

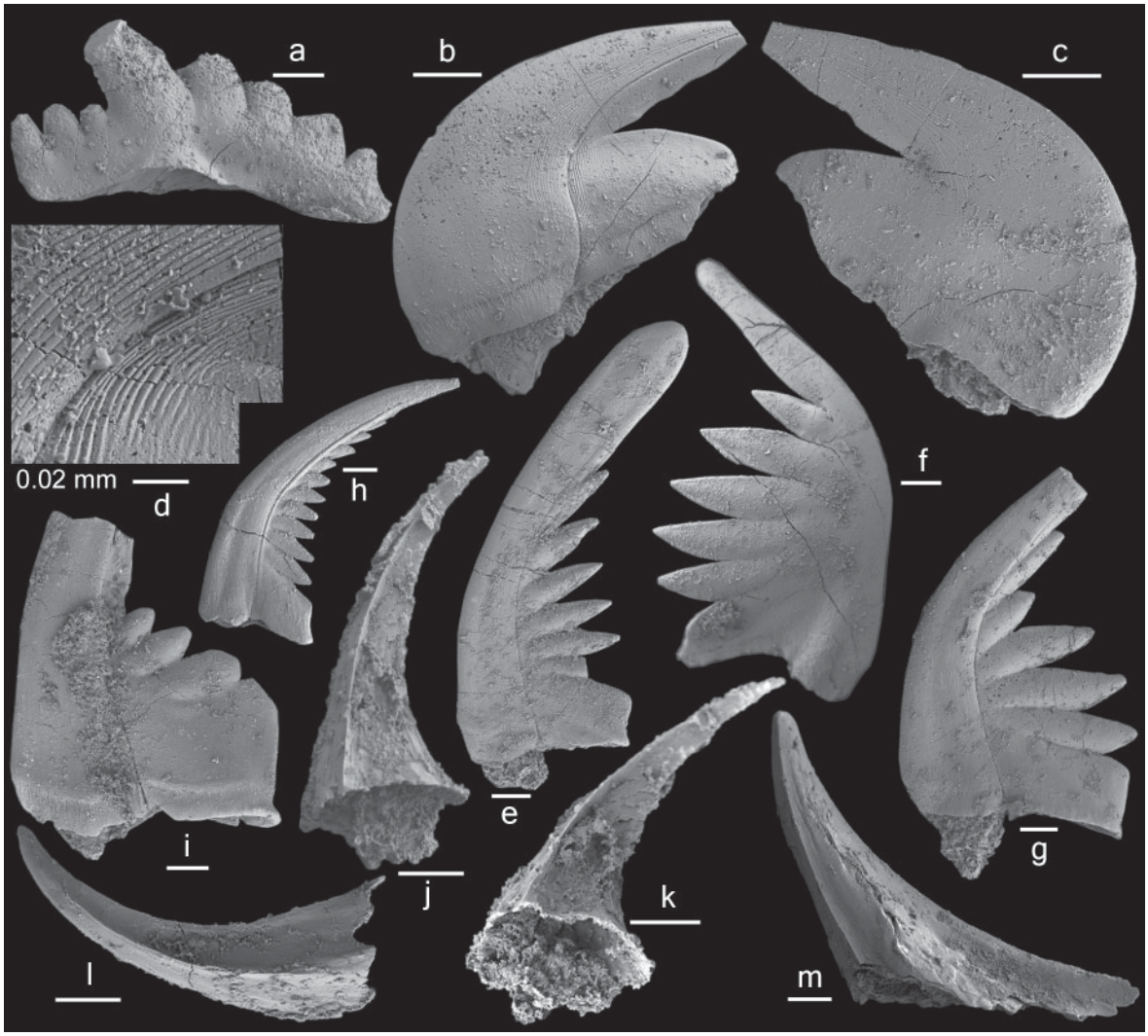

Figure 4. a, *Aphelognathus* sp. Pa element; MMMC4756, KAOS-60, inner-lateral view (IY242-023). b-h, *Belodina confluens* Sweet, 1979. b, d, M (eobelodiniform) element, MMMC4757, KCY-5; b, view of furrowed side (IY233-004), d, view of furrowed side, close-up showing surface striation (IY233-005); c, MMMC4758, KCY-5, view of unfurrowed side (IY233-006); e, S2 (grandiform) element, MMMC4759, KAOS-47.4, view of furrowed side (IY239-007); f-g, S1 (compressiform) element, f, MMMC4760, KCY-5, view of unfurrowed side (IY233-009); g, MMMC4761, KCY-5, view of furrowed side (IY233-009); h, S2 (grandiform) element, MMMC4762, KCY-1, view of furrowed side (IY238-002). i, *Belodina* sp. S2 (grandiform) element, MMMC4763, KAOS-44.8, view of furrowed side (IY243-031). j-m, *Coelocerodontus trigonius* Ethington, 1959. j-k, asymmetrical trigoniform element, MMMC4764, KAOS-42.6, j, outer-lateral view (IY240-016), k, basal-posterior view (IY240-017); l, asymmetrical tetragoniform element, MMMC4765, KAOS-42.6, outer-lateral view (IY240-013); m, long-based, asymmetrical trigoniform element, MMMC4766, KAOS-43.9, outer-lateral view (IY240-016). Scale bars 100 µm.

Material

40 specimens from 10 samples at the Kaos Gully locality (see Table 1).

Discussion

In eastern Australia *B. confluens* had a wide distribution in the Upper Ordovician (Eastonian), reported from the Sofala Volcanics (Pickett 1978; Percival 1999), the Raggatt Volcanics (Pickett and Ingpen 1990), allochthonous limestones in the lower part of the Malongulli Formation (Trotter and Webby 1995), the Cliefden Caves Limestone Subgroup (Savage 1990; Zhen and Webby 1995), the Bowan Park Limestone Subgroup and the basal part of the overlying Malachis Hill Formation (Zhen et al. 1999), and the allochthonous limestones in the Barnby Hills Shale (Zhen et al. 2003) of the Lachlan Orogen in central New South Wales, from the allochthonous

limestones in the Wisemans Arm Formation (Furey-Greig 1999) and in the Drik Drik Formation (Furey-Greig 2000b), formerly the "Trelawney Beds" (Philip 1966), and the "Uralba Beds" (Furey-Greig 2000a) of the New England Orogen in NE New South Wales, from the Fork Lagoons beds of central-east Queensland (Palmieri 1978), and from allochthonous limestones within the Wairuna Formation of the Broken River region, north Queensland (Talent et al. 2002; this study).

Belodina confluens is common in the studied collections from north Queensland, but only M (eobelodiniform), S1 (compressiform), and S2 (grandiform) elements were recovered. The S2 element illustrated herein (Fig. 4e) is identical with that identified by Trotter and Webby (1995, pl. 2, fig. 14) as *Belodina* sp. B. It is characterized by having a broadly swollen tip of the cusp. A comparable specimen was doubtfully referred by Zhen and Webby (1995, pl. 1, fig. 20) to *B. confluens*. The illustrated S1 element (Fig. 4f-g) is less compressed with a gently curved anterior margin and is identical with those illustrated by Palmieri (1978, pl. 3, figs 1-2) as *Belodina* sp. A. We consider that specimen to represent a variant S1 element of *B. confluens*.

Leslie (1997), studying fused clusters of elements from Missouri and Iowa, revised *Belodina compressa* as consisting of a quadrimembrate skeletal apparatus, including eobelodiniform (M), compressiform (S1), grandiform (S2) and dispansiform (S3) elements. He also indicated that *Belodina confluens* was composed of a similar quadrimembrate species apparatus. Morphologically *B. confluens* closely resembles its likely direct ancestral species, *B. compressa*, but can be distinguished from the latter mainly by having a regularly curved antero-basal corner of the anterior margin in the S1 element in lateral view, compared to the corresponding element of *B. compressa* which has a distinctive straight segment (Zhen et al. 2004, pp. 148, 150). Four morphotypes (M, S1, S2 and S3) of elements belonging to *B. confluens* were first recorded from the "Trelawney Beds" of northern NSW (Philip 1966, figs 1-4, 8), and later reported to be widely distributed in the Upper Ordovician of eastern Australia. Palmieri (1978) documented M, S1 and S2 elements of this species (assigned at the time to *Belodina compressa*); additionally some of his specimens illustrated as *Belodina* sp. D s.f. represent the S3 element of *B. confluens* (Palmieri 1978, pl. 3, fig. 18, text-fig. 5.13-5.15). Specimens he assigned to *B*. sp. A and *B*. sp. B are also regarded herein as variants of the S1 and S2 elements of *B. confluens*. Trotter and Webby (1995) only illustrated the M and S1 elements of *B. confluens* from limestone breccia in the lower Malongulli Formation. However, specimens they assigned to *Belodina* sp. A and *Belodina* sp. B are considered herein as representatives of the S2 element of *B. confluens*. In comparison with its rarity in the North American Midcontinent faunas, abundant material of this species (numerically up to 60 percent of the total numbers in some samples – see Zhen and Webby 1995) from eastern Australia shows wider morphological variations in respect to the major characters of the constituent elements. The holotype of *B. confluens* from the Kope Formation (Edenian) of Ohio (Bergström and Sweet 1966, pl. 31, figs 14-16) is an S1 element bearing a strongly reclined cusp with a smoothly curved anterior margin and six denticles along its posterior margin. The paratype, which came from the same sample of the Kope Formation (Bergström and Sweet 1966, pl. 31, figs 17-19), represents the S2 element with a less reclined cusp bearing seven basally-confluent denticles along its posterior margin. The other specimen figured by Bergström and Sweet (1966, pl. 31, figs 12-13) is the geniculate M element bearing a short and recurved cusp and an extended base (heel) with an arched upper margin. The S3 element of *B. confluens*, which is more elongate with five or six smaller denticles obliquely arranged along the posterior margin of the cusp, was documented by Bergström (1990, pl. 3, fig. 9), who originally considered it as doubtful juvenile of an S2 element, and by Barnes (1967, text-figs 1-2) and Nowlan (1979, fig. 35.2) in fused clusters, which were originally assigned to *B. compressa* (see Leslie 1997 p. 924). Among the eastern Australian material referrable to *B. confluens*, S1 elements typically have four or five denticles, and the anterior margin varies from gently curved (Palmieri 1978, pl. 3, figs 1-2; this study Fig. 4f-g), to moderately curved (comparable to the holotype; Philip 1966, fig. 3; Palmieri 1978, pl. 3, figs 23-24; Savage 1990, fig. 9.3-9.4; Zhen and Webby 1995, pl. 1, figs 16, 19; Furey-Greig 1999, pl. 1, fig. 4), and strongly curved (Palmieri 1978, pl. 3, figs 5-6; Trotter and Webby 1995, pl. 2, figs 23-25). Variation of the M element was well-illustrated by Trotter and Webby (1995, pl. 2, figs 267-30) in respect to the degree of the posterior extension of the base and relative size of the cusp. Apparently those specimens occupying the centre of the variation range (Trotter and Webby 1995, pl. 2, fig. 29; Zhen and Webby 1995, pl. 1, fig. 21) are identical with the type specimen illustrated by Bergström and Sweet (1966, pl. 31, figs 12-13), and occur more often in the *Taoqupognathus philipi* Biozone (Ea1, early Katian). Specimens of the M element with a more strongly extended base and a reduced cusp (Trotter and Webby 1995, pl. 2, figs 27-28) are only reported

from the stratigraphically higher *Taoqupognathus tumidus* Biozone (Ea3-4 = Ka2-3). The S2 element of *B. confluens* from eastern Australia has denticles varying from four to ten (typically four to six) along the posterior margin in comparison with the paratype (seven denticles). Some of the grandiform specimens referrable to the S2 element of *B. confluens* exhibit a swollen distal end of the cusp (Trotter and Webby 1995, pl. 2, fig. 14; Zhen and Webby 1995, pl. 1, fig. 20; McCracken 2000, pl. 2, fig. 9; Fig. 4E). The specimen illustrated by Palmieri (1978, pl. 3, fig. 18) from the Fork Lagoons beds of Queensland and by Philip (1966, fig. 1) from the "Trelawney Beds" of NSW were recovered in association with the other elements of *B. confluens*, and are nearly identical with the S3 element of *B. confluens* documented by Bergström (1990, pl. 3, fig. 9) from Scotland, and by Barnes (1967, text-figs 1-2) and Nowlan (1979, fig. 35.2) from Ottawa in Canada. A single S2 (grandiform) element (Fig. 4i) is assigned herein to *Belodina* sp., characterized by having three denticles rooted more or less on the upper margin of the heel rather than on the posterior margin of the cusp as in the typical species of *Belodina.*

Genus BESSELODUS Aldridge, 1982

Type species

Besselodus arcticus Aldridge, 1982.

Discussion

The genus and its type species, *Besselodus arcticus,* were established by Aldridge (1982) based on a fused cluster consisting of seven elements from the Upper Ordovician of North Greenland. Aldridge (1982, p. 428) noted the most important character of the type species to be the presence of prominent oblique striations in all elements. *Besselodus* can be distinguished from *Dapsilodus* Cooper, 1976 mainly by differences in their skeletal apparatus and appearance of the constituent elements. *Besselodus* consists of geniculate M, and distacodiform S and P elements, whereas *Dapsilodus* has non-geniculate M, distacodiform and acodiform S elements. Moreover, the oblique striations are only developed in some S elements of *Dapsilodus*, i.e. they have been only recognized in the acodiform Sb and Sc elements of *Dapsilodus viruensis* (Fåhræus, 1966) documented from South China (Zhen et al. 2009, p. 142, fig. 4).

Unfortunately, Aldridge's study was based on only a small number of specimens and an incomplete species apparatus of the type species, resulting in ongoing difficulty in defining *Besselodus*. Nowlan and McCracken (in Nowlan et al. 1988) described the second species *Besselodus borealis*, from the Northwest Territories of Canada, with a quinquimembrate apparatus including an element (originally referred to as the *c* element) without the oblique striations along the anterior margin. Adhering to the original generic concept of *Besselodus*, this distacodiform element is better assigned to a *Dapsilodus* species in the fauna, and should be excluded from the species apparatus of *B. borealis.* More recently, Leslie (2000) expanded the definition of *Besselodus* by accommodating in it several species including distacodiform, acontiodiform and oistodiform elements that apparently lacked oblique striations along the anterior margin, which would be excluded from *Besselodus* if Aldridge's (1982) original concept is maintained. The new species described below includes only elements bearing these oblique striations.

Besselodus fusus sp. nov.
Fig. 5a-p

Synonymy

?*Besselodus* sp. Trotter and Webby, 1995, pp. 481-482, pl. 3, figs 7, 12-18 (figs 7, 12-14, 16-17 = Sb, figs 15, 18 = M).

Besselodus sp. Zhen et al., 1999, p. 86, *partim* only figs 6.1-6.3. 6.5-6.12 (non 6.4) (figs 6.1-6.3 = Sc, figs 6.5-6.6 = Pb, figs 6.7-6.11 = ?Sb, fig. 6.12 = M).

?*Besselodus* sp. Zhen et al., 2003, fig. 4L-O (= Sb).

Figure 5 (next page). *Besselodus fusus* sp. nov. a-c, M element; a-b, MMMC4767, paratype, KAOS-43.9, a, anterior view (IY240-023), b, enlargement showing striation along inner-lateral margin (IY240-024); c, MMMC4768, paratype, KAOS-43.9, posterior view (IY244-022). d-e, Sa element; d, MMMC4769, paratype, KAOS-43.9, lateral view (IY241-013); e, MMMC4770, paratype, KAOS-43.9, lateral view (IY241-014). f-h, Sb element; f, MMMC4771, paratype, KCY-5, outer-lateral view (IY235-015); g, MMMC4772, paratype, KCY-5, inner-lateral view (IY235-017); h, MMMC4773, paratype, KCY-5, inner-lateral view (IY235-016). i, P element, MMMC4774, paratype, KAOS-41.6, outer-lateral view (IY244-010). j-o, Sc element; j, MMMC4775, holotype, KCY-5, inner-lateral view (IY235-008); k-m, MMMC4776, paratype, KCY-5, k, inner-lateral view (IY235-013), l, posterior view (IY235-010), m, outer-lateral view (IY235-011); n, MMMC4777, paratype, KCY-5, inner-lateral view (IY235-014); o, MMMC4778, paratype, KAOS-43.9, upper view, close-up showing cross section of cusp (IY241-018). p, P element, MMMC4779, paratype, KCY-5, outer-lateral view (IY235-007). Scale bars 100 µm unless otherwise indicated.

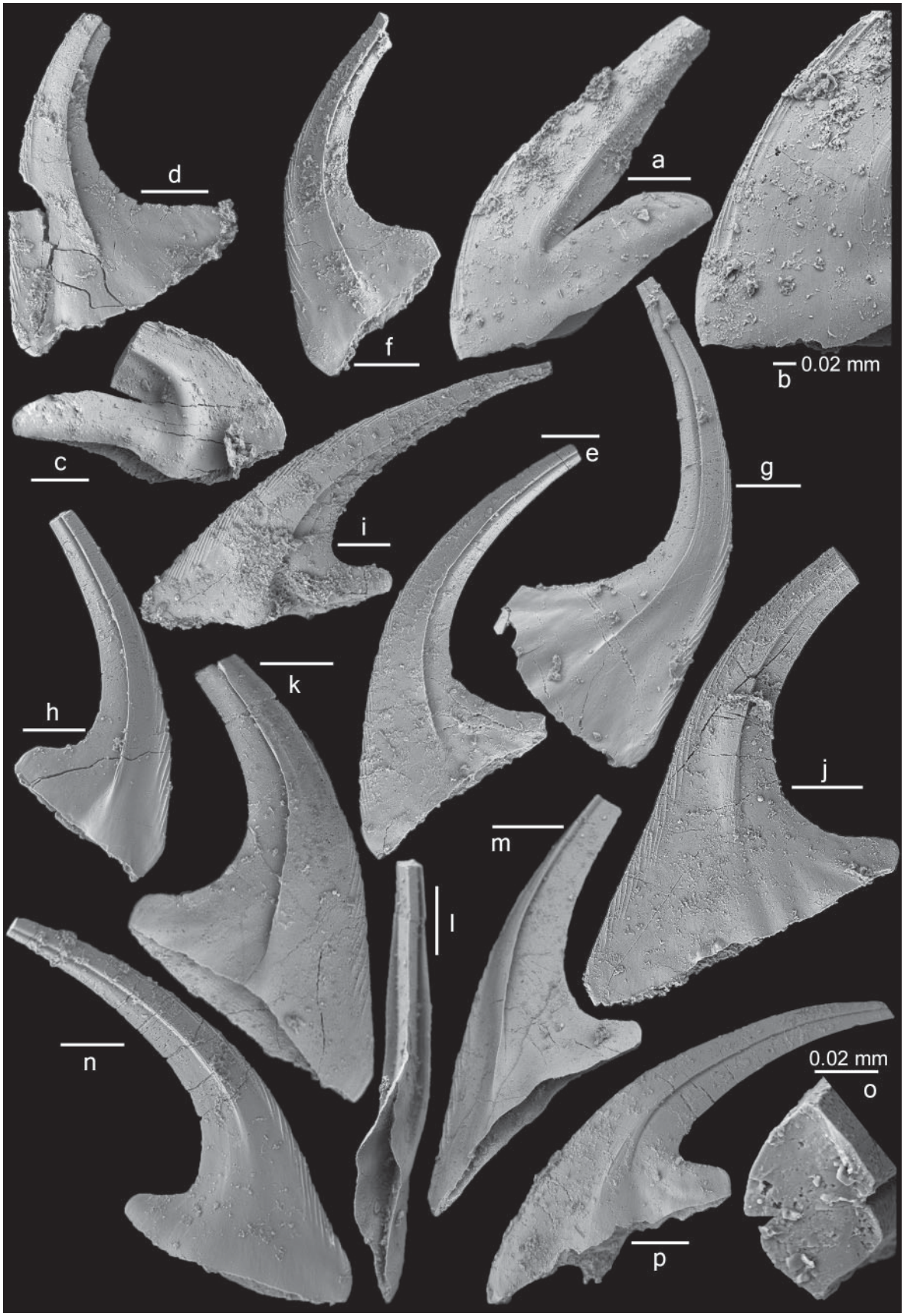
a
b
0.02 mm
c
d
e
f
g
h
i
j
k
l
m
n
o
0.02 mm
p

Material

579 specimens from seven samples at Kaos Gully locality, including the holotype (MMMC4775) and 12 figured paratypes (MMMC4767 to MMMC4774, MMMC4776 to MMMC4779) (see Fig. 5), and an additional two specimens from sample CWZ-1 at Gray Creek locality (see Table 1).

Derivation of name

From Latin *fusus*, extended, alluding to the extended base that characterizes the S and P elements of the species.

Diagnosis

A species of *Besselodus* consisting of a coniform-coniform quinquimembrate species apparatus, with all elements ornamented with oblique striations along the anterior margin (S and P elements) or along the inner-lateral margin (M element); geniculate M element makellate with a strongly recurved cusp and an outer-laterally extended base, long-based distacodiform S elements forming a symmetry transition series (symmetrical Sa, asymmetrical Sb and strongly asymmetrical Sc), and short-based distacodiform P element with a strongly antero-posteriorly extended base and a distally recurved cusp.

Description

Geniculate M element is makellate, strongly compressed antero-posteriorly with sharp inner-lateral and outer-lateral margins, and consists of a robust and outer-laterally strongly recurved cusp bearing a sharp costa on broad anterior and posterior faces, and an outer-laterally extended base (Fig. 5a-c); costae are typically in the median position or situated slightly towards outer-lateral margin on the anterior face (Fig. 5a); base is low and extended outer-laterally, with a straight or gently wavy basal margin and a gently arched upper margin on the long outer-lateral extension; inner-lateral corner short and without prominent extension.

Distacodiform S elements are strongly compressed laterally, and consist of a distally reclined cusp and a longer base, which is more or less triangular in lateral view. The cusp has sharp anterior and posterior margins, and bears a sharp median costa bordered with a deep and narrow groove on the posterior side on each lateral face. Lateral costae and the narrow furrows extend distally to the tip of the cusp, but basally vary from extending to the upper portion of the base (Fig. 5j, n) to near the basal margin (Fig. 5h, k). The anterior margin is gently and smoothly curved in lateral view in extending to the antero-basal corner, and the posterior margin merges with the upper margin of the base through a broadly rounded corner. The Sa element is laterally symmetrical, with a cusp that is basally slightly proclined-suberect and distally reclined, and a posteriorly extended base (Fig. 5d-e). The Sb element is similar to the Sa element, but slightly asymmetrical with anterior margin slightly flexed inner-laterally (Fig. 5g-h) and with a more convex outer-lateral face (Fig. 5f). The Sc element (Fig. 5j-o) is asymmetrical with the base extended posteriorly and also anteriorly to form a prominent basal-anterior corner, which is more or less triangular in outline in lateral view (Fig. 5j).

The distacodiform P element is laterally compressed and asymmetrical with a more strongly developed costa on each lateral side extended to near the basal margin, and displays a distally recurved cusp and a shorter base, which is more open and more strongly extended antero-posteriorly than the S (particularly Sc) elements. Although similar to the Sc element, the P element has a shorter and a more antero-posteriorly extended base (Fig. 5i, p). The posterior margin of the cusp and the upper margin of the base forms an acute angle (Fig. 5i, p), rather than being broadly rounded as in the typical Sc element (Fig. 5j-k).

Discussion

Based on comparison with illustrated specimens representing the M, Sa and Sc elements, *Besselodus* sp. reported from the lower Malongulli Formation of central NSW (Trotter and Webby 1995, pl. 3, figs 7, 12-18) is likely conspecific with *B. fusus* sp. nov. However, the geniculate specimens from the Malongulli Formation display weaker development of the costa (Trotter and Webby 1995, pl. 3, fig. 15), and the Sb and Sc elements are comparable with the Sb element of *B. fusus*, but with a longer base and a more strongly reclined cusp. Trotter and Webby (1995, p. 481) indicated that the symmetrical Sa element was also recognized in the Malongulli fauna, but did not illustrate this.

Elements of *Besselodus* sp. documented from the top part of the Bowan Park Limestone Subgroup of central NSW (Zhen et al. 1999) are closely comparable with the M, Sb, Sc and P elements of the new species and are considered conspecific, although some illustrated specimens with a longer base (Zhen et al. 1999, figs 6.7-6.11) are more similar to some of the type specimens of *Besselodus borealis* (e.g. Nowlan et al. 1988, pl. 2, figs 3-4). Specimens likely representing the Sb element of *B. fusus* were also reported from allochthonous limestones within the Barnby Hills Shale (Zhen et al. 2003).

Both *Besselodus arcticus* Aldridge, 1982 and *Besselodus borealis* Nowlan and McCracken (in Nowlan et al. 1988) are represented only by M and S elements. *B. borealis* differs from the type species mainly by having the costa in the M element situated more towards the outer-lateral margin rather than in the median position in the latter, and by having coarser oblique striations in some S elements that often form a weakly serrated anterior margin. The new species *B. fusus* is readily distinguished from both by having a more antero-posteriorly extended base, particularly its Sc and P elements.

Genus DREPANOISTODUS Lindström, 1971

Type species

Oistodus forceps Lindström, 1955.

Drepanoistodus suberectus (Branson and Mehl, 1933)
Fig. 6a-l

Synonymy

Oistodus suberectus Branson and Mehl, 1933, p. 111, pl. 9, fig. 7.

Drepanoistodus suberectus **(**Branson and Mehl**);** Sweet and Bergström, 1966, pp. 330-333, pl. 35, figs 22-27 (*cum syn.*); Nowlan and Barnes, 1981, pp. 12-13, pl. 4, figs 17-19; Nowlan and McCracken *in* Nowlan et al., 1988, p. 16, pl. 3, figs 19-22 (*cum syn.*); Uyeno, 1990, p. 76, pl. 1, figs 13, 16-18; Dzik, 1994, p. 78, pl. 17, figs 2-6, text-fig. 12b; Trotter and Webby, 1995, p. 482, pl. 5, figs 27-31; Zhen and Webby, 1995, p. 282, pl. 3, figs 8-10 (*cum syn.*); Nowlan et al., 1997, pl. 1, figs 7-9; Zhen et al., 1999, p. 88, fig. 6.1-6.7; Furey-Greig, 1999, p. 310, pl. 2, figs 1-3; Furey-Greig, 2000b, p. 137, fig. 5.8; McCracken, 2000, pl. 1, fig. 12, pl. 2, figs 20, 21; Leslie, 2000, fig. 5.16-5.19; Sweet, 2000, fig. 9.23-9.25; Nowlan, 2002, pl. 1, figs 19-21; Talent et al., 2002, pl. 1, figs C-D; Sansom and Smith, 2005, p. 36, pl. 1, figs 1-2, 7-8, 12; Zhang and Barnes, 2007a, fig. 7.15-7.18; Zhang and Barnes, 2007b, fig. 10.7-10.10; Viira, 2008, fig. 3W-X; Zhang, 2013, fig. 9.36-9.38; Ferretti et al., 2014a, fig. 14M-O; Ferretti et al., 2014c, pl. 2, figs 8-10.

Material

75 specimens from 13 samples at Kaos Gully locality (see Table 1).

Discussion

Elements forming the seximembrate species apparatus of this species are recognized, including makellate M element (Fig. 6a-b) bearing an outer-laterally extended base with a strongly recurved basal margin and a robust cusp; drepanodiform S elements that form a symmetry transition series from symmetrical Sa element (Fig. 6c-e) with a base more flared at the postero-median portion of lateral side, asymmetrical Sb element (Fig. 6f-g), to strongly asymmetrical and laterally compressed Sc element (Fig. 6h-i); drepanodiform Pa element (Fig. 6j-k) with an extended antero-basal corner, and Pb element (Fig. 6l) with a suberect cusp and a short base confined by a strongly recurved basal margin. The Kaos Gully material is identical with specimens from NSW, for instance from the limestone breccia in the lower Malongulli Formation (Trotter and Webby 1995), the Cliefden Caves Limestone Subgroup (Zhen and Webby 1995), the Bowan Park Limestone Subgroup and basal Malachis Hill Formation (Zhen et al. 1999), and from allochthonous limestones within the Barnby Hills Shale (Zhen et al. 2003).

Genus MOLLOYDENTICULUS gen. nov.

Derivation of name

In honour of our co-author, Peter Molloy (deceased) who meticulously processed the samples and picked the conodont residues on which much of this paper is based. Peter studied Silurian conodonts for his Ph.D; combined with *denticulus* (Latin): tooth (diminutive).

Type species

Molloydenticulus bicostatus gen. et sp. nov.

Diagnosis

A genus of Protopanderodontidae consisting of a bimembrate apparatus including laterally-compressed, asymmetrical bicostate (distacodiform) Pa and Pb elements bearing a stout cusp with sharp anterior and posterior margins and with a prominent costa on each lateral face, and a short antero-posteriorly extended base; costa more strongly developed basally into a short, blade-like protoprocess and typically with a deep and narrow groove developed on its posterior side.

Discussion

Molloydenticulus is apparently closely related to *Scabbardella*, but consists of a bimembrate species apparatus with only short based distacodiform elements recognized. These differ from distacodiform elements of *Scabbardella altipes* co-occurring in the fauna in having a stouter cusp with a more strongly

Figure 6. a-l, *Drepanoistodus suberectus* (Branson and Mehl, 1933). a-b, M element; a, MMMC4780, KAOS-42.8, anterior view (IY240-020); b, MMMC4781, KAOS-43.8, anterior view (IY238-018). c-e, Sa element; c, MMMC4782, KAOS-44.8, upper view (IY238-013); d, MMMC4783, KAOS-43.9, lateral view (IY241-004); e, MMMC4784, KAOS-44.8, lateral view (IY238-010). f-g, Sb element, f, MMMC4785, KAOS-42.8, inner-lateral view (IY238-017); g, MMMC4786, KCY-5, inner-lateral view (IY237-023). h-i, Sc element; h, MMMC4787, KAOS-42.6, outer-lateral view (IY240-012); i, MMMC4788, KAOS-42.6, outer-lateral view (IY240-010). j-k, Pa element; j, MMMC4789, KCY-5, outer-lateral view (IY237-021); k, MMMC4790, KAOS-44.8, inner-lateral view (IY238-016). l, Pb element, MMMC4791, KCY-5, inner-lateral view (IY237-016). m, *Drepanodus arcuatus* Pander, 1856. Sa element, MMMC4792, KAOS-44.8, lateral view (IY238-012). n-o, *Paroistodus* sp. M element; n, MMMC4793, KAOS-42.6, posterior view (IY240-011); o, MMMC4794, KAOS-44.8, posterior view (IY238-011). Scale bars 100 µm.

developed costa on the lateral faces and a shorter and more open base. No confirmed P elements comparable with those of the new taxon recognised here were recorded among the abundant material of *S. altipes* from Britain. Therefore the north Queensland specimens are interpreted as representing a new genus (currently monospecific) consisting of a bimembrate species apparatus.

Molloydenticulus bicostatus gen. et sp. nov.
Fig. 7a-m

Synonymy

?*Acodus mutatus* (Branson and Mehl); Palmieri, 1978, *partim* only pp. 6-7, pl. 1, figs 17-18, text-fig. 4a-c (not pl. 2, fig. 19, and text-fig. 5a-c).

Gen. et sp. indet. C Trotter and Webby, 1995, p. 489, pl. 1, figs 16-18.

Nordiodus? sp. Kaljo et al., 2012, figs 5N1, 5N2.

Material

249 specimens from six samples at Kaos Gully locality, including holotype (MMMC4864) and nine figured paratypes (MMMC4858 to MMMC4863, MMMC4865 to MMMC4867) (see Table 1, Fig. 12).

Derivation of name

From Latin *bi*, two, and *cost-*, rib, alluding to the strongly developed costa on each lateral face.

Diagnosis

As for genus.

Description

Two morphotypes of this species are represented (Fig. 7a-m). They are asymmetrical, coniform distacodiform units, more or less triangular in outline in lateral view, and typically with the anterior margin flexed inward (Fig. 7b, i). Both are laterally compressed with sharp anterior and posterior margins. On each lateral face is developed a strong costa, which extends from the tip of cusp to the basal margin, where it is more strongly produced into a blade-like protoprocess. A narrow groove developed on the posterior side of the costa on the lateral faces is deeper and more prominent on the outer-lateral face (Fig. 7f-g, j, l). The base extends antero-posteriorly with a basal cavity of moderate depth (Fig. 7e). The Pa element has a proclined cusp (Fig. 7a-g), while the Pb element has the cusp basally suberect and distally reclined (Fig. 7h-m).

Discussion

Two specimens illustrated by Trotter and Webby (1995, pl. 1, figs 16-18) as Gen. et sp. indet. C, from the lower Malongulli Formation of central NSW, are comparable with the Pa element described herein. A poorly preserved specimen from the Fork Lagoons beds of central Queensland illustrated by Palmieri (1978, pl. 2, figs 17-18) and identified as *Acodus mutatus* (Branson and Mehl) appears to be generally comparable with the Pa element of the new species although it is said to be acodiform (Palmieri 1978, p. 7). Therefore it is only doubtfully assigned to *Molloydenticulus bicostatus*.

The new species also occurs in the lower part of the Tirekhtyakh Formation in the Mirny Creek section of NE Russia, correlated by Kaljo et al. (2012) with the lower part of the *A. ordovicicus* Biozone. However, resolution of the conodont zonation established in NE Russia is still low with the *A. ordovicicus* fauna overlying the long-ranging *Belodina compressa* fauna that spanned the entire Sandbian to middle Katian (Zhang and Barnes 2007a, fig. 2). Recognition of *M. bicostatus* in the Mirny Creek section implies a more precise Ka2-3 age, based on the eastern Australian occurrences.

Genus NORDIODUS Serpagli, 1967

Type species

Nordiodus italicus Serpagli, 1967.

Discussion

Nordiodus was erected based on two form species (*N. italicus* Serpagli, 1967 and *N. proclinatus* Serpagli, 1967) from the Upper Ordovician (Katian) of the Carnic Alps of Italy. In the conodont Treatise (Clark et al. 1981, p. W144), the type species was revised as consisting of a trimembrate apparatus, including a geniculate element (= form species *Oistodus rhodesi* Serpagli, 1967; referred to herein as representing the M element), and two types of nongeniculate elements represented by the form species *N. italicus* Serpagli, 1967 and *N. proclinatus* Serpagli, 1967. The latter are reinterpreted as representing the Pa (=*N. proclinatus*) and Pb (=*N. italicus*) elements. It is likely that the specimens ascribed to *Acodus trigonius* (Schopf, 1966) and *Acodus trigonius aequilateralis* Serpagli, 1967 by Serpagli (1967) may belong to the same species, representing the asymmetrical and symmetrical S elements, respectively, of *N. italicus*.

Nordiodus italicus Serpagli, 1967
Fig. 8a-k

Synonymy

Nordiodus proclinatus Serpagli, 1967, pp. 78-79, pl. 19, figs 1a-6c (= Pa element).

Acodus trigonius (Schopf); Serpagli, 1967, pp. pp.

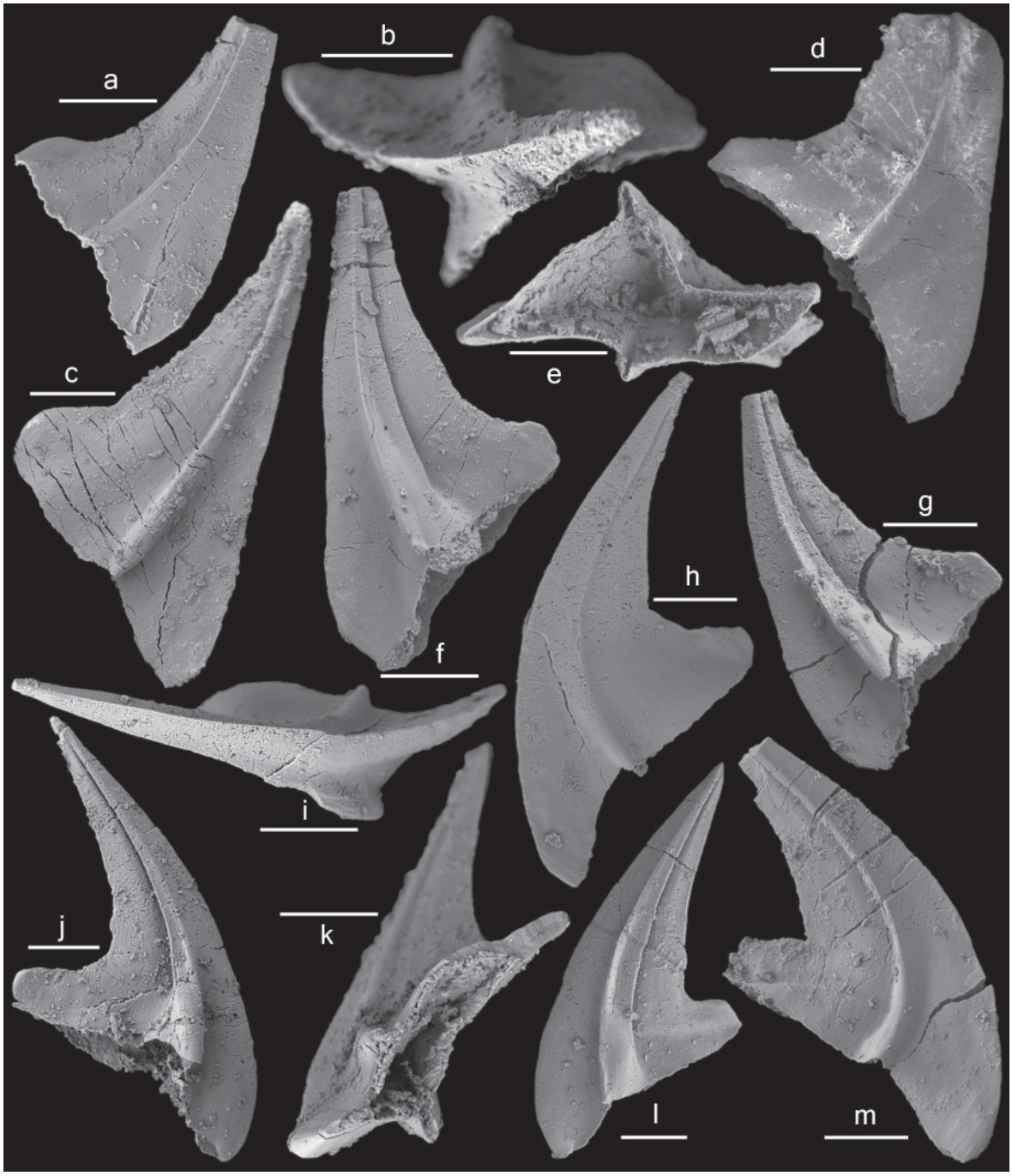

Figure 7. ***Molloydenticulus bicostatus*** **gen. et. sp. nov. a-g, Pa element; a, MMMC4858, paratype, KAOS-43.9, inner-lateral view (IY240-032); b-c, MMMC4859, paratype, KAOS-43.9, b, upper view (IY240-027), c, inner-lateral view (IY240-026); d-e, MMMC4860, paratype, KAOS-43.9, d, outer-lateral view (IY241-010), e, basal view (IY241-008); f, MMMC4861, paratype, KAOS-43.9, outer-lateral view (IY241-006); g, MMMC4862, paratype, KCY-5, outer-lateral view (IY235-003). h-m, Pb element; h-i, MMMC4863, paratype, KAOS-43.9, h, inner-lateral view (IY241-012), i, upper view (IY241-009); j, MMMC4864, holotype, KCY-5, outer-lateral view (IY234-027); k, MMMC4865, paratype, KCY-5, basal, inner-lateral view (IY234-024); l, MMMC4866, paratype, KCY-5, outer-lateral view (IY235-004); m, MMMC4867, paratype, KCY-5, inner-lateral view (IY235-006). Scale bars 100 µm.**

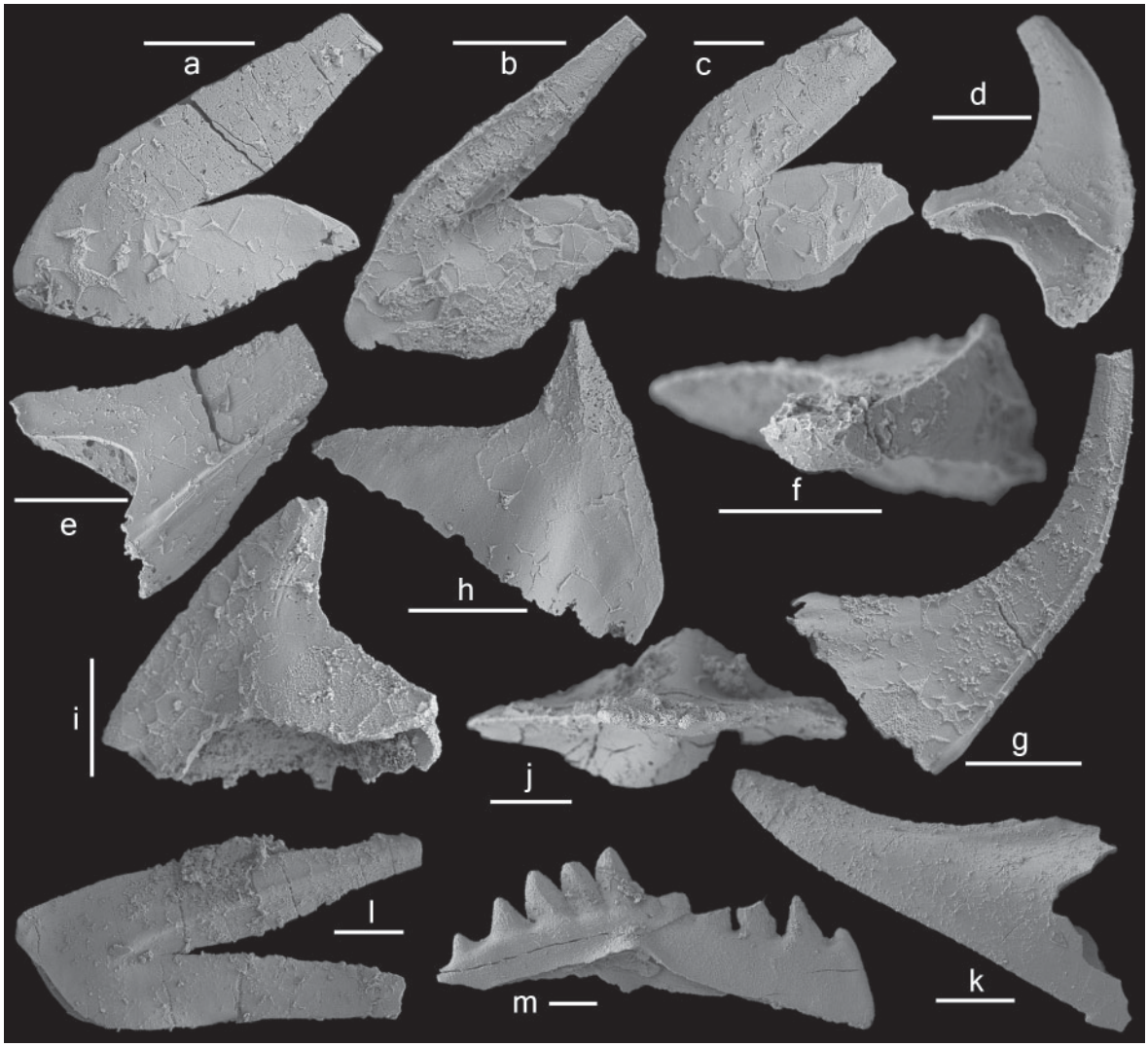

Figure 8. a-k, *Nordiodus italicus* Serpagli, 1967. From sample CWZ-1. a-c, M element; a, MMMC4795, anterior view (IY243-021); b, MMMC4796, posterior view (IY243-022); c, MMMC4797, anterior view (IY243-015). d-g, Sb element; d, MMMC4798, basal-inner-lateral view (IY243-024); e, MMMC4799, outer-lateral view (IY243-026); f, MMMC4800, upper view (IY243-027); g, MMMC4801, inner-lateral view (IY243-025). h-j, P element; h, MMMC4802, outer-lateral view (IY243-016); i, MMMC4803, inner-lateral view (IY243-019); j, MMMC4804, upper view (IY243-014). k, Sc element, MMMC4805, outer-lateral view (IY253-002). l, *Paroistodus? nowlani* Zhen, Webby and Barnes, 1999, M element, MMMC4806, KCY-5, anterior view (IY253-002). m, *Yaoxianognathus* sp., Pa element, MMMC4807, KCY-1, anterior view (IY253-002). Scale bars 100 µm.

44-45, pl. 8, figs 1a-10c (= Sb element).

Acodus trigonius aequilateralis Serpagli, 1967, p. 45, pl. 8, figs 11a-c (= Sa element).

"*Oistodus*" *rhodesi* Serpagli 1967, pp. 81-82, pl. 19, figs 13a-18d (= M element).

Nordiodus italicus Serpagli, 1967, pp. 77-78, pl. 19, figs 7a-12c (= Pb element); Clark et al., 1981, p. W144, fig. 92.2a-c; Ferretti, 1998, p. 133, pl. 1, fig. 18a-b.

Material

17 specimens from sample CWZ-1 at Gray Creek locality and two specimens from sample CWZ-2 at Gray Creek bank locality (see Table 1).

Description

Four albid coniform morphotypes, assigned to the M, Sb, Sc and P elements with a deep basal cavity

that likely represent a single species, were recovered from a bulk sample collected from limestone exposed in Gray Creek. The M element is geniculate makellate and strongly compressed antero-posteriorly, bearing a robust cusp and an outer-laterally extended base with a gently arched upper margin and a wavy basal margin in the anterior or posterior view (Fig. 8a-c). The cusp is recurved outer-laterally and also distally slightly bent inward with sharp inner-lateral and outer-lateral margins and smooth anterior and posterior faces. The Sb element is strongly asymmetrical with a proclined cusp and a posteriorly weakly extended base (Fig. 8d-g). The cusp is more or less triangular in cross section (Fig. 8f) with sharp anterior and posterior margins, a flat and smooth inner lateral face and a convex outer-lateral face bearing a sharp blade-like antero-lateral costa (Fig. 8e). The anterior margin is often flexed inward (Fig. 8g). The asymmetrical Sc element is strongly compressed laterally with sharp anterior and posterior margins, and smooth lateral faces, the outer lateral face more convex (Fig. 8k). The P element is asymmetrical and laterally compressed with a small, suberect cusp, and a large, antero-posteriorly extended base with a deep basal cavity (Fig. 8h-j). The cusp is more or less triangular in outline in lateral view (Fig. 8h) with sharp anterior and posterior margins and a broad median carina. The base is flared in the median potion and tapers distally (Fig. 8j) with a posterior extension, which is triangular in outline in lateral view with straight upper and basal margins (Fig. 8h-i).

Discussion

The P and Sb elements in the material from North Queensland are comparable with type material of this species defined herein as representing the Pb (Serpagli, 1967, pp. 77-78, pl. 19, figs 7a-12c), and the Sb (Serpagli 1967, pp. 44-45, pl. 8, figs 1a-10c) elements. The M element of this species in our collection is also comparable with some of the illustrated M elements (Serpagli 1967, pp. 81-82, pl. 19, fig. 13a-d), but other illustrated type specimens show a prominent costa on both anterior and posterior faces (Serpagli 1967, pp. 81-82, pl. 19, figs 14a-18d).

Genus PERIODON Hadding, 1913

Type species

Periodon aculeatus Hadding, 1913.

Periodon grandis (Ethington, 1959)
Fig. 9m-o

Synonymy

Loxognathus grandis Ethington, 1959, p. 281, pl. 40, fig. 6.

Periodon grandis (Ethington); Bergström and Sweet, 1966, pp. 363-365, pl. 30, figs 1-8 (*cum syn.*); Lindström, in Ziegler, 1981, p. 243-244, pl. 1, figs 13-18; ?McCracken and Nowlan, 1989, p. 1889, pl. 3, figs 7-9; Bergström, 1990, p. 11, pl. 3, fig. 7; Zhang and Chen, 1992, pl. 1, figs 13-16; Ding et al. in Wang, 1993, p. 190, pl. 35, figs 18-21; Fowler and Iwata, 1995, *partim* only fig. 2.1, 2.4-2.5; ?Trotter and Webby, 1995, p. 484, pl. 4, figs 13-14, 27-28; Zhen and Webby, 1995, p. 284, pl. 4, figs 3-4; Stouge and Rasmussen, 1996, pp. 62-63, pl. 1, fig. 19; Furey-Greig, 1999, pp. 310-311, pl. 2, figs 21-22, pl. 3, figs 1-2; Zhen et al., 1999, pl. 4, figs 19-21; Talent et al., 2002, pl. 1, figs F-G; Zhen et al., 2003, pp. 41-43, fig. 6D-L; ?Nowlan, 2002, p. 195, pl. 1, figs 32-37; ?Tolmacheva and Roberts, 2007, fig. 4G-H; Ortega et al., 2008, fig. 6.14; Tolmacheva et al., 2009, pp. 1506-1509, figs 4, 5a-5o; Wang et al., 2011, pp. 198-199, pl. 84, figs 16-19; Zhang, 2011, fig. 20.10-20.12; Zhang, 2013, fig. 11.1-11.4.

Material

Four specimens from four samples at Kaos Gully locality and one doubtfully assigned specimen from sample CWZ-1 at Gray Creek locality (see Table 1).

Discussion

Periodon grandis is the youngest known species of the genus, whose skeletal species construction has been well-established as consisting of a seximembrate or septimembrate apparatus. According to Bergström and Sweet (1966, p. 365) and Lindström (in Ziegler 1981, p. 243), it can be distinguished from its likely direct ancestor, *P. aculeatus*, mainly by the M element having a large, subtriangular base with an essentially straight basal margin and by developing a greater number of smaller denticles between the cusp and the largest denticle on the posterior process of the S elements. However, Zhang and Chen (1992, fig. 1, table 1) indicated that the shape of the base and basal margin of the M element were variable among specimens referable to *P. grandis*, and suggested that it could be differentiated from *P. aculeatus* using the following criteria: *P. grandis* has more than nine denticles between the cusp and the largest denticle on the posterior process of the S elements, displays five to seven denticles along the inner-lateral margin of the M element, and has four to six denticles on the anterior process of the P elements.

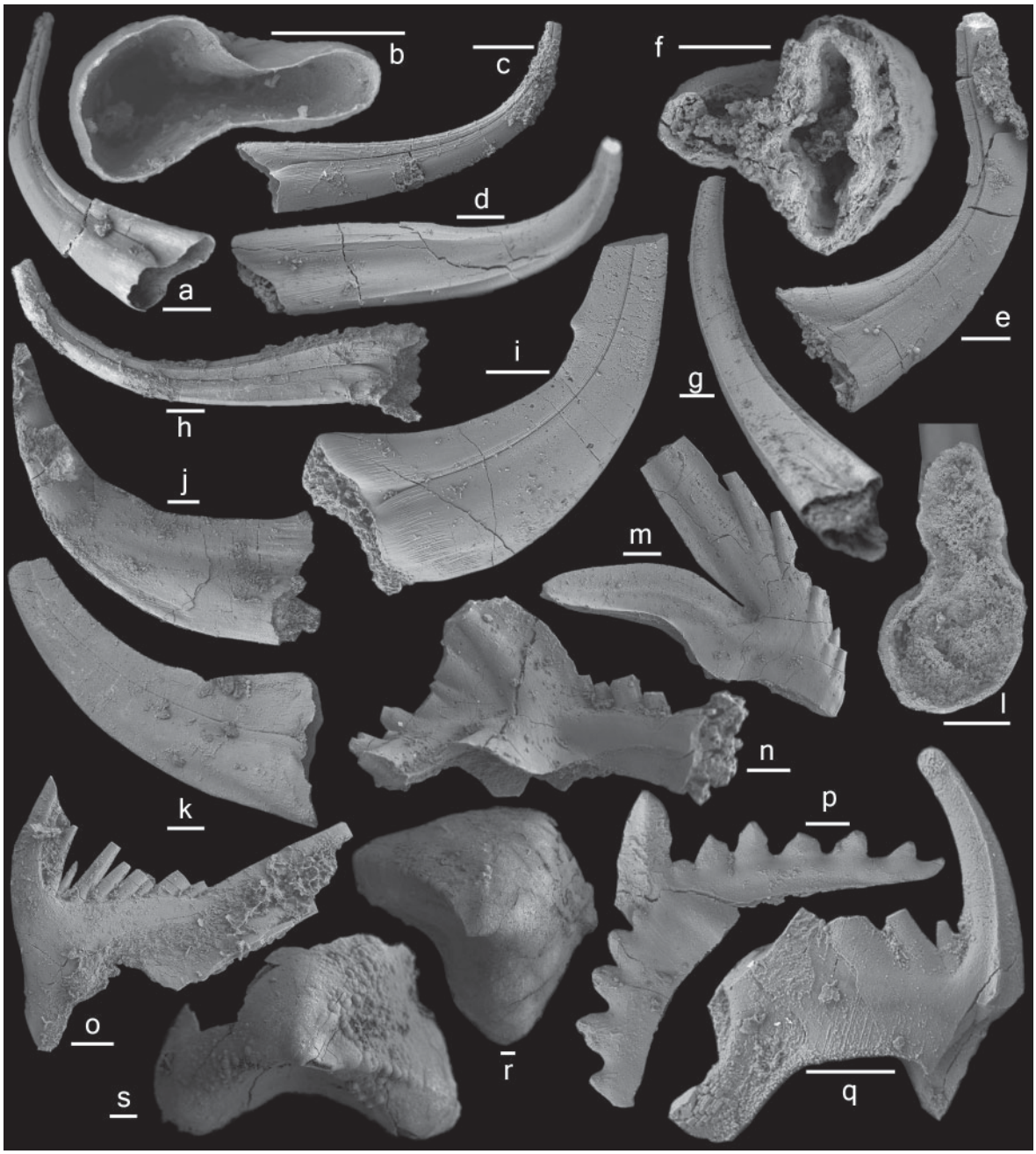

Figure 9. a-h, *Panderodus gracilis* (Branson and Mehl, 1933). a-d, similiform element, a-b, MMMC4808, KAOS-42.2, a, outer-lateral view (IY244-012), b, basal view (IY244-013); c, MMMC4809, KCY-5, outer-lateral view (IY237-015); d, MMMC4810, KCY-5, inner-lateral view (IY237-013). e, falciform element, MMMC4811, KAOS-42.2, outer-lateral view (IY244-011); f-h, symmetrical ae element, f-g, MMMC4812, KCY-5, f, basal view (IY244-007), g, postero-lateral view (IY244-005). h, MMMC4813, KAOS-42.6, postero-lateral view (IY240-014). i, *Panderodus nodus* Zhen, Webby and Barnes, 1999. Long-based element, MMMC4814, KCY-5, outer-lateral view (IY237-011). j-l, *Panderodus* sp. j, MMMC4815, KAOS-18.2, inner-lateral view (IY238-007); k-l, MMMC4816, KAOS-18.2, k, outer-lateral view (IY240-022), l, basal view (IY240-021). m-o, *Periodon grandis* (Ethington, 1959). m, M element, MMMC4817, KCY-5, posterior view (IY233-003); n, Pa element, MMMC4818, KCY-5, inner-lateral view (IY236-019); o, Sc element, MMMC4819, KAOS-47.1, outer-lateral view (IY238-018). p-q, *Phragmodus undatus* Branson and Mehl, 1933. p, Pa element, MMMC4820, KCY-1, posterior view (IY238-009); q, Sb element, MMMC4821, KCY-1, outer-lateral view (IY243-030). r-s, *Pseudooneotodus mitratus* (Moskalenko, 1973). r, MMMC4822, KAOS-48.2, upper view (IY239-011); s, MMMC4823, KAOS-47.1, upper view (IY239-004). Scale bars 100 μm.

Periodon grandis is relatively rare in allochthonous limestones within the Wairuna Formation, and morphology of the M element suggests that it represents an advanced form of the species (see Zhang and Chen 1992, fig. 1).

Genus PROTOPANDERODUS Lindström, 1971

Type species

Acontiodus rectus Lindström, 1955.

Discussion

Under the currently accepted concept of the genus, *Protopanderodus* includes three groups of species, represented by bicostate coniform species (such as the type species, *P. rectus*), multicostate species (such as *P. calceatus* and *P. liripipus*), and denticulate and multicostate species (represented by only one species, *P. insculptus*).

Protopanderodus insculptus (Branson and Mehl, 1933)
Fig. 10a-o

Synonymy

Phragmodus insculptus Branson and Mehl, 1933, *partim* only p. 124, pl. 10, figs 32-33; non fig. 34 = ?Pb element of *Protopanderodus varicostatus* (Sweet and Bergström, 1962).

Protopanderodus insculptus (Branson and Mehl); Palmieri, 1978, p. 25, pl. 2, figs 26, ?27-29, text-fig. 4.10; Harris et al., 1979, pl. 4, fig. 2; An et al., 1981, pl. 1, fig. 26; An, 1981, pl. 3, fig. 28; Lenz and McCracken, 1982, *partim* only pl. 1, figs 15-16; Zeng et al., 1983, pl. 12, fig. 37; Wang and Luo, 1984, pp. 277-278, pl. 8, figs 4-5; Lin et al., 1984, pl. 2, fig. 10; An et al., 1985, pl. 11, fig. 18; An, 1987, p. 172, pl. 11, figs 16, 23, pl. 15, fig. 21; Ni and Li, 1987, p. 431, pl. 60, fig. 54; McCracken, 1989, pp. 16-18, *partim* only text-fig. 3o-p (denticulate); not pl. 3, figs 9-14, 17, 19, text-fig. 3k-n (adenticulate) (*cum syn.*); Trotter and Webby, 1995, p. 485, pl. 4, figs 1, 7-8, 10-11, ?9, ?12; Zhen et al., 1999, pp. 90, 92, fig. 9.6-9.9; Sweet, 2000, fig. 9.21-9.22; Talent et al., 2002, pl. 1, figs L-N; Zhang and Barnes, 2007a, pp. 503-504, fig. 8.11-8.15; ?Kaljo et al., 2008, fig. 8N; Wang et al., 2011, p. 210, pl. 89, figs 13-17, pl. 160, fig. 22.

Protopanderodus aff. *P. insculptus* (Branson and Mehl); Nowlan et al., 1997, *partim*, only fig. 2.10.

Material

91 specimens from 23 samples at Kaos Gully locality (see Table 1).

Diagnosis

Denticulate and multicostate species of *Protopanderodus* consisting of a seximembrate (or possibly septimembrate) ramiform-ramiform apparatus including nongeniculate makellate M1 and M2 elements with a smooth convex anterior face, a costate posterior face and an outer-laterally inclined single denticle on the outer-lateral process, and multicostate S and P elements with two strong costae separated by a deep groove on each lateral side, and with a reclined-recurved single denticle on the posterior process; S elements forming a symmetry transition series from symmetrical Sa and asymmetrical Sb, to strongly asymmetrical and laterally compressed Sc elements; P element similar to S elements, but developing a prominent antero-basal corner, which is triangular in outline in lateral view.

Description

The M elements are nongeniculate and ramiform bearing an outer-laterally reclined cusp with sharp inner-lateral and outer-lateral margins, and an outer-laterally extended base with a wavy basal margin and a non-extended inner-lateral corner; they are antero-posteriorly compressed with an acostate and more convex anterior face, and a multicostate posterior face (Fig. 10a-d). Located near the distal end of the long outer-lateral process is a single denticle, which is variable in size, separated from the cusp by a wide U-shaped gap, and strongly recurved outer-laterally. The M1 element has two weakly developed costae separated by a weak and shallow groove on the posterior face (Fig. 10a-b); the M2 element (fig. 10c-d) has two strongly developed costae separated by a deeper groove and often with short secondary costae developed towards outer-lateral margin (fig. 10c).

The S elements are ramiform bearing a robust multicostate cusp and a long posterior process, which bears a single denticle near the distal end. The cusp and the denticle on the posterior process are laterally compressed with sharp anterior and posterior margins. The cusp is reclined distally with two sharp costae separated by a deep and open groove on each lateral side. The denticle is strongly recurved posteriorly, variable in size, and separated from the cusp by a wide U-shaped gap. Three types of S elements have been recognized, forming a symmetry transition series. The Sa element is symmetrical and biconvex (Fig. 10e-f). The Sb element is similar to the Sa element, but asymmetrical with a more convex outer lateral face (Fig. 10g-j). The Sc element is strongly asymmetrical with anterior margin more antero-basally extended and inner-laterally flexed (Fig. 10k-n).

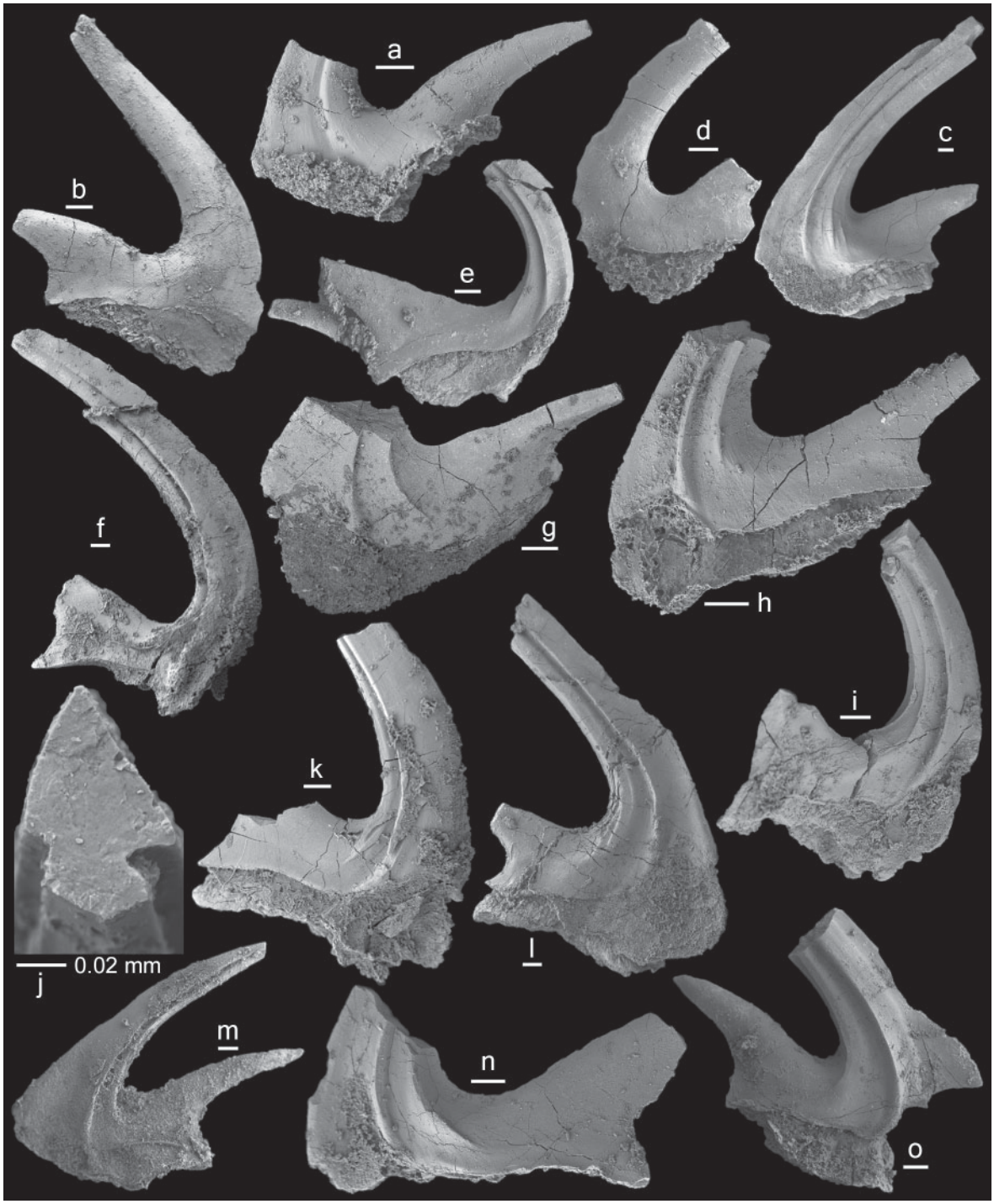

Figure 10. ***Protopanderodus insculptus*** **(Branson and Mehl, 1933). a-b, M1 element; a, MMMC4824, KCY-5, posterior view (IY234-015); b, MMMC4825, KCY-5, anterior view (IY234-014). c-d, M2 element; c, MMMC4826, KAOS-47.1, posterior view (IY238-024); d, MMMC4827, KAOS-47.1, anterior view (IY238-025). e-f, Sa element; e, MMMC4828, KAOS-43.9, lateral view (IY244-018); f, MMMC4829, KAOS-48.2, lateral view (IY239-013). g-j, Sb element; g, MMMC4830, KAOS-48.2, outer-lateral view (IY244-005); h, MMMC4831, KCY-5, inner-lateral view (IY234-016); i, MMMC4832, KCY-5, inner-lateral view (IY234-021); j, MMMC4833, KAOS-44.8, upper view, close-up showing cross section of cusp (IY243-033). k-n, Sc element; k, MMMC4834, KAOS-47.1, outer-lateral view (IY239-003); l, MMMC4835, KAOS-47.1, inner-lateral view (IY239-002); m, MMMC4836, KAOS-48.2, outer-lateral view (IY239-017); n, MMMC4837, KAOS-47.1, inner-lateral view (IY239-001); o, P element, MMMC4838, KAOS-43.9, outer-lateral view (IY242-008). Scale bars 100 µm unless otherwise indicated.**

The P element is similar to Sc element, but weakly asymmetrical with a prominent antero-basal corner, which is strongly antero-basally extended and more or less triangular in outline in lateral view (Fig. 10o).

Discussion

Protopanderodus insculptus is characterized by having a single denticle on all the constituent elements, that is on the outer-lateral process of the M element and on the posterior process of the S and P elements. Among the three cotypes illustrated by Branson and Mehl (1933), two (Branson and Mehl 1933, pl. 10, figs 32-33; the specimen figured in pl. 10, fig. 32 is selected herein as the lectotype), although rather poorly preserved, showed the appearance of this distinctive denticle. However, the other cotype exhibits a posteriorly less extended base without the denticle, and has a suberect cusp and short base with strongly recurved basal margin. This specimen most likely represents the Pb element of *Protopanderodus varicostatus* (Sweet and Bergström 1962). This latter species was recently revised as consisting of a septimembrate apparatus, based on the topotype material from the Pratt Ferry Formation of Alabama (Zhen et al. 2011).

McCracken (1989) revised *P. insculptus* according to the multielement concept as consisting of a quinquimembrate species apparatus including both denticulate and adenticulate elements. Although this species definition was subsequently accepted by some authors, An (1987, p. 172) recognized a scandodiform element assignable to the M position of this species (also confirmed from central NSW: Zhen et al. 1999, fig. 9.8-9.9 = M2), and suggested that *P. insculptus* should include only denticulate elements. Relatively abundant material of this species from the allochthonous limestones within the Wairuna Formation, with six denticulate morphotypes recognized representing the M1, M2, Sa, Sb, Sc and P elements, strongly supports this latter view. Therefore, the species definition of *P. insculptus* is revised herein as consisting of a seximembrate (or possibly septimembrate, if the Pa and Pb elements can be differentiated) ramiform-ramiform apparatus including only denticulate elements.

Protopanderodus liripipus Kennedy, Barnes and Uyeno, 1979
Figs 11a-o, 12a-l

Synonymy

Scolopodus insculptus (Branson and Mehl); Bergström and Sweet, 1966, pp. 398-400, pl. 34, figs 26-27, text-fig. 13B.

Scolopodus? *insculptus* (Branson and Mehl); Serpagli, 1967, pp. 97-99, pl. 28, figs 1a-6b.

Protopanderodus insculptus (Branson and Mehl); Dzik, 1976, fig. 16h, k.

Protopanderodus liripipus Kennedy, Barnes and Uyeno, 1979, pp. 546-550, pl. 1, figs 9-19; An, 1981, pl. 3, fig. 29; An et al., 1981, pl. 1, figs 16-17; Nowlan, 1981, p. 14, pl. 5, figs 6-8; An and Ding, 1982, pl. 2, figs 4, 13; Zeng et al., 1983, pl. 12, fig. 34; Burrett et al., 1983, p. 184, fig. 9A and B; Chen and Zhang, 1984, p. 129, pl. 2, figs 22-24; Wang and Lou, 1984, p. 278, pl. 8, figs 6-10; An and Xu, 1984, pl. 1, fig. 21; An et al., 1985, pl. 12, figs 5-9; Savage and Bassett, 1985, p. 708, pl. 86, fig. 15; An, 1987, p. 173, pl. 11, figs 4, 11-14; Ding, 1987, pl. 5, fig. 28; Nowlan and McCracken, in Nowlan et al., 1988, p. 29, pl. 11, figs 18, 20 (*cum syn.*); Chen and Zhang, 1989, pl. 4, figs 26, ?27; McCracken, 1989, pp. 18-20, pl. 3, figs 15-16, 18, 20-25, text-fig. 3G-J (*cum syn.*); McCracken and Nowlan, 1989, p. 1890, pl. 4, fig. 1; An and Zheng, 1990, pl. 6, figs ?5, 9-10; Bergström, 1990, pl. 2, figs 7-8, pl. 4, figs 1-4; Duan, 1990, pl. 3, figs 2, 4; Gao, 1991, p. 135, pl. 12, fig. 8; Ding et al. in Wang, 1993, p. 195, pl. 38, fig. 17; Dzik, 1994, pp. 74-75, pl. 14, figs 6-7, text-fig. 11c; Trotter and Webby, 1995, p. 485, pl. 4, figs 2-6; Stouge and Rasmussen, 1996, p. 63, pl. 1, fig. 18; Zhen et al., 1999, p. 92, fig. 9.10-9.13 (*cum syn.*); Leslie, 2000, p. 1125, fig. 6.19-6.24; Zhao et al., 2000, p. 217, pl. 20, figs 1-2, 5, 7, 10-13; McCracken, 2000, pl. 3, fig. 10; Pyle and Barnes, 2001, pl. 2, figs 6-7; Wang, 2001, pl. 1, fig. 12; Wang and Qi, 2001, pl. 1, figs 5, 22; Talent et al., 2002, pl. 1, figs H-J; Agematsu et al., 2007, p. 29, fig. 13.4-13.5, 13.8, 13.10 (*cum syn.*); Zhang and Barnes, 2007a, p. 505, fig. 8.7-8.10; Agematsu et al., 2008, p. 969, fig. 12.23-12.28; Zhen et al., 2011, pp. 243-245, fig. 23C-E; Zhang, 2011, fig. 20.15-20.16; Zhang, 2013, fig. 11.21-11.22; Bergström and Ferretti, 2015, fig. 13A-C.

Material

572 specimens from 32 samples at Kaos Gully locality (see Table 1).

Diagnosis

A multicostate coniform species of *Protopanderodus* consisting of a septimembrate apparatus including nongeniculate makellate M elements bearing a robust suberect cusp with a smooth and more convex anterior face and a costate

Figure 11. ***Protopanderodus liripipus*** **Kennedy, Barnes and Uyeno, 1979. a-e, M1 element; a, MMMC4839, KCY-5, posterior view (IY233-031); b, MMMC4840, KCY-5, posterior view (IY233-030); c, MMMC4841, KCY-5, posterior view (IY233-028); d, MMMC4842, KAOS-43.9, anterior view (IY244-017); e, MMMC4843, KCY-5, posterior view (IY233-026); f, M2 element; MMMC4844, KAOS-39.3, posterior view (IY244-009). g-j, Sa element; g-h, MMMC4845, KAOS-43.9, g, upper-posterior view (IY242-009), h, lateral view (IY242-010); i, MMMC4846, KAOS-43.9, lateral view (IY242-013); j, MMMC4847, KCY-5, lateral view (IY233-025). k-o, Sb element; k-m, MMMC4848, KCY-5, k, inner-lateral view (IY233-021), l, outer-lateral view (IY233-023), m, upper view, close-up showing cross section of cusp (IY233-019); n-o, MMMC4849, KCY-5, n, outer-lateral view (IY233-024), o, basal view (IY233-020). Scale bars 100 µm unless otherwise indicated.**

posterior face, and an outer-laterally extended base; multicostate S and P elements typically bearing two strong costae separated by a deep groove on each lateral side of the cusp and a long and distally tapering posteriorly-extended base; S elements forming a symmetry transition series from symmetrical Sa to asymmetrical Sb and Sc elements; P elements with a strongly developed antero-basal extension, which is triangular in outline in lateral view.

Description

The M elements (Fig. 11a-f) are nongeniculate, bearing a robust, outer-laterally more or less suberect cusp with sharp inner-lateral and outer-lateral margins, and an outer-laterally extended base with a wavy basal margin; they are antero-posteriorly compressed with an acostate and more convex anterior face, and a multicostate posterior face characterized by a prominent median groove between two costae (Fig. 11a-c, e-f). The costae and groove vary from weakly (Fig. 11a, c) to strongly developed (Fig. 11e). The posterior extension of the base varies from short (Fig. 11a) to relatively long and low (Fig. 11c-d, f). The M1 element has a gently rounded antero-basal corner (Fig. 11a-e), while the M2 element (Fig. 11f) has a basally extended, anticusp-like antero-basal extension.

The S elements are multicostate, bearing a robust, distally reclined cusp with two sharp costae separated by a deep groove on each lateral face, and a base with a long, distally tapering posterior extension and a short anticusp-like antero-basal extension. The median groove and its bordering costae on each lateral face are located slightly towards the posterior margin (Fig. 11m). The Sa element is symmetrical and biconvex bearing a basally suberect and distally reclined cusp with sharp anterior and posterior margins (Fig. 11g-j). The Sb element is similar to the Sa element, but asymmetrical with a more convex outer lateral face (Fig. 11k-o). The Sc element (Fig. 12a-e) is strongly asymmetrical with a longer posterior process and with the small anticusp-like antero-basal extension often slightly flexed inward (Fig. 12b).

The P elements are similar to S elements, but with a long anticusp-like antero-basal extension of the base (Fig. 12f-l). The Pa element has a more strongly reclined cusp with the angle of about 50-60^0 between the posterior margin of the cusp and the upper margin of the posterior extension of the base (Fig. 12f-i). The Pb element (Fig. 12j-l) has a suberect cusp, which is distally bowed inward (Fig. 12k), and a strongly extended antero-basal corner, which is triangular in outline in lateral view (Fig. 12j, l).

Discussion

Kennedy et al. (1979) established *P. liripipus* as consisting of a quadrimembrate apparatus including four elements, which are interpreted herein as representing the M (= scandodiform), Sa (=symmetrical), Sb (= slightly asymmetrical), and Sc (= markedly asymmetrical) elements. Kennedy et al. (1979, p. 547) described the markedly asymmetrical element as having "two costae on one side and one on the other". However, no comparable specimens of the Sc element were present in our collections, and therefore the markedly asymmetrical element described by Kennedy et al. (1979) is interpreted herein as representing an atypical variant. All Sc elements as defined herein from the Wairuna Formation limestones have two sharp costae separated by a deep groove on both lateral faces (Fig. 12a-e). One illustrated paratype (Kennedy et al. 1979, pl. 1, figs 10-11) exhibits a long base and an inwardly flexed antero-basal corner, and is more comparable with the Sc element defined and illustrated herein, but some specimens illustrated by Kennedy et al. (1979) as representing the slightly asymmetrical element (Kennedy et al. 1979, pl. 1, fig. 16) and markedly asymmetrical element (Kennedy et al. 1979, pl. 1, fig. 17) exhibited a shorter base and lacked the anticusp-like antero-basal extension developed in S elements in our collection. Zhen et al. (2011) suggested that material previously ascribed to *P. liripipus* from eastern Gondwana and peri-Gondwana exhibited a prominent anticusp-like antero-basal extension, and might represent a separate species. However, Kennedy et al. (1979) and McCracken (1989) included in the S elements of *P. liripipus* forms showing wider variations in respect to the number and position of the costae (as discussed above), length of the posterior extension of the base, and the development of the anticusp-like antero-basal extension. This wide variation among the type material was illustrated by the holotype and several paratypes (Kennedy et al. 1979, pl. 1, fig. 14, 16, 17) that appear to lack the anticusp-like antero-basal extension, compared to other paratypes (Kennedy et al. 1979, pl. 1, figs 9, 11, 13) that exhibit such an extension. Specimens of *P. liripipus* illustrated by McCracken (1989) from the northern Yukon Territory of Canada also included some with a prominent anticusp-like antero-basal extension (McCracken 1989, pl. 3, fig. 21), but most others display a more or less regularly curved basal margin in lateral view (McCracken1989, pl. 3, figs 15-16, 18, 22-24). Pa and Pb elements from the north Queensland samples are asymmetrical, characterized by having a strongly developed antero-basal extension (Fig. 12f-l), comparable with the P

Figure 12. ***Protopanderodus liripipus*** **Kennedy, Barnes and Uyeno, 1979. a-e, Sc element; a-c, MMMC4850, KCY-5, a, outer-lateral view (IY234-011), b, inner-lateral view (IY234-012), c, upper view (IY234-010); d, MMMC4851, KCY-5, outer-lateral view (IY234-009); e, MMMC4852, KCY-5, upper-posterior view (IY233-011). f-i, Pa element; f, MMMC4853, KCY-5, inner-lateral view (IY234-007); g, MMMC4854, KCY-5, outer-lateral view (IY234-006); h, MMMC4855, KCY-5, outer-lateral view (IY233-013); i, MMMC4856, KAOS-47.1, outer-lateral view (IY244-002). j-l, Pb element, MMMC4857, KAOS-45.6, j, inner-lateral view (IY238-019), k, anterior view (IY238-020), l, outer-lateral view (IY238-021). Scale bars 100 µm.**

elements recognized in *P. insculptus* (Fig. 10o), and also in the likely ancestor, *P. varicostatus* (see Zhen et al. 2011, fig. 22N-O, referred to as Sd but herein reinterpreted as a Pa element).

P. liripipus differs from *P. insculptus* in lacking a denticle, and is distinguished from *P. varicostatus* by having a longer, distally tapering posterior extension (S and P elements) and outer-lateral extension of the base (M element).

Genus SCABBARDELLA Orchard, 1980

Type species

Drepanodus altipes Henningsmoen, 1948 (amended by Orchard, 1980).

Scabbardella altipes (Henningsmoen, 1948) amend. Orchard, 1980
Figs 13-15

Synonymy

Drepanodus altipes Henningsmoen, 1948, p. 420, pl. 25, fig. 14 (drepanodiform = Sc element); Wang and Lou, 1984, p. 257, pl. 2, figs 3-4, 15, 17.

Scabbardella altipes (Henningsmoen); Orchard, 1980, p. 26, pl. 5, figs 2-5, 7-8, 12, 14, 18, 20, 23-24, 28, 30, 33, 35, text-fig. 4C (*cum syn*.); Nowlan, 1983, p. 668, pl. 1, figs 6-7, 11-14; Chen and Zhang, 1984, pl. 2, figs 29-30; Ni and Li, 1987, p. 437, pl. 55, figs 19-20, pl. 59, figs 21-22, 31-32; McCracken, 1987, pl. 2, figs 1-9, 11-13; Nowlan and McCracken, in Nowlan et al., 1988, p. 36, pl. 16, figs 7-20, pl. 17, figs 1-3, 5-6, 8-9 (*cum syn*.); Chen and Zhang, 1989, pl. 5, figs 8-9; non Rasmussen and Stouge, 1989, fig. 3M, P., Q; Bergström, 1990, pl.4, fig. 14; Pohler and Orchard, 1990, pl. 2, fig. 18; Gao, 1991, 137, pl. 12, fig. 18; Ferretti and Serpagli, 1991, pl. 2, figs 12-14; Leone et al., 1991, pl. 1, figs 14-15; Bergström and Massa, 1992, p. 1339, pl. 1, figs 1, 3, 4; Ding et al. in Wang, 1993, 199, pl. 12, figs 26-27; Dzik, 1994, pp. 64-66, pl. 11, figs 36-39, text-fig. 6e; Trotter and Webby, 1995, p. 487, pl. 3, figs 1-6, 8-11; Stouge and Rasmussen, 1996, p. 63, pl. 1, figs 1-6 (*cum syn*.); Wang et al., 1996, pl. 1, fig. 18; Ferretti and Barnes, 1997, p. 34, pl. 1, figs 17-22 (*cum syn*.); Nowlan et al., 1997, fig. 2.21-2.22; Wang and Zhou, 1998, pl. 2, fig. 3; Ferretti and Serpagli, 1999, pl. 2, figs 17-23; Leslie, 2000, fig. 3.36-3.37; Sweet, 2000, fig. 9.14-9.15; Zhao et al., 2000, p. 221-222, pl. 23, figs 10-12; Rasmussen, 2001, p. 130, pl. 17, figs 4-5; Talent et al., 2002, pl. 1, fig. P, ?fig. O; Agematsu et al., 2007, p. 29-30, fig. 11.4, 11.8-11.10, 11.12-11.17 (*cum syn*.); Zhang and Barnes, 2007a, p. 505, fig. 8.16-8.20; Agematsu et al., 2008, p. 969, fig. 10.25-10.34; Tolmacheva et al., 2009, pp. 1509-1510, fig. 6a-6e, 6h; Rodríguez-Cañero et al., 2010, fig. 5.9-5.12; Zhen et al., 2011, p. 252, fig. 9D-O (*cum syn*.); Wang, et al., 2011, p. 225, pl. 95, figs 6-12, pl. 179, figs 1-4; Ferretti et al., 2014a, fig. 13N-P; Ferretti et al., 2014b, fig. 3S-U; Bagnoli and Qi, 2014, pl. 4, figs 13-14; Bergström and Ferretti, 2015, fig. 1I-M.

Scabbardella sp. cf. *S. altipes* (Henningsmoen); Zhen et al., 1999, p. 94, figs 9.16-9.19, 10.1-10.9, 10.23.

Dapsilodus similaris (Rhodes); An, 1981, pl. 3, figs 4-5; An and Ding, 1982, pl. 1, figs 17-18; An et al., 1983, p. 91, pl. 15, fig. 22; An and Xu, 1984, pl. 1, figs 8, 15; An et al., 1985, pl. 11, figs 9-10, 13-14; Ding, 1987, pl. 5, fig. 23; Duan, 1990, pl. 3, figs 13-15.

Scabbardella similaris (Rhodes); An, 1987, pp. 179-180, pl. 5, figs 14-17, 19-24, 26-27; Ding et al. in Wang, 1993, p. 199, pl. 17, figs 22-28.

Material

836 specimens from 37 samples at Kaos Gully locality and seven specimens from sample CWZ-2 at Gray Creek bank locality (see Table 1).

Diagnosis

A species of *Scabbardella* consisting of a seximembrate apparatus, including drepanodiform long-based M1 and short-based M2 elements with smooth lateral faces, distacodiform long-based Sa and short-based Sd elements with a broad carina or a prominent costa bordering a deep and narrow groove on each lateral side, and acodiform long-based Sb and short-based Sc elements with a smooth inner-lateral face and a broad carina or a prominent costa bordering a deep and narrow groove on the outer-lateral face; all elements laterally compressed and nongeniculate, bearing a procline to suberect cusp with sharp anterior and posterior margins and a base triangular in outline with a non-flared basal cavity of moderate depth.

Description

The drepanodiform M elements (Fig. 13a-j) are weakly asymmetrical, laterally strongly compressed with sharp anterior and posterior margins, and biconvex, typically with outer-lateral face slightly more convex (Fig. 13h). The lateral faces are smooth and broadly rounded, often more sharply thinning towards posterior margin to form a narrow and thin posterior edge (Fig. 13a-d, f, i-j), and more or less spade-like in cross section (Fig. 13d, h). The surface is ornamented with fine striae (Fig. 13e). The M1 element has a long base that is antero-posteriorly less extended (Fig. 13a-e), while the M2 has a short base that is more extended antero-posteriorly (Fig. 13f-j).

The distacodiform Sa element (Fig. 14g-i) is symmetrical or nearly symmetrical and laterally strongly compressed, bearing a suberect cusp with sharp anterior and posterior margins and a long base. The lateral faces have a deep and narrow groove located more towards the posterior margin and a broadly rounded median carina (Fig. 14h-i).

The distacodiform Sd element (Fig. 14j-m) is slightly asymmetrical and laterally strongly compressed, bearing a suberect cusp with sharp

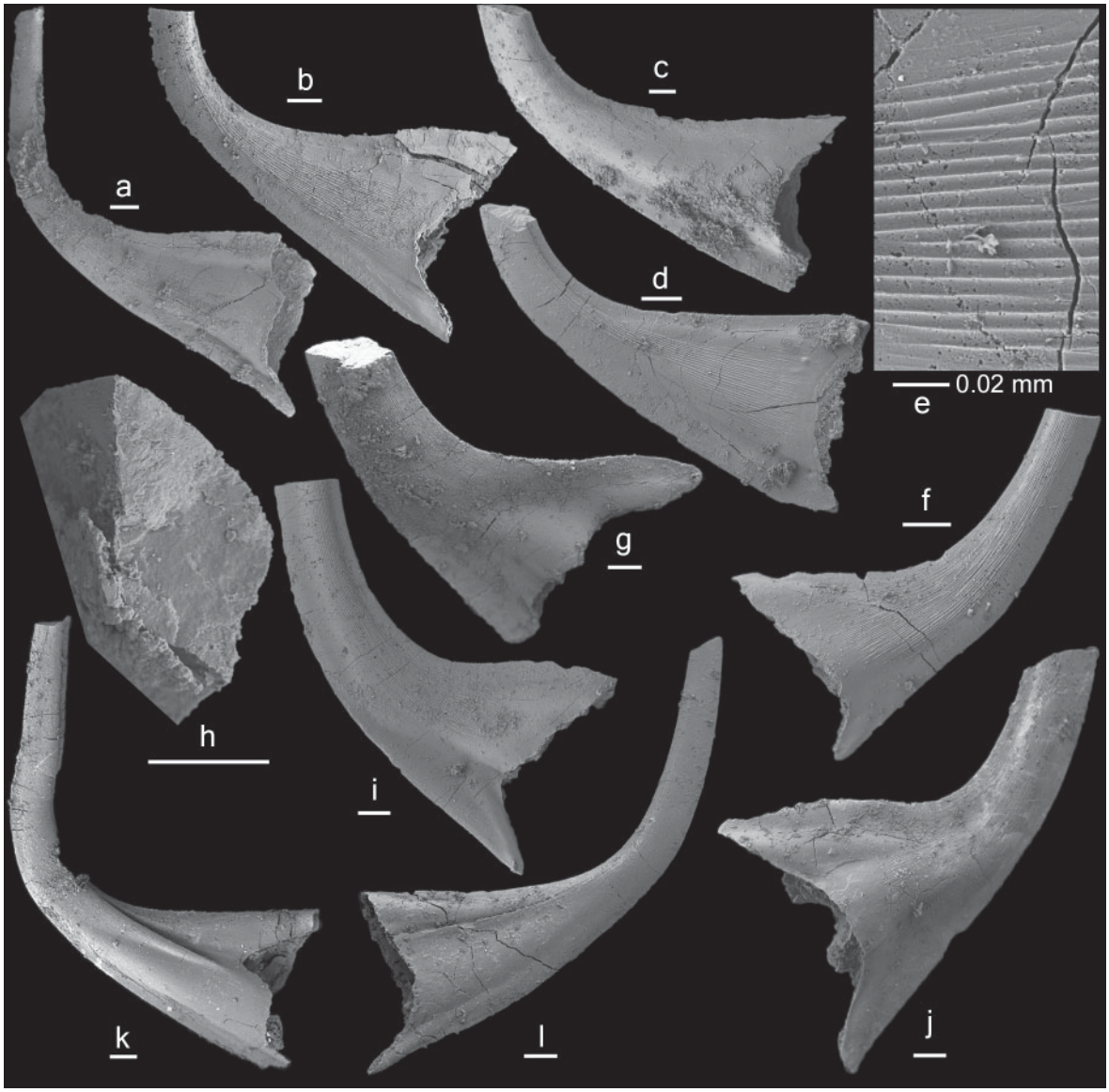

Figure 13. ***Scabbardella altipes*** **(Henningsmoen, 1948). a-e, M1 (long-based drepanodiform) element; a, MMMC4868, KAOS-47.5, inner-lateral view (IY239-006); b, MMMC4869, KAOS-47.5, outer-lateral view (IY239-005); c, MMMC4870, KCY-5, outer-lateral view (IY235-018); d-e, MMMC4871, KCY-5, d, inner-lateral view (IY235-019), e, close up showing surface striation (IY235-020). f-j, M2 (short-based drepanodiform) element; f, MMMC4872, KCY-5, outer-lateral view (IY236-032); g-h, MMMC4873, KCY-5, g, inner-lateral view (IY236-033), h, close-up showing cross section of cusp (IY236-034); i, MMMC4874, KCY-5, inner-lateral view (IY236-010); j, MMMC4875, KCY-5, outer-lateral view (IY236-015). k-l, Sb (long-based acodiform) element; k, MMMC4876, KAOS-41.6, outer-lateral view (IY240-009); l, MMMC4877, KAOS-43.9, outer-lateral view (IY241-005). Scale bars 100 µm unless otherwise indicated.**

anterior and posterior margins and a short and antero-posteriorly more extended base. The lateral faces have a sharp costa located more towards the posterior margin (Fig. 14m), and a deep and narrow groove bordering the posterior side of the costa (Fig. 14j). The cusp has a more convex outer-lateral face and is diamond-shaped in cross section (Fig. 14m). The costa on the lateral faces is more strongly developed around the curvature of the cusp and extends onto the base, but not to the basal margin.

The acodiform Sb element (Figs 13k-l, 15a-f) is asymmetrical and laterally strongly compressed,

Figure 14. ***Scabbardella altipes*** **(Henningsmoen, 1948). a-f, Sc (short-based acodiform) element; a-b, MMMC4878, KCY-5, a, basal view (IY236-035), b, outer-lateral view (IY236-036); c, MMMC4879, KAOS-41.6, inner-lateral view (IY240-002); d, MMMC4880, KCY-5, outer-lateral view (IY236-020); e, MMMC4881, KAOS-41.6, basal view (IY240-004); f, MMMC4882, KCY-5, outer-lateral view (IY236-019). g-i, Sa (long-based distacodiform) element; g, MMMC4883, KAOS-43.9, lateral view (IY244-015); h, MMMC4884, KAOS-48.2, lateral view (IY239-010); i, MMMC4885, KAOS-48.2, lateral view (IY239-009). j-m, Sd (short-based distacodiform) element; j, MMMC4886, KCY-5, outer-lateral view (IY236-024); k-m, MMMC4887, KCY-5, k, inner-lateral view (IY236-031), l, outer-lateral view (IY236-030), m, upper view, close-up showing cross section of cusp (IY236-029). Scale bars 100 µm unless otherwise indicated.**

Figure 15. ***Scabbardella altipes*** **(Henningsmoen, 1948). a-f, Sb (long-based acodiform) element; a, MMMC4888, KCY-5, outer-lateral view (IY235-026); b, MMMC4889, KCY-5, outer-lateral view (IY235-024); c, f, MMMC4890, KCY-5, c, basal view (IY235-022), f, outer-lateral view (IY235-021); d, MMMC4891, KCY-5, outer-lateral view (IY235-027); e, MMMC4892, KCY-5, inner-lateral view (IY235-025). g-j, Sc (short-based acodiform) element; g-h, MMMC4893, KAOS-43.9, g, outer-lateral view (IY242-014), h, showing regrowth (pathological repair) of distal part of cusp (IY242-015); i, MMMC4894, KAOS-41.6, inner-lateral view (IY240-008); j, MMMC4895, KAOS-41.6, outer-lateral view (IY240-001). k-l, Sc (medium-based acodiform) element; k, MMMC4896, KCY-5, inner-lateral view (IY236-009); l, MMMC4897, KCY-5, inner-lateral view (IY236-008). Scale bars 100 µm.**

bearing a proclined to suberect cusp with sharp anterior and posterior margins and a long base. The inner-lateral face is less convex and smooth (Fig. 15e), and the outer-lateral face is more convex, with a deep, narrow groove located more towards the posterior margin and a broadly rounded median carina to its anterior side (Figs 13k-l, 15f).

The acodiform Sc element (Figs 14a-f, 15k-l) is asymmetrical and laterally strongly compressed, bearing a suberect or distally reclined cusp with sharp anterior and posterior margins and a short and antero-posteriorly more extended base. The inner-lateral face has a broadly rounded carina (Figs 14c, 15i), and the outer-lateral face is more convex, with a deep and narrow groove located more towards the posterior margin and a broadly rounded median carina to its anterior side (Figs 14b, d, 15j). One specimen (Fig. 15g-h) shows the regrowth of a broken or damaged

distal end of the cusp, demonstrating the capacity of the conodont animal to self-repair damaged parts of the elements.

All elements display well preserved fine surface striae, and also show the gradational change from long-based M1, Sa and Sb elements to short-based M2, Sd and Sc elements respectively (Fig. 15k-l).

Discussion

Scabbardella altipes was originally erected as a form species represented by a drepanodiform element (Henningsmoen 1948, pl. 25, fig. 14) from the Fjacka Shale (*P. linearis* Zone, Katian, Late Ordovician) of Sweden. It was later revised by Orchard (1980) as consisting of six morphotypes including two drepanodiform, two acodiform and two distacodiform elements. Orchard (1980, figs 1, 4) also considered these elements to represent the 'M', 'Sc-Sb' and 'Sa' positions respectively. Following the multielement species concept of Orchard (1980), *S. altipes* is here recognized as consisting of a seximembrate apparatus including long-based drepanodiform (= M1), short-based drepanodiform (= M2), long-based distacodiform (= Sa), short-based distacodiform (= Sd), long-based acodiform (= Sb), and short-based acodiform (= Sc) elements. Although Zhen et al. (2011) acknowledged the existence of a medium-based acodiform element, the abundant material of this species from the Wairuna Formation of north Queensland demonstrates that medium length forms exist in all elements of the species, which vary from long-based to short-based.

Orchard (1980) identified two subspecies representing populations from north England (*S. altipes* subsp. A) and from north Wales (*S. altipes* subsp. B), mainly based on differences of curvature of the cusp and the extension of the base. However, our material shows a wide variation in respect of these two features. Therefore we recognize only a single species *S. altipes* rather than subspecies (e.g. Trotter and Webby 1995) or even two separate species as suggested by some other authors (e.g. Stouge and Rasmussen, 1996).

Distacodiform elements (Sa and Sd) of this species are superficially similar to the S elements of both *Besselodus* (also co-occurring in the Wairuna Formation fauna) and *Dapsilodus*, but can be easily distinguished from those genera. In the collections from Queensland, specimens of *S. altipes* are generally larger in size in comparison with co-occurring *Besselodus fusus* and also *Molloydenticulus bicostatus*. More importantly *S. altipes* differs in having a very different species apparatus, which also includes drepanodiform M, and acodiform Sb and Sc elements. Furthermore, although specimens of *S. altipes* from the Wairuna Formation exhibit well-developed fine surface striae, apparently no distinctive oblique striations such as those characterizing *Besselodus fusus* were developed along the anterior margins of the S elements of *S. altipes*.

Genus STRACHANOGNATHUS Rhodes, 1955

Type species

Strachanognathus parvus Rhodes, 1955.

Strachanognathus parvus Rhodes, 1955
Fig. 16a-g

Synonymy

Strachanognathus parvus Rhodes, 1955, p. 132, pl. 7, fig. 16, pl. 8, figs 1-4 text-fig. 5; Bergström, 1962, pp. 54-55, pl. 3, figs 1-6, text-figs 2B, 3H-I; Serpagli, 1967, p. 99, pl. 29, figs 4a-5c; Löfgren, 1978, p. 112, pl. 1, fig. 29 (*cum syn.*); Palmieri, 1978, p. 27, pl. 6, figs 27-28, text-fig. 6 (8a-8c); Kennedy, Barnes and Uyeno, 1979, p. 550, pl. 1, fig. 24 (*cum syn.*); Orchard, 1980, p. 26, pl. 14, figs 34-35; Nowlan, 1981, pl. 3, fig. 18, pl. 5, fig. 5; Lenz and McCracken, 1982, p. 1318, pl. 2, fig. 21; Lin et al., 1984, pl. 2, fig. 16; Sarmiento, 1990, pl. 5, fig. 4; Bergström, 1990, pl. 1, fig. 10; Pohler and Orchard, 1990, pl. 1, fig. 6; McCracken, 1991, p. 52, pl. 2, fig. 36 (*cum syn.*); Dzik, 1994, pp. 62-63, pl. 13, figs 1-6, text-fig. 5; Pohler, 1994, pl. 8, fig.3; Trotter and Webby, 1995, p. 487, pl. 4, figs 24-26; Armstrong, 1997, pp. 790-791, pl. 5, figs 1-3, ?4-5; Nowlan et al., 1997, fig. 2.24; Furey-Greig, 1999, p. 311, pl. 3, fig. 16; Armstrong, 2000, pl. 5, figs 6-12, ?13-16; Zhao et al., 2000, p. 226, pl. 26, figs 19, 24 (*cum syn.*); Leslie, 2000, fig. 3.35; McCracken, 2000, pl. 3, fig. 19; Sweet, 2000, fig. 9.11; Talent et al., 2002, pl. 1, figs Q-R; Löfgren, 2000, fig. 4ab; Löfgren, 2003, fig. 8AA; Löfgren, 2004, fig. 7r; Wang et al., 2011, p. 245, pl. 107, figs 18-19; Bergström and Ferretti, 2015, fig. 10AB-AD.

Material

20 specimens from three samples at Kaos Gully locality (see Table 1).

Discussion

Strachanognathus parvus has a distinctive morphology characterized by a strongly laterally compressed robust cusp with sharp anterior and

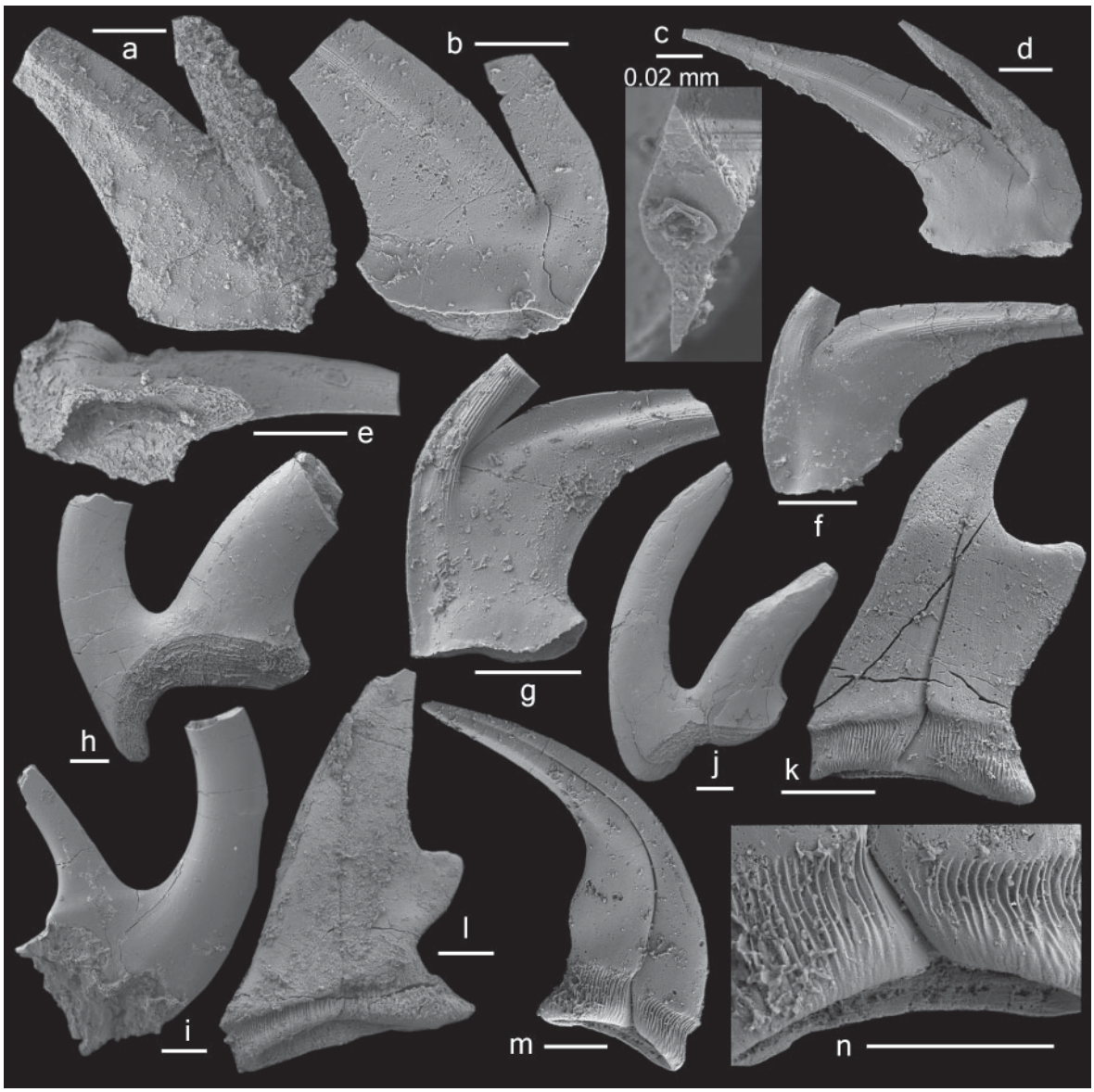

Figure 16. a-g, *Strachanognathus parvus* Rhodes, 1955. a-e, proclined, short-based element; a, MMMC4898, KAOS-43.9, outer-lateral view (IY241-021); b, MMMC4899, KAOS-43.9, inner-lateral view (IY241-016); c, MMMC4900, KAOS-43.9, upper view, close-up showing cross section of cusp (IY241-025); d, MMMC4901, KAOS-43.9, outer-lateral view (IY242-006); e, MMMC4902, KAOS-43.9, basal view (IY241-029). f, suberect, short-based element, MMMC4903, KAOS-43.9, outer-lateral view (IY241-027); g, suberect, long-based element, MMMC4904, KAOS-43.9, inner-lateral view (IY241-026). h-j, *Spinodus spinatus* (Hadding, 1913). h-i, Sb element; h, MMMC4905, KAOS-50.5, inner-lateral view (IY242-021); i, MMMC4906, KAOS-46.8, inner-lateral view (IY238-022). j, Sc element, MMMC4907, KAOS-50.5, outer-lateral view (IY242-022). k-n, *Taoqupognathus tumidus* Trotter and Webby, 1995. k, Sb3 element, MMMC4908, KAOS-43.9, outer-lateral view (IY242-018); l, Sc3 element, MMMC4909, KAOS-43.9, outer-lateral view (IY242-018); m-n, Sc2 element, MMMC4910, KCY-5, M, outer-lateral view (IY233-001), n, close-up showing coarse striation near basal margin and panderodid furrow (IY233-002). Scale bars 100 µm unless otherwise indicated.

posterior margins, and a short anterior process represented by a single denticle (Fig. 16a-g). It was originally erected as a form species represented by a single element, but the illustrated types from north Wales include short-based (Rhodes 1955, pl. 7, fig. 16, pl. 8, fig.3) to long-based elements (Rhodes 1955, pl. 8, fig.4), and the curvature of the cusp varies from suberect with anterior margin of the cusp more or less normal to the basal margin (Rhodes 1955, text-fig. 5) to procline with the gently curved anterior margin of the cusp smoothly merging into the base (Rhodes 1955, pl. 8, figs 1-2). Therefore at least three (or possibly four) morphotypes can be differentiated among the type material. Based on abundant material of this species from erratic limestone boulders of the Tvären area of southeastern Sweden, Bergström (1962, pp. 54-55) also recognized three morphotypes as illustrated by the types, and indicated that they "only represented stages in a long, continuous series of variations, so that it seemed impossible to draw sharp limits between different types". Specimens representing these three types are also present in our collections from north Queensland, and are referred to herein as a procline, short-based element (Fig. 16a-e), a less common suberect, short-based element (Fig. 16f) and a suberect, long-based element (Fig. 16g).

Armstrong (1997) proposed a quinquimembrate apparatus for *S. parvus* by including two (symmetrical and asymmetrical) coniform elements, which were generally accepted as part of *Parapanderodus* species apparatus. However, these striate coniform elements were not recovered from the allochthonous limestones within the Wairuna Formation of Queensland.

Strachanognathus parvus was pandemic and had a relatively long range extending from the Darriwilian to late Katian. In eastern Australia, it has been only reported from the *T. tumidus* Biozone, such as from allochthonous limestone clasts in the lower part of the Malongulli Formation (Trotter and Webby 1995), from allochthonous limestones in the Wisemans Arm Formation (Furey-Greig 1999) of New South Wales, from the Fork Lagoons beds (Palmieri 1978) and allochthonous limestones within the Wairuna Formation of Queensland (Talent et al. 2002; and this study).

Genus TAOQUPOGNATHUS An, 1985

Type species

Taoqupognathus blandus An, 1985.

Discussion

Three species belonging to this genus are recorded from eastern Gondwana and peri-Gondwana, including eastern Australia, South China, North China and the Tarim Basin. Zhen (2001) indicated that it had a distribution restricted to the Australasian Superprovince. However, Nowlan (2002, p. 195, p. 2, figs 25-26, 29-31, 36-37) reported a species referred to as *Taoqupognathus* sp. nov. A, represented by 16 specimens from Late Ordovician subsurface core material of Alberta, Canada. As noted by Nowlan (2002), although the slender M element is comparable to the corresponding element of *T. philipi*, this North American species (consisting of slender elements without posterior extension) is significantly different from the three known Australasian species, which have a prominent lobe-like posterior extension. If more detailed study can confirm that this North American species belongs to *Taoqupognathus*, it may represent the morphologically most primitive species among the known representatives of this genus. McCracken (2000, p. 194, pl. 1, fig. 28) also illustrated a single specimen referred to *Taoqupognathus philipi* from the Upper Ordovician of the Foxe Basin of Baffin Island.

Taoqupognathus tumidus Trotter and Webby, 1995
Fig. 16k-n

Synonymy

Drepanodus? *altipes*? Palmieri, 1978, pl. 2, figs 24, 25.

gen. unident. Pickett, 1978, cover photo, fig. 4.

?*Belodina beiguoshanensis* Yu and Wang, 1986, p. 100, pl. 1, figs 6, 9-11.

Belodina cf. *B. blandus* (An); Duan, 1990, p. 31, pl. 5, fig. 7.

Taoqupognathus tumidus Trotter and Webby, 1995, pp. 487-488, pl. 7, figs 10-24; Zhen et al., 1999, p. 96, fig. 14.1-14.9; Percival, 1999, fig. 3.1-3.2, 3.5; Packham et al., 1999, fig. 3.14-3.16; Furey-Greig, 1999, p. 312, pl. 4, figs 1-9; Zhao et al., 2000, pp. 226-227, pl. 26, figs 1-6, 10-13, 17-18, ?15-16; Furey-Greig, 2000a, p. 94, fig. 6B-H; Talent et al., 2003, pl. 1, fig. 12; Zhen et al., 2003, pp. 43-45, fig. 7K; Wang et al., 2011, p. 247-248, pl. 108, figs 5-11.

Taoqupognathus ani Wang and Zhou, 1998, p. 190, pl. 3, fig. 4.

Material

Four specimens from two samples at Kaos Gully locality (see Table 1).

Discussion

Taoqupognathus tumidus is a morphologically distinctive species, known only from the middle

Katian (Ka2-3; see Fig. 3) in eastern Australia and in the three major Chinese blocks (North China, South China and Tarim plates; see Zhen 2001). In eastern Australia, it is widely reported from allochthonous limestone clasts, such as within the Sofala Volcanics (Pickett 1978; Percival 1999), in the lower part of the Malongulli Formation (Trotter and Webby 1995), in limestone breccias in the basal part of the Malachis Hill Formation overlying the Bowan Park Limestone Subgroup (Zhen et al. 1999), from allochthonous limestones in the Barnby Hills Shale (Zhen et al. 2003), from a limestone body (?allochthonous) within the Forest Reefs Volcanics exposed adjacent to Sheahan-Grants minesite (subsequently destroyed by mining activities; Packham et al. 1999) at Junction Reefs in central NSW, from allochthonous limestones in the Wisemans Arm Formation (Furey-Greig 1999) of the New England Orogen in northeastern NSW, from the Fork Lagoons beds of central-east Queensland (Palmieri 1978), and from allochthonous limestones within the Wairuna Formation of the Broken River region, north Queensland (Talent et al. 2003; this study). *T. tumidus* also occurs in association with *P. insculptus* in the Downderry Limestone Member at the top of the Bowan Park Limestone Subgroup (Zhen et al. 1999), which is autochthonous limestone interpreted as representing shelf edge deposits.

Belodina beiguoshanensis Yu and Wang, 1986 was considered by Wang et al. (2011, p. 247) as a junior synonym of *Taoqupognathus blandus* An, 1985. However, Zhen (2001) suggested that it was morphologically closely related to *Taoqupognathus tumidus*, but with a more stout and short outline in lateral view, and might be either a senior synonym of the latter representing its end member (a subspecies representing the most advanced forms) or a separate species derived from the latter. It has been treated herein as a doubtful senior synonym of *T. tumidus* pending further detailed study of this species from the upper Beiguoshan Formation (middle Katian) in the Ordos Basin of North China. This designation is also supported by the recognition of several elements assignable to typical *T. tumidus* from a sample at the top of the Taoqupo Formation exposed near Yaoxian in the Ordos Basin of North China (Zhen et al. 2003).

BRACHIOPODS (Percival)

Almost all brachiopod taxa encountered in the fauna from the Kaos Gully section in north Queensland are being described elsewhere from more abundant material obtained from the Malongulli Formation and correlative units in NSW; accordingly the brachiopods are documented herein merely by brief taxonomic notes and illustrations. For brevity, authors of Family/Subfamily level taxonomic hierarchy and above are not cited in the References, as these are readily obtainable from the *Treatise on Invertebrate Paleontology* (Williams et al. 2000).

Subphylum Linguliformea Williams, Carlson, Brunton, Holmer and Popov, 1996
Class Lingulata Goryansky and Popov, 1985
Order Lingulida Waagen, 1885
Superfamily Linguloidea Menke, 1828
Family Obolidae King, 1846
Subfamily Elliptoglossinae Popov and Holmer, 1994

Genus ELLIPTOGLOSSA Cooper, 1956
Elliptoglossa adela Percival, 1978 (Fig. 17a-d)

Figure 17 (next page). a-d, *Elliptoglossa adela* Percival, 1978. a, interior view of incomplete dorsal? valve, MMMC4911, KAOS-50.4, (PI CWL-3041); b, interior view of incomplete ventral valve, MMMC4912, KAOS-50.4, (PI CWL-3040); c, fragment of posterior end of ventral? valve interior, MMMC4913, KAOS-50.4, (PI CWL-3042); d, interior view of incomplete ventral valve, MMMC4914, KAOS-49.8, (PI CWL-3035). e-g, indeterminate lingulide. e, interior view of incomplete ventral valve, MMMC4915, KAOS-42.8, (PI CWL-3011); f, fragment of ventral valve pseudointerarea showing pedicle groove, MMMC4916, KCY-5, (PI CWL-1012); g, interior view of incomplete dorsal valve, MMMC4917, KCY-5, (PI CWL-1011). h, *Paterula malongulliensis* Percival, 1978, interior view of dorsal valve, MMMC4918, KAOS-47.5, (PI CWL-3030); accompanying scale bar is 500 µm. i-k, n, *Glossella* sp. i, exterior view of incomplete valve showing smooth post-larval shell flanked by shell ornamented by concentric rows of fine elongate tubercles separated by pits, MMMC4919, KCY-5, (PI CWL-2024). j, fragment of shell exterior, and k, enlargement of lower right side of j to show rows of elongate tubercles, some having the appearance of hollow spines, MMMC4920, KCY-5, (PI CWL-1008, PI CWL-1009 respectively); scale bar for k is 100 µm. n, fragment of shell exterior displaying more widely-separated tubercles, presumably from a more anterior position on the valve, MMMC4921, KAOS-44.8, (PI CWL-3028). l, fragment of shell exterior cf. *Westonia*, MMMC4922, KCY-5, (PI CWL-1006). m, fragment of shell exterior cf. *Dictyonina*, MMMC4923, KCY-5, (PI CWL-1010). Unless otherwise indicated, scale bars represent 1 mm; scale bar to right of specimen e relates to specimens a, b, c, d, e, f and g; scale bar beneath specimen i relates to specimens i, j and l; scale bar between specimens m and n relates only to those two specimens.

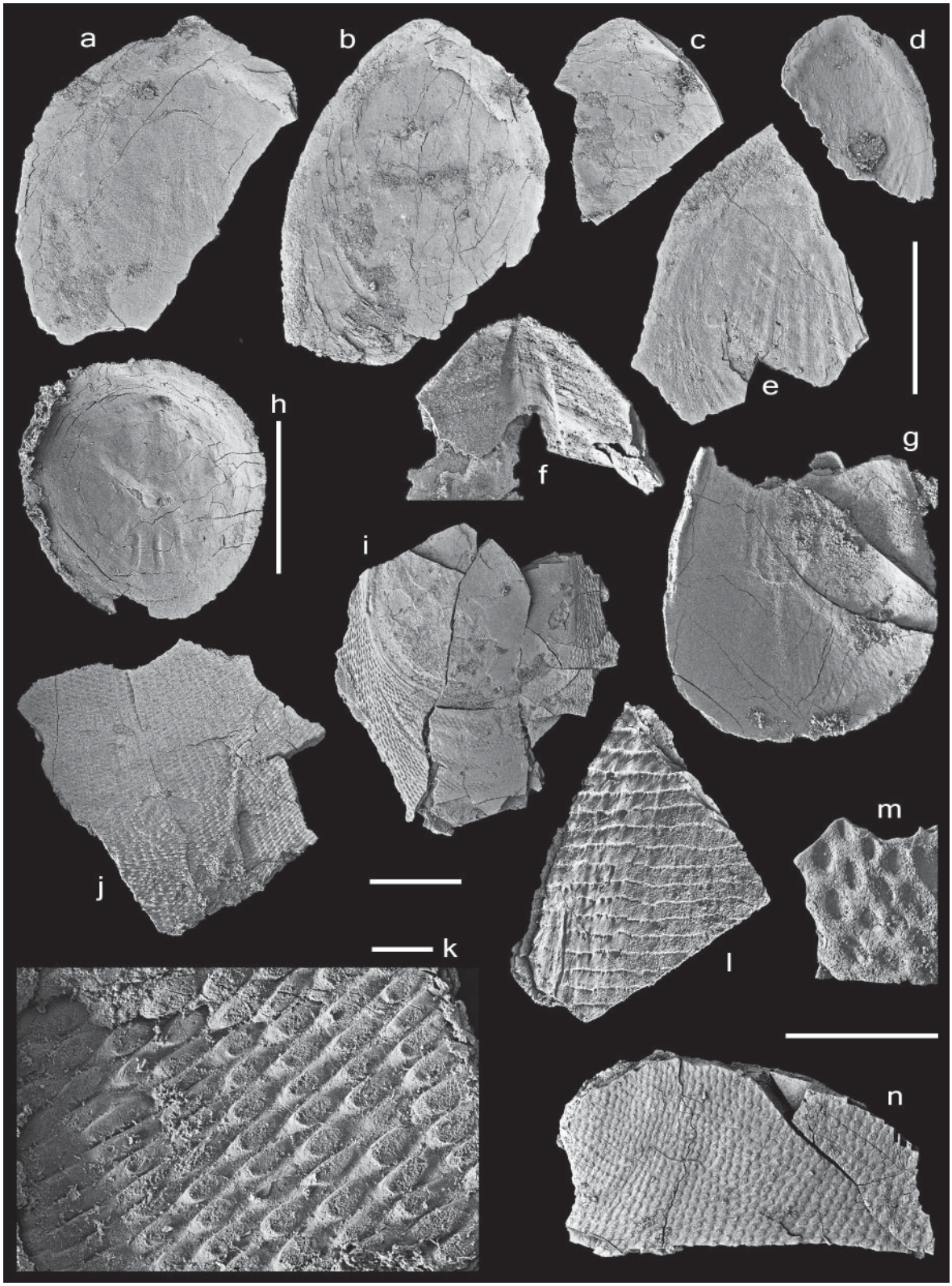
a
b
c
d
e
f
g
h
i
j
k
l
m
n

Remarks

The type material of this species was described from internal and external moulds preserved in graptolitic siltstone and spiculite of the Malongulli Formation in central NSW. The isolated valves from the Kaos Gully limestone are at the lower end of the observed range in length and width for *E. adela* measured by Percival (1978). Since the length/width ratio is comparable in both suites and morphological details (or obscurity thereof) are identical, these specimens are confidently identified as *E. adela*.

Distribution

KAOS 49.8, 50.4

Subfamily Obolinae King, 1846

Genus ATANSORIA Popov, 2000 (Fig. 18a-c)

Remarks

Atansoria was first described by Popov (2000) from the Mayatas Formation of Katian age, in the Atansor Lake region of north-central Kazakhstan, solely on the basis of its distinctive dorsal valve. Likewise, no ventral valves were identified in the Carriers Well material, and it is postulated that *Atansoria* was cemented to the substrate by that valve. The dorsal valve is concave, with a large ovoid to diamond-shaped visceral field bounded by strong ridges. *Atansoria* from north Queensland is identical to the new species recognized from the Macquarie Volcanic Province of New South Wales, which differs from the type (and only other known) species *A. concava* Popov, 2000 in exhibiting concentric growth rings, whereas *A. concava* is smooth externally. Furthermore, *A. concava* possesses a far more prominent median septum in the dorsal valve than does the Australian species.

Distribution

KCY-5, KAOS 43.9

Unidentified lingulide

Remarks

Three illustrated fragments (Fig. 17e-g) of comparable size are regarded as conspecific and representative of a lingulide that is restricted in distribution to just two levels in the section. The well-developed pedicle groove is flanked by moderately long propareas (Fig. 17f). Three low divergent ridges extend through the ventral visceral field to about mid length (Fig. 17e). The presumed associated dorsal valve (Fig. 17g) has a suboval visceral field terminating at about mid length and is marked by several indistinct muscle scars and surrounded by low ridges; a faint median ridge extends well into the anterior part of the valve.

Distribution

KCY-5, KAOS 42.8

Genus WESTONIA Walcott, 1901 (Fig. 17l)

Remarks

A fragment tentatively referred to *Westonia*? displays an ornament of terrace lines typical of (but not unique to) this genus. No other material similar to this was found in the residues from the Kaos Gully section.

Distribution

KCY-5

Subfamily Glossellinae Cooper, 1956

Genus GLOSSELLA Cooper, 1956 (Fig. 17i-k, n)

Remarks

Specimens referred to *Glossella* sp. are recognizable by their papillose ornament on the flanks and anterior of the valves. All material is fragmentary, and no useful interior details are known. Thick-shelled fragments with a similar ornament are plentiful in acid-resistant residues from the lower Malongulli Formation of the Macquarie Volcanic Province in central NSW.

Distribution

KCY-5; KAOS 44.8

Family Paterulidae Cooper, 1956

Genus PATERULA Barrande, 1879
Paterula malongulliensis Percival, 1978 (Fig. 17h)

Remarks

The sole dorsal valve was recovered from the limestone at Carriers Well is identical to the type specimens of this species, described from the Malongulli Formation in NSW, in having an undivided umbonal muscle scar.

Distribution

KAOS 47.5

Superfamily Discinoidea Gray, 1840
Family Discinidae Gray, 1840

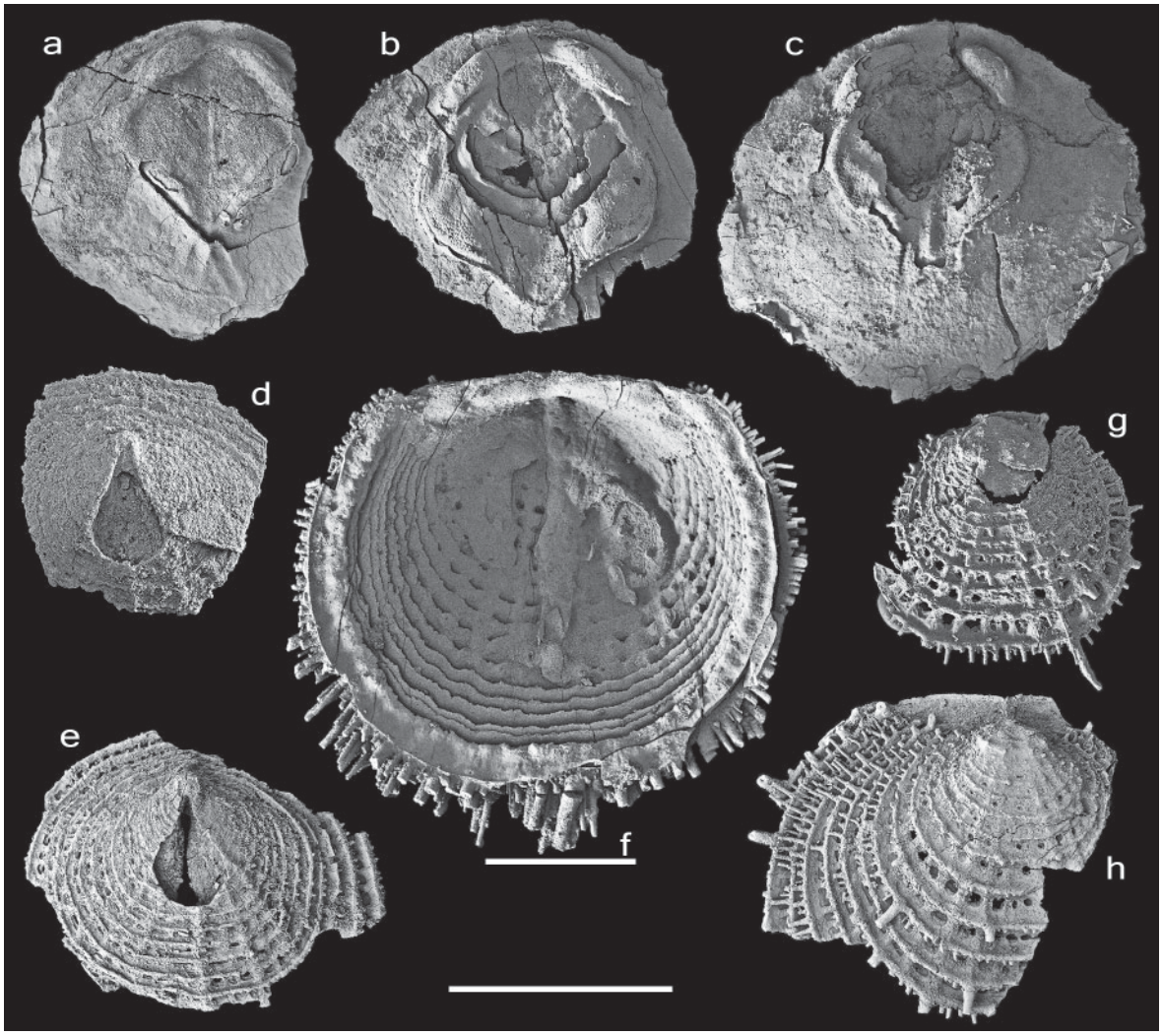

Figure 18. a-c, *Atansoria* sp. nov. a, interior view of incomplete dorsal valve, MMMC4924, KAOS-43.9, (PI CWL-3014); b, interior view of incomplete dorsal valve, MMMC4925, KCY-5, (PI CWL-1002); c, interior view of dorsal valve, MMMC4926, KCY-5, (PI CWL-1001). d-h, *Nushbiella* sp. nov. d, exterior view of incomplete ventral valve, MMMC4927, KCY-5, (PI CWL-1004); e, exterior view of incomplete ventral valve, MMMC4928, KAOS-42.8, (PI CWL-3012); f, interior view of dorsal valve, MMMC4929, KCY-5, (PI CWL-1007); g, exterior view of dorsal valve, MMMC4930, KCY-5, (PI CWL-1003); h, exterior view of incomplete dorsal valve, MMMC4931, KAOS-41.6, (PI CWL-3005). Scale bar (1 mm) beneath f relates only to that specimen; scale bar (1 mm) for all other specimens is at lower centre of figure.

Genus ACROSACCUS Willard, 1928 (Fig. 19a-e)

Remarks

Acrosaccus is the most common linguliformean brachiopod encountered in acid-resistant residues of the limestone from the Kaos Gully section, where it is mostly found as fragments, recognizable by their ornament of strong concentric ridges. Among the more complete specimens, only dorsal valves have been recovered (Fig. 19a-d). One shell (Fig. 19d, e) revealed a previously unrecognised ornament of fine regular micropitting.

These specimens from north Queensland exhibit the same trend as observed in those from central NSW (being described as a new species) where the dorsal apex migrates during ontogeny from a submarginal (e.g. Fig. 19d) to a subcentral position. An intermediate point on this journey is shown in Fig. 19c, illustrating a specimen that is not yet fully grown in comparison to those from the Malongulli Formation and Downderry Limestone Member of the Ballingoole Limestone of the Macquarie Volcanic Province.

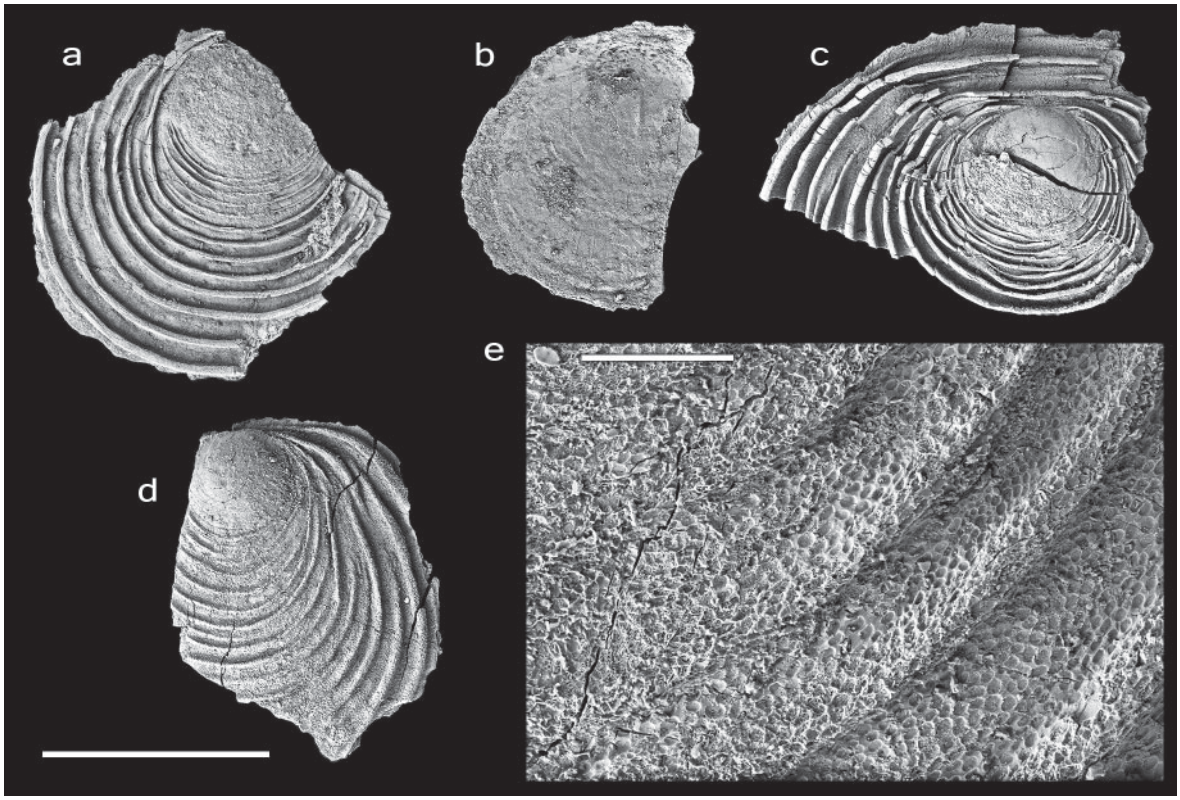

Figure 19. a-e, *Acrosaccus* sp. nov. a, exterior view of incomplete dorsal valve, MMMC4932, KAOS-42.2, (PI CWL-3010); b, interior view of incomplete dorsal valve, MMMC4933, KAOS-43.9, (PI CWL-3018); c, exterior view of incomplete dorsal valve, MMMC4934, KAOS-47.5, (PI CWL-3029); d, exterior view of incomplete dorsal valve, and e, enlargement of micropitting on surface of post-larval shell, MMMC4935, KAOS-43.9, (PI CWL-3016 and PI CWL-3017 respectively). Scale bar (1 mm) beneath in lower left corner relates to specimens a-d; scale bar within e is 100 µm.

Distribution

KAOS 42.2, 43.9, 47.5

Order Siphonotretida Kuhn, 1949
Superfamily Siphonotretoidea Kutorga, 1848
Family Siphonotretidae Kutorga, 1848

Genus NUSHBIELLA Popov in Kolobova and Popov, 1986 (Fig. 18d-h)

Remarks

Spinose exterior fragments of *Nushbiella* are readily apparent in the acid-resistant residues from Carriers Well, though complete specimens (e.g. Fig. 18f) are rare. Ventral valves are characterised by a large pedicle foramen that may be partly or entirely closed anteriorly by two plates growing inwards from the sides of the aperture (Fig. 18d, e), exactly as is shown by specimens from central NSW. The radial ornament, which in some other species of *Nushbiella* – including the type species *N. dubia* (Popov, 1977) – is relatively prominent on the dorsal valve, is much more subdued (even absent) in the Carriers Well specimens (Fig. 18g, h).

Distribution

KCY-5; KAOS 41.6, 42.8

Order Acrotretida Kuhn, 1949
Superfamily Acrotretoidea Schuchert, 1893
Family Acrotretidae Schuchert, 1893

Genus CONOTRETA Walcott, 1889 (Fig. 20a-e)

Remarks

Both valves of this species generally resemble those of *Conotreta*? *mica* described by Holmer (1989) from Västergötland and Dalarna, Sweden, but a conservative approach to the identification is taken in view of the relatively few specimens available from the Kaos Gully section and so this material is referred here to *Conotreta* sp. Dorsal valves of the Swedish specimens have a median septum bearing up to three

anterior spines or denticles, whereas those from the Carriers Well limestone display two (Fig. 20d).

Distribution

KCY-5; KAOS 44.8, 50.4

Genus HISINGERELLA Henningsmoen in Waern et al., 1948

Hisingerella hetera (Percival, 1978) (Fig. 20f-o)

Remarks

Ventral valves of this species (originally described from spiculitic siltstones of the lower Malongulli Formation of central NSW) are common in the Carriers Well residues, dorsal valves much less so. Specimens are smaller and more delicate than those assigned to *Conotreta* sp., but there are other morphological differences confirming that the distinction between the two is not indicative merely of juvenile and gerontic individuals of the one taxon. For example, some ventral valves of *H. hetera* display a weak but distinct interridge crossing the pseudointerarea (Fig. 20h) which is not present in *Conotreta* sp. Similarities in shell construction, such as the presence of twin spines on the anterior edge of the median septum (constructed in both species of concentric layers of bacular lamellae, shown in Fig. 20d for *Conotreta* sp., and Fig. 20j for *H. hetera*) demonstrate the close phylogenetic relationship of these acrotretides.

Distribution

KCY-5; KAOS 43.9, 44.8

Family Scaphelasmatidae Rowell, 1965

Genus SCAPHELASMA Cooper, 1956 (Fig. 21a, b)

Remarks

The species depicted in Fig. 21a-b has a distinctive transversely oval to subquadrate outline and its ventral valve is deeper, more rounded and inflated than is typical for *Scaphelasma*. The presence of a well-developed apical process in front of the internal foramen (Fig. 21b) is reminiscent of *Scaphelasma scutula* Popov, Nõlvak and Holmer, 1994, which has also been recognized in several formations of late Katian age in the Macquarie Volcanic Province of central NSW.

Distribution

KCY-5; KAOS 39.3

Family Biernatidae Holmer, 1989

Genus BIERNATIA Holmer, 1989 (Fig. 21c-e)

Remarks

The species of *Biernatia* in the Carriers Well limestone is characterized by a high, strongly apsacline ventral valve with the intertrough barely visible (Fig. 21c) and two distinct sizes of pitting developed on the larval shell (Fig. 21d) – larger flat-bottomed pits surrounded by multiple micropits. The dorsal valve (Fig. 21e) has a very short, narrow pseudointerarea, prominent cardinal muscle scars, and a relatively short, flat-topped, anteriorly-expanding surmounting plate supported by the median septum. Of the two

Figure 20 (next page). a-e, *Conotreta* sp. a, exterior view of incomplete ventral valve, MMMC4936, KCY-5, (PI CWL-2023); b, interior view of incomplete ventral valve, MMMC4937, KCY-5, (PI CWL-2001); c, fragment of dorsal valve interior, showing pseudointerarea and median septum, and d, enlargement of broken anterior end of median septum displaying concentric layers forming cross sections of two spines, MMMC4938, KAOS-44.8, (PI CWL-3022 and PI CWL-3023 respectively); e, interior view of incomplete dorsal valve, MMMC4939, KAOS-50.4, (PI CWL-3039). f-o, *Hisingerella hetera* (Percival, 1978). f, exterior of ventral valve in plan view with posterior margin uppermost, MMMC4940, KCY-5, (PI CWL-2012); g, oblique interior view of ventral valve, MMMC4941, KCY-5, (PI CWL-2005); h, oblique posterior view of ventral valve pseudointerarea showing weakly defined interridge, MMMC4942, KCY-5, (PI CWL-2007); i, fragment of dorsal valve interior, showing median septum, and j, enlargement of broken anterior end of median septum displaying concentric layers forming cross sections of two spines (lowermost cut off against edge of image), MMMC4943, KAOS-43.9, (PI CWL-3019 and PI CWL-3020 respectively); k, oblique interior view of ventral valve, MMMC4944, KAOS-44.8, (PI CWL-3024); l, exterior of incomplete ventral valve in plan view with posterior margin uppermost, MMMC4945, KCY-5, (PI CWL-2002); m, oblique interior view of ventral valve, MMMC4946, KCY-5, (PI CWL-2006); n, exterior of incomplete ventral valve in plan view with posterior margin at lower right, and o, enlargement of margin of pedicle foramen to show micropitting on larval shell, MMMC4947, KAOS-44.8, (PI CWL-3025 and PI CWL-3027 respectively). Scale bar (1 mm) in lower left corner relates to all specimens except j and o which have their own 10 µm scale bars, and d with a 20 µm scale bar.

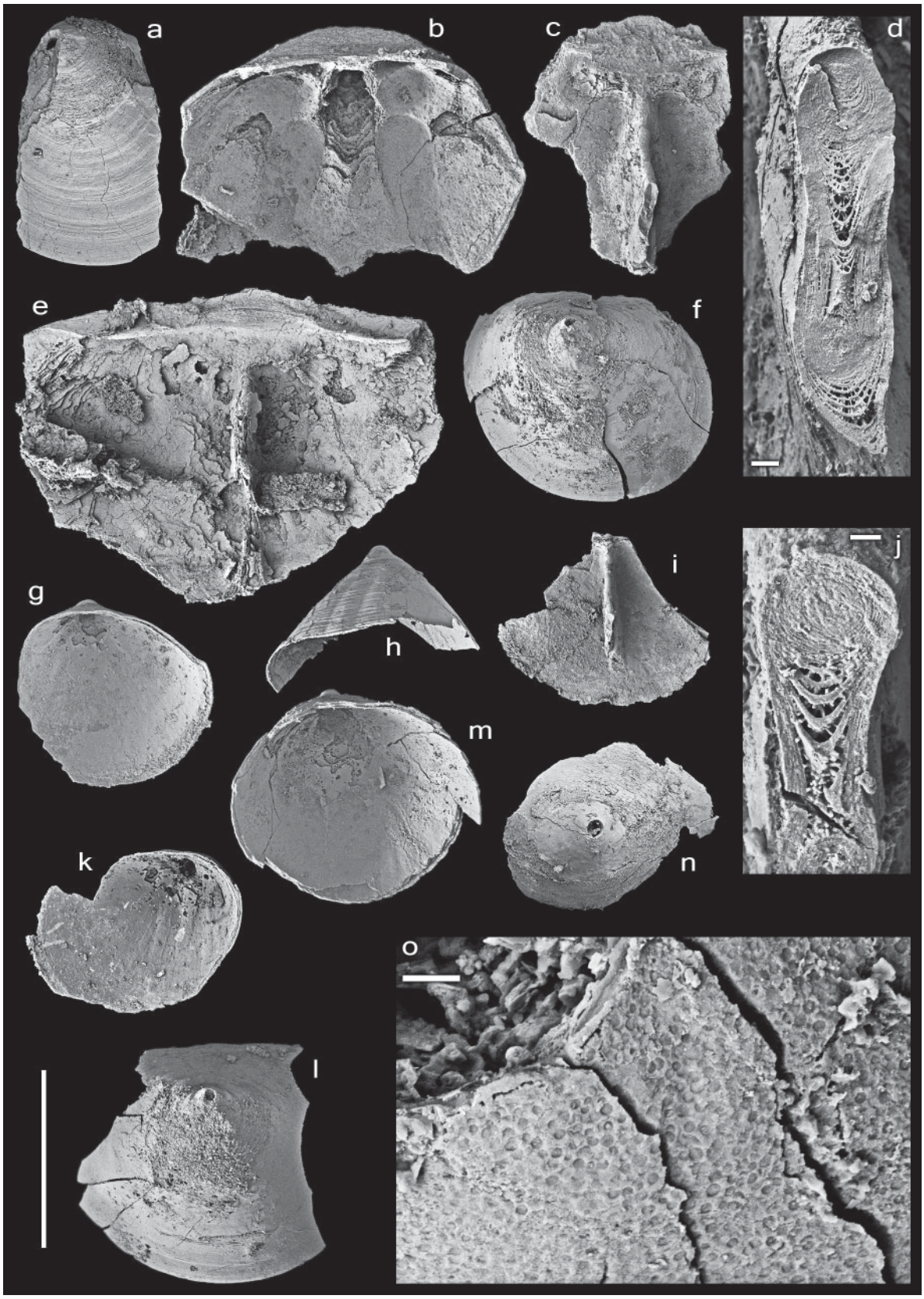
a
b
c
d
e
f
g
h
i
j
k
l
m
n
o

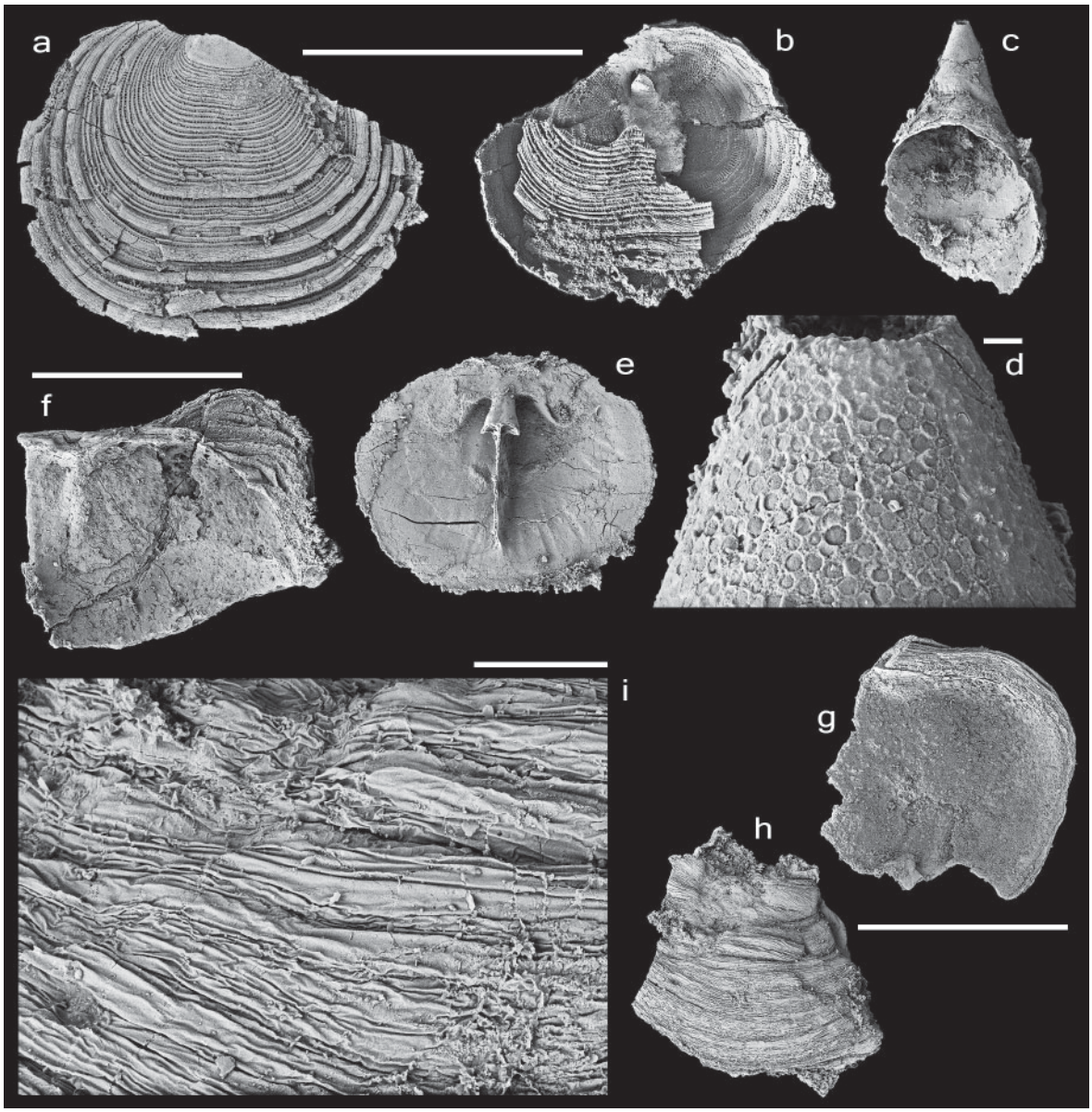

Figure 21. a, b, *Scaphelasma* sp. nov. a, exterior view of incomplete dorsal valve, MMMC4948, KCY-5, (PI CWL-2019); b, view of incomplete conjoined valves from dorsal side, showing apical process in interior of ventral valve, MMMC4949, KAOS-39.3, (PI CWL-3004). c-e, *Biernatia* sp. nov., c, oblique view of ventral valve from dorsal perspective, and d, enlargement of larval shell showing micropitting of two distinct sizes, MMMC4950, KAOS-48.2, (PI CWL 3032 and PI CWL 3033); e, interior view of dorsal valve showing surmounting plate on median septum, MMMC4951, KAOS-48.2, (PI CWL 3031); f-i, *Undiferina* sp. f, interior view of incomplete dorsal valve showing short pseudointerarea and weak median septum, MMMC4952, KAOS-43.9, (PI CWL-3013); g, interior view of incomplete dorsal valve, MMMC4953, KCY-5, (PI CWL-2018); h, fragment of valve exterior, and i, enlargement to show irregular banded ornament, MMMC4954, KAOS-49.8, (PI CWL 3037 and PI CWL 3038 respectively). Scale bar (1 mm) for a, b, c, e is situated at top of figure; scale bar (1 mm) for f is above the latter; scale bar (1 mm) for g and h is in lower right corner of figure; scale bars for enlargements are immediately adjacent to d (10 µm) and i (100 µm).

new species (as yet undescribed) of *Biernatia* that are present in the Malongulli Formation and correlative units of the Macquarie Volcanic Province in NSW, the Carriers Well form is almost certainly conspecific with that having the more suboval outline.

Distribution
KAOS 48.2

Family Eoconulidae Rowell, 1965

Genus UNDIFERINA Cooper, 1956 (Fig. 21f-i)

Remarks
The few available specimens (Fig. 21f-h), although confined to incomplete dorsal valves, display the distinctive ornament of this genus characterised by irregular, wavy distortions (Fig. 21i). They appear to be close to, if not identical with, material from the Malongulli Formation and Downderry Limestone Member at the top of the Ballingoole Limestone in central NSW, that in turn resembles the type species *U. rugosa* Cooper, 1956 from the Pratt Ferry Formation of Alabama, of slightly older latest Middle Ordovician to earliest Late Ordovician age.

Distribution
KCY-5; KAOS 43.9, 49.8

Class Paterinata Williams, Carlson, Brunton, Holmer and Popov, 1996
Order Paterinida Rowell, 1965
Superfamily Paterinoidea Schuchert, 1893
Family Paterinidae Schuchert, 1893

Genus DICTYONINA Cooper, 1942 (Fig. 17m)

Remarks
Identification of this fragment as *Dictyonina*? is necessarily tentative, although the presence of large pits through the shell material suggests this is a reasonable choice.

Distribution
KCY-5

ACKNOWLEDGMENTS

We express our gratitude to John Talent and Ruth Mawson for introducing us to the Broken River region, and for providing samples for us to work on. Field work in Queensland by Zhen in 2010 was supported by a grant from the Betty Mayne Scientific Research Fund of the Linnean Society of New South Wales. B. Webby, A. Cook and R. Jones are thanked for their assistance during the field trip. Paul Meszaros (Geological Survey of New South Wales) assisted with acid leaching and residue separation. Scanning electron microscope photographs were prepared in the Electron Microscope Unit of the Australian Museum. We thank Barry Webby and an anonymous referee for their perceptive and constructive reviews of the manuscript. The study is a contribution to IGCP Project 591: The Early to Middle Paleozoic Revolution. Zhen and Percival publish with permission of the Executive Director, Geological Survey of New South Wales.

REFERENCES

Agematsu, S., Sashida, K. and Ibrahim, B. (2008). Biostratigraphy and Paleobiogeography of Middle and Late Ordovician Conodonts from the Langkawi Islands, Northwestern Peninsular Malaysia. *Journal of Paleontology* **82**, 957-973.

Agematsu, S., Sashida, K., Salyapongse, S. and Sardsud, A. (2007). Ordovician conodonts from the Satun area, southern Peninsular Thailand. *Journal of Paleontology* **81**, 19-37.

Aldridge, R.J. (1982). A fused cluster of coniform conodont elements from the Late Ordovician of Washington Land, western North Greenland. *Palaeontology* **25**, 425-430.

An, T.X. (1981). Recent progress in Cambrian and Ordovician conodont biostratigraphy of China. *Geological Society of America Special Paper* **187**, 209-226.

An, T.X. (1987). 'Early Paleozoic conodonts from South China'. 238 pp. (Peking University Publishing House: Beijing). (in Chinese with English abstract).

An, T.X. and Ding, L.S. (1982). Preliminary studies and correlations on Ordovician conodonts from the Ningzhen Mountains, China. *Acta Petroleum Sinica* **3** (4), 1-11. (in Chinese).

An, T.X., Du, G.Q. and Gao, Q.Q. (1985). 'Ordovician conodonts from Hubei'. 64 pp. (Geological Publishing House: Beijing). (in Chinese with English abstract).

An, T.X., Du, G.Q., Gao, Q.Q., Chen, X.B. and Li, W.T. (1981). Ordovician conodont biostratigraphy of the Huanghuachang area of Yichang, Hubei. In 'Selected Papers of the First Symposium of the Micropalaeontological Society of China' (Ed. Micropalaeontological Society of China), pp. 105-113 (Science Press: Beijing). (in Chinese).

An, T.X. and Xu, B.Z. (1984). Ordovician System and conodonts of Tungshan and Xianning, Hubei. *Acta Scientiarum Naturalium Universitatis Pekinensis* **5**, 73-87. (in Chinese with English abstract).

An, T.X., Zhang, F., Xiang, W.D., Zhang, Y.Q., Xu, W.H., Zhang, H.J., Jiang, D.B., Yang, C.S., Lin, L.D., Cui,

Z.T. and Yang, X.C. (1983). 'The conodonts in North China and adjacent regions'. 223 pp. (Science Press: Beijing). (in Chinese with English abstract).

An, T.X. and Zheng, S.C. (1990). 'The conodonts of the marginal areas around the Ordos Basin, North China'. 199 pp. (Science Press: Beijing). (in Chinese with English abstract).

Armstrong, H.A. (1997). Conodonts from the Ordovician Shinnel Formation, southern Uplands, Scotland. *Palaeontology* **40**, 763-797.

Armstrong, H.A. (2000). Conodont micropalaeontology of mid-Ordovician aged limestone clasts from Lower Old Red Sandstone conglomerates, Lanark and Strathmore basins, Midland Valley, Scotland. *Journal of Micropalaeontology* **19**, 45-59.

Bagnoli, G. and Qi, Y.P. (2014). Ordovician conodonts from the Red Petrified Forest, Hunan Province, China. *Bollettino della Società Paleontologica Italiana* **53** (2), 93-104.

Barrande, J. (1879). 'Systême Silurien du Centre de la Bohême. Ière Partie. Recherches Paléontologiques, vol. 5. Classe des Mollusques: Ordre des Brachiopodes'. 226 pp., 153 pls. (Published by the author: Paris).

Barnes, C.R. (1967). A questionable conodont assemblage from Middle Ordovician limestones, Ottawa, Canada. *Journal of Paleontology* **41**, 1557-1560.

Bergström, S.M. (1962). Conodonts from the Ludibundus Limestone (Middle Ordovician) of the Tvären area (S.E. Sweden). *Arkiv för Geologi och Mineralogi* **3** (1), 1-61.

Bergström, S.M. (1990). Biostratigraphic and biogeographic significance of Middle and Upper Ordovician conodonts in the Girvan succession, south-west Scotland. *Courier Forschungsinstitut Senckenberg* **118**, 1-43.

Bergström, S.M. and Bergström, J. (1996). The Ordovician-Silurian boundary successions in Östergötland and Västergötland, S. Sweden. *GFF* **118**, 25-42.

Bergström, S.M. and Massa, D. (1992). Stratigraphic and biogeographic significance of Upper Ordovician conodonts from northwestern Libya. In 'The Geology of Libya' (eds M.J. Salem, O.S. Hammuda and B.A. Eliagoubi) 4, 1323-1342.

Bergström, S.M., Chen, X., Gutiérrez-Marco, J.C. and Dronov, A. (2009). The new chronostratigraphic classification of the Ordovician System and its relations to major regional series and stages and to δ13C chemostratigraphy. *Lethaia* **42**, 97–107.

Bergström, S.M. and Ferretti, A. (2015). Conodonts in the Upper Ordovician Keisley Limestone of northern England: taxonomy, biostratigraphical significance and biogeographical relationships. *Papers in Palaeontology* **1** (1), 1-32 (published online 2014). http://dx.doi.org /10.1002/spp2.1003.

Bergström, S.M. and Sweet, W.C. (1966). Conodonts from the Lexington Limestone (Middle Ordovician) of Kentucky and its lateral equivalents in Ohio and Indiana. *Bulletin of American Paleontology* **50** (229), 271-441.

Branson, E.B. and Mehl, M.G. (1933). Conodont studies. *University of Missouri Studies* **8**, 1-349.

Brime, C., Talent, J.A. and Mawson, R. (2003). Low-grade metamorphism in the Palaeozoic sequences of the Townsville hinterland, northeastern Australia. *Australian Journal of Earth Sciences* **50** (5), 751-767.

Burrett, C.F., Stait, B.A. and Laurie, J. (1983). Trilobites and microfossils from the Middle Ordovician of Surprise Bay, southern Tasmania, Australia. *Memoir of the Australian Association of Palaeontologists* **1**, 177-193.

Chen, M.J. and Zhang, J.H. (1984). Middle Ordovician conodonts from Tangshan, Nanjing. Acta *Micropalaeontologica Sinica* **1**, 120-137. (in Chinese with English abstract).

Chen, M.J. and Zhang, J.H. (1989). Ordovician conodonts from the Shitai region, Anhui. *Acta Micropalaeontologica Sinica* **6** (3), 213-228. (in Chinese with English abstract).

Chen, X., Bergström, S.M., Zhang, Y.D. and Wang, Z.H. (2013). A regional tectonic event of Katian (Late Ordovician) age across three major blocks of China. *Chinese Science Bulletin* **58** (34), 4292-4299.

Clark, D.L., Sweet, W.C., Bergström, S.M., Klapper, G., Austin, R.L., Rhodes, F.H.T., Müller, K.J., Ziegler, W., Lindström, M., Miller, J.F. and Harris, A.G. (1981). Conodonta. In 'Treatise on Invertebrate Paleontology, part W, Miscellanea, supplement 2'. (Ed. R.A. Robison). 202 pp. (The Geological Society of America: Boulder, and the University of Kansas: Lawrence).

Cooper, G.A. (1942). New genera of North American brachiopods. *Washington Academy of Sciences, Journal* **32** (8), 228-235.

Cooper, G.A. (1956). Chazyan and related brachiopods. *Smithsonian Miscellaneous Collections* **127**, 1-1245.

Cooper, B.J. (1976). Multielement conodonts from the St. Clair Limestone (Silurian) of southern Illinois. *Journal of Paleontology* **50** (2), 205-217.

Ding, L.S. (1987). Preliminary probes into Ordovician conodont biostratigraphy from the Kunshan area, Jiangsu, China. In 'Symposium on petroleum stratigraphy and palaeontology (1987)', pp. 41-53, pp. 375-380. (Geological Publishing House: Beijing). (in Chinese with English abstract).

Dixon, O.A. and Jell, J.S. (2012). Heliolitine tabulate corals from Late Ordovician and possibly early Silurian allochthonous limestones in the Broken River Province, Queensland, Australia. *Alcheringa* **36** (1), 69-98.

Duan, J.Y. (1990). Ordovician conodonts from northern Jiangsu and indices of their colour alteration. *Acta Micropalaeontologica Sinica* **7** (1), 19-41. (in Chinese with English abstract).

Dumoulin, J.A., Harris, A.G. and Repetski, J.E. (2014). Carbonate rocks of the Seward Peninsula, Alaska:

Their correlation and paleogeographic significance. *Geological Society of America, Special Paper* **506**, 59-110.

Dzik, J. (1976). Remarks on the evolution of Ordovician conodonts. *Acta Palaeontologica Polonica* **21**, 395-455.

Dzik, J. (1994). Conodonts of the Mójcza Limestone. In 'Ordovician carbonate platform ecosystem of the Holy Cross Mountains' (eds J. Dzik, E. Olempska, and A. Pisera). *Palaeontologia Polonica* **53**, 43-128.

Epstein, A., Epstein, J.B. and Harris, L.D. (1977). Conodont color alteration: an index to organic metamorphism. *Geological Survey Professional Paper* **995**, 1-27.

Ethington, R.L. (1959). Conodonts of the Ordovician Galena Formation. *Journal of Paleontology* **33**, 257-292.

Fåhræus, L.E. (1966). Lower Viruan (Middle Ordovician) conodonts from the Gullhögen Quarry, Southern Central Sweden. *Sveriges Geologiska Undersökning C* **610**, 1-40.

Ferretti, A. (1998). Late Ordovician conodonts from the Prague Basin, Bohemia. In Proceedings of the Sixth European Conodont Symposium (ECOS VI) (ed. H. Szaniawski), *Palaeontologia Polonica* **58**, 123-139.

Ferretti, A. and Barnes, C.R. (1997). Upper Ordovician conodonts from the Kalkbank Limestone of Thuringia, Germany. *Palaeontology* **40**, 15-42.

Ferretti, A., Bergström, S.M. and Barnes, C.R. (2014a). Katian (Upper Ordovician) conodonts from Wales. *Palaeontology* **57** (4), 801-831.

Ferretti, A., Messori, A. and Bergström, S.M. (2014b). Composition and significance of the Katian (Upper Ordovician) conodont fauna of the Vaux Limestone ('Calcaire des Vaux') in Normandy, France. *Estonian Journal of Earth Sciences* **63** (4), 214-219.

Ferretti A., Bergström S.M. and Sevastopulo, G.D. (2014c). Katian conodonts from the Portrane Limestone: the first Ordovician conodont fauna described from Ireland. *Bollettino della Società Paleontologica Italiana* **53** (2), 1-15.

Ferretti, A. and Serpagli, E. (1991). First record of Ordovician conodonts from southwestern Sardinia. *Revista Italia Paleontologia et Stratigraphia* **97**, 27-34.

Ferretti, A. and Serpagli, E. (1999). Late Ordovician conodont faunas from southern Sardinia, Italy: biostratigraphic and paleogeographic implications. *Bollettino della Società Paleontologia Italiana* **37**, 215-236.

Fowler, T.J. and Iwata, K. (1995). Darriwilian-Gisbornian conodonts from the Triangle Group, Triangle Creek area, New South Wales. *Australian Journal of Earth Sciences* **42** (2), 119-122.

Furey-Greig, T.M. (1999). Late Ordovician conodonts from the olistostromal Wisemans Arm Formation (New England Region, Australia). *Abhandlungen der Geologischen Bundesanstalt* **54**, 303–321.

Furey-Greig, T.M. (2000a). Late Ordovician and Early Silurian conodonts from the "Uralba Beds", northern New South Wales. *Alcheringa* **24**, 83-97.

Furey-Greig, T.M. (2000b). Late Ordovician (Eastonian) conodonts from the Early Devonian Drik Drik Formation, Woolomin area, eastern Australia. *Records of the Western Australian Museum Supplement* **58**, 133-143.

Gao, Q.Q. (1991). Conodonts. In 'Sinian to Permian stratigraphy and Palaeontology of the Tarim Basin II, Keping-Bachu area' (Ed. Xinjiang Petroleum Administration Bureau and the Jianghan Petroleum Administration Bureau), pp. 125-149. (Petroleum Industry Press: Beijing). (in Chinese with English abstract).

Glen, R.A. (2005). The Tasmanides of Eastern Australia. In 'Terrane Processes at the Margins of Gondwana' (Eds A. Vaughan, P. Leat and R. Pankhurst). *Geological Society of London Special Publication* **246**, 23-96.

Glen, R.A. (2013). Refining accretionary orogen models for the Tasmanides of eastern Australia. *Australian Journal of Earth Sciences* **60**, 315-370.

Goldman, D., Leslie, S.A., Nõlvak, J., Young, S., Bergström, S.M. and Huff, W.D. (2007). The Global Stratotype Section and Point (GSSP) for the base of the Katian Stage of the Upper Ordovician Series at Black Knob Ridge, Southeastern Oklahoma, USA. *Episodes* **30** (4), 258-270.

Hadding, A.R. (1913). Undre dicellograptusskiffern i Skåne jämte några dågra därmed ekvivalenta bildningar. *Lunds Universitets Årsskrift, Ny Följd, Afdelning 2* **9** (15), 1-90.

Harris, A.G., Bergström, S.M., Ethington, R.L. and Ross, R.J. jr. (1979). Aspects of Middle and Upper Ordovician conodont biostratigraphy of carbonate facies in Nevada and southeast California and comparison with some Appalachian successions. *Brigham Young University Geology Studies* **2** (3), 7-44.

Henderson, R.A., Innes, B.M., Fergusson, C.L., Crawford, A.J. and Withnall, I.W. (2011). Collisional accretion of a Late Ordovician oceanic island arc, northern Tasman Orogenic Zone, Australia. *Australian Journal of Earth Sciences* **58**, 1-19.

Henderson, R.A., Donchak, P.J.T. and Withnall, I.W. (2013). Chapter 4: Mossman Orogen. In 'Geology of Queensland' (Ed. P.A. Jell), pp. 225-304. (Geological Survey of Queensland: Brisbane).

Henningsmoen, G. (1948). The Tretaspis Series of the Kullatorp Core, pp. 374-432. In Waern, B., Thorslund, P. and Henningsmoen, G. Deep boring through Ordovician and Silurian strata at Kinnekulle, Vastergötland. *Bulletin of the Geological Institutions of the University of Uppsala* **32**, 337-474.

Holmer, L.E. (1989). Middle Ordovician phosphatic inarticulate brachiopods from Västergötland and Dalarna, Sweden. *Fossils and Strata* **26**, 1-172.

Jenkins, C.J. (1978). Llandovery and Wenlock stratigraphy of the Panuara area, central New South Wales. *Proceedings of the Linnean Society of New South Wales* **102**, 109-130.

Kaljo, D., Hints, L., Männik, P. and Nõlvak, J. (2008). The succession of Hirnantian events based on data from Baltica: brachiopods, chitinozoans, conodonts, and carbon isotopes. *Estonian Journal of Earth Sciences* **57** (4), 197-218.

Kaljo, D., Männik, P., Martma, T. and Nõlvak, J. (2012). More about the Ordovician–Silurian transition beds at Mirny Creek, Omulev Mountains, NE Russia: carbon isotopes and conodonts. *Estonian Journal of Earth Sciences* **61** (4), 277-294.

Kennedy, D.J., Barnes, C.R. and Uyeno, T.T. (1979). A middle Ordovician faunule from the Tetagouche Group, Camel Back Mountain, New Brunswick. *Canadian Journal of Earth Sciences* **16**, 540-551.

Kolobova, I.M. and Popov, L.E. (1986). K paleontologitscheskoi kharakteristike anderkenskogo gorizonta srednego ordovika v Chu-Iliyskikh Gorakh (Juzhnyi Kazakhstan). *Ezhegodnik Vsesoyuznogo Paleontologicheskogo Obshchestva* **29**, 246-261. (in Russian).

Lenz, A.C. and McCracken, A.D. (1982). The Ordovician-Silurian boundary, northern Canadian Cordillera: graptolite and conodont correlation. *Canadian Journal of Earth Sciences* **19**, 1308-1322.

Leone, F., Hammann, W., Laske, R., Serpagli, E. and Villas, E. (1991). Lithostratigraphic units and biostratigraphy of the post-sardic Ordovician sequence in south-west Sardinia. *Bollettino della Societa Paleontologica Italiana* **30** (2), 201-235.

Leslie, S.A. (1997). Apparatus architecture of *Belodina* (Conodonta): Interpretations based on fused clusters of *Belodina compressa* (Branson and Mehl, 1933) from the Middle Ordovician (Turinian) Plattin Limestone of Missouri and Iowa. *Journal of Paleontology* **71**, 921-926.

Leslie, S.A. (2000). Mohawkian (Upper Ordovician) conodonts of eastern North America and Baltoscandia. *Journal of Paleontology* **74**, 1122-1147.

Lin, B.Y., Qiu, H.R. and Xu, C.C. (1984). New observations of Ordovician strata in Shetai District of Urad Front Banner, Nei Mongol (Inner Mongolia). *Geological Review* **30**, 95-105. (in Chinese with English abstract).

Lindström, M. (1955). Conodonts from the lowermost Ordovician strata of south-central Sweden. *Geologiska Föreningen i Stockholm Förhandlingar* **76**, 517-604.

Lindström, M. (1971). Lower Ordovician conodonts of Europe. In 'Symposium on conodont biostratigraphy' (Eds W.C. Sweet and S.M. Bergström). *Geological Society of America, Memoir* **127**, 21-61.

Löfgren, A. (1978). Arenigian and Llanvirnian conodonts from Jämtland, northern Sweden. *Fossils and Strata* **13**, 1-129.

Löfgren, A. (2000). Conodont biozonation in the upper Arenig of Sweden. *Geological Magazine* **137** (1), 53-65.

Löfgren, A. (2003). Conodont faunas with *Lenodus variabilis* in the upper Arenigian to lower Llanvirnian of Sweden. *Acta Palaeontologica Polonica* **48**, 417-436.

Löfgren, A. (2004). The conodont fauna in the Middle Ordovician *Eoplacognathus pseudoplanus* Zone of Baltoscandia. *Geological Magazine* **141**, 505-24.

Männik, P. and Viira, V. (2012). Ordovician conodont diversity in the northern Baltic. *Estonian Journal of Earth Sciences* **61** (1), 1-14.

McCracken, A.D. (1987). Description and correlation of Late Ordovician conodonts from the *D. ornatus* and *P. pacificus* graptolite zones, Road River Group, northern Yukon Territory. *Canadian Journal of Earth Sciences* **24**, 1450-1464.

McCracken, A.D. (1989). *Protopanderodus* (Conodontata) from the Ordovician Road River Group, Northern Yukon Territory, and the evolution of the genus. *Geological Survey of Canada Bulletin* **388**, 1-39.

McCracken, A.D. (1991). Middle Ordovician conodonts from the Cordilleran Road River Group, northern Yukon Territory, Canada. In 'Ordovician to Triassic conodont paleontology of the Canadian Cordillera' (Eds M.J. Orchard and A.D. McCracken). *Geological Survey of Canada, Bulletin* **417**, 41-63.

McCracken, A.D. (2000). Middle and Late Ordovician conodonts from the Foxe Lowland of southern Baffin Island, Nunavut. In 'Geology and paleontology of the southeast Arctic Platform and southern Baffin Island' (Eds A.D. McCracken and T.E. Bolton). *Geological Survey of Canada, Bulletin* **557**, 159-216.

McCracken, A.D. and Nowlan, G.S. (1989). Conodont paleontology and biostratigraphy of Ordovician carbonates and petroliferous carbonates on Southampton, Baffin, and Akpatok islands in the eastern Canadian Arctic. *Canadian Journal of Earth Sciences* **26**, 1880-1903.

Mei, S.L. (1995). Biostratigraphy and tectonic implications of Late Ordovician conodonts from Shiyanhe Formation, Neixiang, Henan. *Acta Palaeontologica Sinica* **34** (6), 674-687. (in Chinese with English abstract).

Mellgren, J.S. and Eriksson, M.E. (2006). A model of reconstruction for the oral apparatus of the Ordovician conodont genus *Protopanderodus* Lindström, 1971. *Transactions of the Royal Society of Edinburgh: Earth Sciences* **97**, 97-112.

Moors, H.T. (1970). Ordovician graptolites from the Cliefden Caves area, Mandurama, N.S.W., with a re-appraisal of their stratigraphic significance. *Proceedings of the Royal Society of Victoria* **83**, 253-287.

Moskalenko, T.A. (1973). Conodonts of the Middle and Upper Ordovician on the Siberian Platform. *Akademiy Nauk SSSR, Sibirskoe Otdelenie, Trudy Instituta Geologii i Geofiziki* **137**, 1-143. (in Russian).

Ni, S.Z. and Li, Z.H. (1987). Conodonts. In Wang, X.F., Ni, S.Z., Zeng, Q.L., Xu, G.H., Zhou, T.M., Li, Z.H., Xiang, L.W. and Lai, C.G. 'Biostratigraphy of the Yangtze Gorge area 2: Early Palaeozoic Era' pp. 386-447, 549-555, 619-632 (Geological Publishing House: Beijing). (in Chinese with English abstract).

Nowlan, G.S. (1979). Fused clusters of the conodont genus *Belodina* Ethington from the Thumb Mountain Formation (Ordovician), Ellesmere Island, District of Franklin. *Current Research, Part A, Geological Survey of Canada, Paper* **79-1A**, 213-218.

Nowlan, G.S. (1981). Some Ordovician conodont faunules from the Miramichi Anticlinorium, New Brunswick. *Geological Survey of Canada, Bulletin* **345**, 1-35.

Nowlan, G.S. (1983). Biostratigraphic, paleogeographic, and tectonic implications of Late Ordovician conodonts from the Grog Brook Group, northwestern New Brunswick. *Canadian Journal of Earth Sciences* **20**, 650-670.

Nowlan, G.S. (2002). Stratigraphy and conodont biostratigraphy of Upper Ordovician strata in the subsurface of Alberta, Canada. *Special Papers in Palaeontology* **67**, 185-203.

Nowlan, G.S. and Barnes, C.R. (1981). Late Ordovician conodonts from the Vauréal Formation, Anticosti Island, Québec; Part 1. *Geological Survey of Canada, Bulletin* **329**, 1-49.

Nowlan, G.S., McCracken, A.D. and Chatterton, B.D.E. (1988). Conodonts from Ordovician-Silurian boundary strata, Whittaker Formation, Mackenzie Mountains, Northwest Territories. *Geological Survey of Canada, Bulletin* **373**, 1-99.

Nowlan, G.S., McCracken, A.D. and McLeod, M.J. (1997). Tectonic and paleogeographic significance of Late Ordovician conodonts in the Canadian Appalachians. *Canadian Journal of Earth Sciences* **34**, 1521-1537.

Orchard, M.J. (1980). Upper Ordovician conodonts from England and Wales. *Geologica et Palaeontologica* **14**, 9-44.

Ortega, G., Albanesi, G.L., Banchig, A.L. and Peralta, G.L. (2008). High resolution conodont-graptolite biostratigraphy in the Middle-Upper Ordovician of the Sierra de La Invernada Formation (Central Precordillera, Argentina). *Geologica Acta* **6** (2), 161-180.

Packham, G.H., Percival, I.G. and Bischoff, G.C.O. (1999). Age constraints on strata enclosing the Cadia and Junction Reefs ore deposits of central New South Wales, and tectonic implications. *Geological Survey of New South Wales, Quarterly Notes* **110**, 1-12.

Palmieri, V. (1978). Late Ordovician conodonts from the Fork Lagoons Beds, Emerald area, central Queensland. *Geological Survey of Queensland Publication 369, Palaeontological Paper* **43**, 1-55.

Pander, C.H. (1856). 'Monographie der fossilen Fische des Silurischen Systems der Russisch-Baltischen Gouvernements'. 91 pp. (Akademie der Wissenschaften: St. Petersburg).

Pei, F. and Cai, S.H. (1987). 'Ordovician conodonts from Henan Province'. 128 pp. (Press of the Wuhan College of Geosciences: Wuhan). (in Chinese).

Percival, I.G. (1976). The geology of the Licking Hole Creek area, near Walli, central-western New South Wales. *Journal and Proceedings of the Royal Society of New South Wales* **109**, 7-23.

Percival, I.G. (1978). Inarticulate brachiopods from the Late Ordovician of New South Wales, and their palaeoecological significance. *Alcheringa* **2,** 117-141.

Percival, I.G. (1999). Late Ordovician biostratigraphy of the northern Rockley-Gulgong Volcanic Belt. *Geological Survey of New South Wales, Quarterly Notes* **108**, 1-7.

Percival, I.G., Kraft, P., Zhang, Y.D. and Sherwin, L. (2015). A long-overdue systematic revision of Ordovician graptolite faunas from New South Wales, Australia. The Ordovician Exposed: Short Papers and Abstracts for the 12th International Symposium on the Ordovician System, Harrisonburg, USA, June 2015. *Stratigraphy* **12** (2), 47-53.

Philip, G.M. (1966). The occurrence and palaeogeographic significance of Ordovician strata in northern New South Wales. *Australian Journal of Science* **29**, 112-113.

Pickett, J.W. (1978). Further evidence for the age of the Sofala Volcanics. *Geological Survey of New South Wales, Quarterly Notes* **31**, 1-4.

Pickett, J.W. and Ingpen, I.A. (1990). Ordovician and Silurian strata south of Trundle, New South Wales. *Geological Survey of New South Wales, Quarterly Notes* **78**, 1-14.

Pohler, S.M.L. (1994). Conodont biofacies of Lower to lower Middle Ordovician megaconglomerates, Cow Head Group, western Newfoundland. *Geological Survey of Canada, Bulletin* **459**, 1-71.

Pohler, S.M.L. and Orchard, M.J. (1990). Ordovician conodont biostratigraphy, western Canadian Cordillera. *Geological Survey of Canada Paper* **90**-15, 1-37.

Popov, L.E. (1977). Novye vidy sredneordovikskikh bezzamkovykh brachiopod krebta Chingiz (Vostochnyy Kazakhstan). *Novye vidy drevnikh rastenii i bespozvonochnykh SSSR* **4**, 102-105. (in Russian).

Popov, L.E. (2000). Late Ordovician linguliformean microbrachiopods from north-central Kazakhstan. *Alcheringa* **24**, 257-275.

Popov, L.E., Nõlvak, J. and Holmer, L.E. (1994). Late Ordovician lingulate brachiopods from Estonia. *Palaeontology* **37**, 627-650.

Pyle, L.J. and Barnes, C.R. (2001). Conodonts from the Kechika Formation and Road River Group (Lower to Upper Ordovician) of the Cassiar Terrane, northern British Columbia. *Canadian Journal of Earth Sciences* **38**, 1387-1401.

Rasmussen, J.A. (2001). Conodont biostratigraphy and taxonomy of the Ordovician shelf margin deposits in the Scandinavian Caledonides. *Fossils and Strata* **48**, 1-180.

Rasmussen, J.A. and Stouge, S. (1989). Middle Ordovician conodonts from allochthonous limestones at Høyberget, southeastern Norwegian Caledonides. *Norsk Geologisk Tidsskrift* **69**, 103-110.

Rhodes, F.H.T. (1955). The conodont fauna of the Keisley Limestone. *Quarterly Journal of the Geological Society of London* **11**, 117-142.

Rodríguez-Cañero, R., Martín-Algarra, A., Sarmiento, G.N. and Navas-Parejo, P. (2010). First Late Ordovician conodont fauna in the Beltic Cordillera (South Spain): a palaeobiogeographical contribution. *Terra Nova* **22**, 330-340.

Saltzman, M.R., Edwards, C.T., Leslie, S.A., Dwyer, G.S., Bauer, J.A., Repetski, J.E., Harris, A.G. and Bergström, S.M. (2014). Calibration of a conodont apatite-based Ordovician 87Sr/86Sr curve to biostratigraphy and geochronology: implications for stratigraphic resolution. *Geological Society of America Bulletin* **126** (11-12), 1551-1568.

Sansom, I.J. and Smith, M.P. (2005). Late Ordovician vertebrates from the Bighorn Mountains of Wyoming, USA. *Palaeontology* **48** (1), 31-48.

Sarmiento, G. (1990). Conodontos ordovicicos de Argentina. *Treballs del Museu de Geologia de Barcelona* **1**, 135-161.

Savage, N.M. (1990). Conodonts of Caradocian (Late Ordovician) age from the Cliefden Caves Limestone, southeastern Australia. *Journal of Paleontology* **64**, 821-831.

Savage, N.M. and Bassett, M.G. (1985). Caradoc-Ashgill conodont faunas from Wales and the Welsh Borderland. *Palaeontology* **28**, 679-713.

Schopf, T.J. (1966). Conodonts of the Trenton Group (Ordovician) in New York, southern Ontario, and Quebec. *New York State Museum and Science Service Bulletin* **405**, 1-105.

Serpagli, E. (1967). I conodonti dell'Ordoviciano Superiore (Ashgilliano) delle Alpi Carniche. *Bollettino della Società Paleontologica Italiana* **6**, 30-111.

Simpson, A. (1997). Late Ordovician conodonts from Gray Creek and the headwaters of Stockyard Creek, north Queensland. *Geological Society of Australia Abstracts*, Number **48**, 111.

Simpson, A. (2000). Late Ordovician conodonts from the "Carriers Well Formation", north-eastern Australia. *Geological Society of Australia Abstracts*, Number **61**, 177-178.

Stouge, S. and Rasmussen, J.A. (1996). Upper Ordovician conodonts from Bornholm and possible migration routes in the Palaeotethys Ocean. *Bulletin of the Geological Society of Denmark* **43**, 54-67.

Sweet, W.C. (1979). Late Ordovician conodonts and biostratigraphy of the western Midcontinent Province. *Brigham Young University Geology Studies* **26**, 45-86.

Sweet, W.C. (2000). Conodonts and biostratigraphy of Upper Ordovician strata along a shelf to basin transect in central Nevada. *Journal of Paleontology* **74**, 1148-1160.

Sweet, W.C. and Bergström, S.M. (1962). Conodonts from the Pratt Ferry Formation (Middle Ordovician) of Alabama. *Journal of Paleontology* **36**, 1214-1252.

Talent, J.A., Mawson, R. and Simpson, A. (2003). The "lost" Early Ordovician-Devonian Georgetown Carbonate Platform of northeastern Australia. *Courier Forschungsinstitut Senckenberg* **242**, 71-80.

Talent, J.A., Mawson, R., Simpson, A. and Brock, G.A. (2002). Palaeozoics of NE Queensland: Broken River Region: Ordovician-Carboniferous of the Townsville hinterland: Broken River and Camel Creek regions, Burdekin and Clarke River basins. International Palaeontological Congress Post-5, Field Excursion Guidebook. Special Publication No. 1, Macquarie University Centre for Ecostratigraphy and Palaeobiology. (Macquarie University: Sydney).

Teichert, C. and Glenister, B.F. (1952). Fossil nautiloid faunas from Australia. *Journal of Paleontology* **26**, 730-752.

Tolmacheva, T.Y. and Roberts, D. (2007). New data on Upper Ordovician conodonts from the Trondheim Region, Central Norwegian Caledonides. *Norges geologiske undersøkelse Bulletin* **447**, 5-15.

Tolmacheva, T.Y., Degtyarev, K.E., Ryazantsev, A.V. and Nikitina, O.I. (2009). Conodonts from the Upper Ordovician Siliceous Rocks of Central Kazakhstan. *Paleontological Journal* **43** (11), 1498-1512.

Trotter, J.A. and Webby, B.D. (1995). Upper Ordovician conodonts from the Malongulli Formation, Cliefden Caves area, central New South Wales. *AGSO Journal of Australian Geology and Geophysics* **15** (4), 475-499.

Uyeno, T.T. (1990). Biostratigraphy and conodont faunas of Upper Ordovician through Middle Devonian rocks, eastern Arctic Archipelago. *Geological Survey of Canada, Bulletin* **401**, 1-211.

Viira, V. (2008). Conodont biostratigraphy in the Middle–Upper Ordovician boundary beds of Estonia. *Estonian Journal of Earth Sciences* **57** (1), 23-38.

Walcott, C.D. (1889). Description of a new genus and species of inarticulate brachiopod from the Trenton Limestone. *Proceedings of the United States National Museum* (advance copy) **12**, 365-366.

Walcott, C.D. (1901). Cambrian Brachiopoda: *Obolella*, subgenus *Glyptias*; *Bicia*; *Obolus*, subgenus *Westonia*; with descriptions of new species. *Proceedings of the United States National Museum* **23**, 669-695.

Wang, C.Y. (ed.) (1993). 'Conodonts of the Lower Yangtze Valley - an index to biostratigraphy and organic metamorphic maturity'. 326 pp. (Science Press: Beijing). (in Chinese with English abstract).

Wang, Z.H. (2001). Ordovician conodonts from Kalpin of Xinjiang and Pingliang of Gansu across the base of Upper Ordovician Series. *Acta Micropalaeontologica Sinica* **18** (4), 349-363.

Wang, Z.H., Bergström, S.M. and Lane, H.R. (1996). Conodont provinces and biostratigraphy in Ordovician of China. *Acta Palaeontologica Sinica* **35** (1), 26-59.

Wang, Z.H. and Luo, K.Q. (1984). Late Cambrian and Ordovician conodonts from the marginal areas of the Ordos Platform, China. *Bulletin, Nanjing Institute*

of Geology and Palaeontology, Academia Sinica **8,** 237-304. (in Chinese with English abstract).

Wang, Z.H. and Qi, Y.P. (2001). Ordovician conodonts from drillings in the Taklimakan desert, Xinjiang, NW China. *Acta Micropalaeontologica Sinica* **18** (2), 133-148. (in Chinese with English abstract).

Wang, Z.H., Qi, Y.P. and Wu, R.C. (2011). 'Cambrian and Ordovician conodonts in China', 388 pp. (China University of Science and Technology Press: Hefei). (in Chinese with English abstract).

Wang, Z.H. and Zhou, T.R. (1998). Ordovician conodonts from western and northeastern Tarim and their significance. *Acta Palaeontologica Sinica* **37** (2), 173-193.

Webby, B.D. (1992). Ordovician island biotas: New South Wales record and global implications. *Journal and Proceedings of the Royal Society of New South Wales* **125**, 51-77.

Webby, B.D., Cooper, R.A., Bergström, S.M. and Paris, F. (2004). Stratigraphic framework and time slices. In 'The Great Ordovician Biodiversification Event' (Eds B.D. Webby, F. Paris, M.L. Droser and I.G. Percival), pp. 41-47. (Columbia University Press: New York).

Willard, B. (1928). The brachiopods of the Ottosee and Holston formations of Tennessee and Virginia. *Bulletin of the Harvard Museum of Comparative Zoology* **68**, 255-292.

Williams, A., Brunton, C.H.C., Carlson, S.J. et al. (2000). 'Treatise on Invertebrate Paleontology, Part H, Brachiopoda (Revised) Volume 2: Linguliformea, Craniformea, and Rhynchonelliformea (part)'. (The Geological Society of America: Boulder and The University of Kansas: Lawrence).

Withnall, I.W. and Lang, S.C. (eds) (1993). Geology of the Broken River Province, north Queensland. *Queensland Geology* **4**, 1-289.

Withnall, I.W., Blake, P.R., Crouch, S.B.S., Tenison Woods, K., Grimes, K.G., Hayward, M.A., Lam, J.S., Garrard, P. and Rees, I.D. (1995). Geology of the southern part of the Anakie Inlier, central Queensland. *Queensland Geology* **7**, 1-245.

Yu, F.L. and Wang, Z.H. (1986). Conodonts from Beiguoshan Formation in Long Xian, Shaanxi. *Acta Micropalaeontologica Sinica* **3** (1), 99-105. (in Chinese with English abstract).

Zeng, Q.L., Ni, S.Z., Xu, G.H., Zhou, T.M., Wang, X.F., Li, Z.H., Lai, C.G. and Xiang, L.W. (1983). Subdivision and correlation on the Ordovician in the eastern Yangtze Gorges, China. *Bulletin of the Yichang Institute of Geology and Mineral Resources, Chinese Academy of Geological Sciences* **6**, 1-68.

Zhang, J.H. (1998). Conodonts from the Guniutan Formation (Llanvirnian) in Hubei and Hunan Provinces, south-central China. *Stockholm Contributions in Geology* **46**, 1-161.

Zhang, J.H., Barnes, C.R. and Cooper, B.J. (2004). Early Late Ordovician conodonts from the Stokes Siltstone, Amadeus Basin, central Australia. Courier *Forschungsinstitut Senckenberg* **245**, 1-37.

Zhang, J.H. and Chen, M.J. (1992). Evolutionary trends and stratigraphic significance of *Periodon*. *Acta Micropalaeontologica Sinica* **9** (4), 391-396. (in Chinese with English abstract).

Zhang, S.X. (2011). Late Ordovician conodont biostratigraphy and redefinition of the age of oil shale intervals on Southampton Island. *Canadian Journal of Earth Sciences* **48** (3), 619-643.

Zhang, S.X. (2013). Ordovician conodont biostratigraphy and redefinition of the age of lithostratigraphic units on northeastern Melville Peninsula, Nunavut. *Canadian Journal of Earth Sciences* **50**, 808-825.

Zhang, S.X. and Barnes, C.R. (2007a). Late Ordovician to Early Silurian conodont faunas from the Kolyma Terrane, Omulev Mountains, northeast Russia, and their paleobiogeographic affinity. *Journal of Paleontology* **81**, 490-512.

Zhang, S.X. and Barnes, C.R. (2007b). Late Ordovician–Early Silurian conodont biostratigraphy and thermal maturity, Hudson Bay Basin. *Bulletin of Canadian Petroleum Geology* **55** (3), 179-216.

Zhang, S.X. and Pell, J. (2013). Study of sedimentary rock xenoliths from kimberlites on Hall Peninsula, Baffin Island, Nunavut. In Summary of Activities 2012, Canada-Nunavut Geoscience Office, pp. 107-112.

Zhang, S.X., Tarrant, G.A. and Barnes, C.R. (2011). Upper Ordovician conodont biostratigraphy and the age of the Collingwood Member, southern Ontario, Canada. *Canadian Journal of Earth Sciences* **48**, 1497-1522.

Zhao, Z.X., Zhang, G.Z. and Xiao, J.N. (2000). 'Paleozoic stratigraphy and conodonts in Xinjiang'. 340 pp. (Petroleum Industry Press: Beijing). (in Chinese with English abstract).

Zhen, Y.Y. (2001). Distribution of the Late Ordovician conodont genus *Taoqupognathus* in eastern Australia and China. *Acta Palaeontologica Sinica* **40** (3), 351-361.

Zhen, Y.Y. and Percival, I.G. (2004). Darriwilian (Middle Ordovician) conodonts from the Weemalla Formation, south of Orange, New South Wales. *Memoir of the Association of Australasian Palaeontologists* **30**, 153-178.

Zhen, Y.Y., Percival, I.G. and Farrell, J.R. (2003). Late Ordovician allochthonous limestones in Late Silurian Barnby Hills Shale, central western New South Wales. *Proceedings of the Linnean Society of New South Wales* **124**, 29-51.

Zhen, Y.Y., Percival, I.G. and Webby, B.D. (2004). Conodont faunas from the Mid to Late Ordovician boundary interval of the Wahringa Limestone Member (Fairbridge Volcanics), central New South Wales. *Proceedings of the Linnean Society of New South Wales* **125**, 141-164.

Zhen, Y.Y., Wang, Z.H., Zhang, Y.D., Bergström, S.M., Percival, I.G. and Cheng, J.F. (2011). Middle to Late Ordovician (Darriwilian-Sandbian) conodonts from the Dawangou section, Kalpin area of the Tarim

Basin, northwestern China. *Records of the Australian Museum* **63**, 203-266.

Zhen, Y.Y. and Webby, B.D. (1995). Upper Ordovician conodonts from the Cliefden Caves Limestone Group, central New South Wales, Australia. *Courier Forschungsinstitut Senckenberg* **182**, 265-305.

Zhen, Y.Y., Webby, B.D. and Barnes, C.R. (1999). Upper Ordovician conodonts from the Bowan Park succession, central New South Wales, Australia. *Geobios* **32**, 73-104.

Zhen, Y.Y., Zhang, Y.D. and Percival, I.G. (2009). Early Sandbian (Late Ordovician) conodonts from the Yenwashan Formation, western Zhejiang, South China. *Alcheringa* **33** (2), 133-161.

Zhen, Y.Y., Zhang, Y.D., Wang, Z.H. and Percival, I.G. (2015). Huaiyuan Epeirogeny – shaping Ordovician stratigraphy and sedimentation on the North China Platform. *Palaeogeography, Palaeoclimatology, Palaeoecology*. http://dx.doi.org/10.1016/j.palaeo.2015.07.040

Ziegler, W. (ed.) (1981). 'Catalogue of Conodonts, Vol. 4'. 445 pp. (Schweizerbart'sche Verlagsbuchhandlung: Stuttgart).